Floating Piles

An investigative study into the behavior of friction piles installed within a settling soil profile

Master of Science Thesis

Joris Bol
September 2012

Floating Piles

An investigative study into the behavior of friction piles installed within a settling soil profile

Master of Science Thesis

Student:	J.G. Bol 4052390
Date:	September 2012
Professor:	Prof. Ir. A.F. van Tol
Supervisors:	Dr. Ir. K.J. Bakker Dr. M. Cunningham (Shell Global Solutions) Dr. Ir. J. Dijkstra Ing. H.J. Everts

Preface

This report is submitted in partial fulfillment of the requirements to obtain the degree Master of Science at Delft University of Technology at the faculty of Civil Engineering and Geosciences. The last nine months I have been working on this research project focusing on consolidation settlements in a certain soil profile.

This project would not have been possible without the help of numerous people. I would like to express my gratitude and thanks to my committee, Prof. Frits van Tol, Bert Everts, Klaas Jan Bakker, Jelke Dijkstra and Mark Cunningham. Special thanks goes out to Jelke Dijkstra and Han de Visser for the support during the physical model testing, and their valuable input during the entire process. My gratitude goes to Mark Cunningham for giving me the opportunity to do this study at Shell Global Solutions, and his daily support throughout the project.

I would like to thank all the graduate students, both at Delft University of Technology and Shell Global Solutions in Rijswijk, for the interesting discussions and their input. During the numerous coffee breaks and lunch time debates I have learned an awful lot, maybe not all applicable to this particular research.

Furthermore I would like to show my appreciation to my friends for their discussions on the topic. Also I would like to thank my brother and sister for their support throughout this entire period. Last but not least my thanks go out to my parents for giving me the opportunity to study, and for always supporting me.

Rijswijk, September 5th 2012

Joris Bol

Abstract

The construction of an artificial island is one of the solutions to be able to drill for oil safely in the Caspian Sea. On this island the required facilities are installed. Construction of an artificial island however, results in loading of the subsoil and will trigger settlements. Consolidation is one of the processes which cause the settlement. Differential settlements can damage the shallow foundations on the island. In order to prevent this, an alternative foundation on piles needs to be considered.

Piles placed in a thick, soft soil layer will have low end bearing capacity, and thus need to activate skin friction. Since the surrounding soft soil is consolidating, these piles will have their own challenges. The relative movement between pile and soil determines the zones of negative and positive skin friction. Positive skin friction will need to be mobilized to support pile loading. Applying load on the head creates additional pile settlements, thus expanding the zone of positive skin friction. The consequence of this is that the bearing capacity of the pile is increased.

This research looks into the two dominant parts of these friction piles in a consolidating soil profile. The driving mechanism, consolidation and subsequent settlement of the subsoil, is studied. Besides that the behavior of the interface between the soil and the installed piled is considered.

Site investigations performed at the reference project are interpreted and a ‘Caspian’ soil profile can be determined. Besides this general profile a ‘Centrifuge’ soil profile is determined, which is revised to fit the specifications of the centrifuge. A one layer ‘benchmark’ situation is created to check the different calculation methods. The reaction of the ‘centrifuge’ and ‘benchmark’ soil profiles to the new loading situation is calculated and can be checked with centrifuge measurements.

Recreating a two layer soil profile, containing stiff and soft clay, is done in the centrifuge. Msettle, a Hand Calculation and the Plaxis Soft Soil model give an accurate representation of the settlement in the physical model. The settlement in time seems to be described accurately as well. Calculations are done with a constant permeability. The “settlement in time” lines are calculated with Msettle and give a good image of the decrease in permeability during the performed centrifuge tests.

The measured compression parameters for Kaolin Clay agree well with the values found in the literature. These compression parameters are tested in an oedometer test, and are given in a one dimensional stress space. Recalculation of the compression parameters into isotropic stress dependent parameters does not give the same settlement predictions. The used relationships given in the Plaxis 2D Material Models manual do not seem to give an accurate relation.

The performed direct shear box tests show that the peak friction on the pile-soil interface is mobilized at displacements of about one millimeter. Further shearing led to a decrease in maximum shear stress, the so called residual value.

Table of Contents

List of Figures

List of Tables

1 Introduction

1.1 General introduction

Natural resources are becoming scarce. So called “easy oil”, locations where natural resources can be won without too many difficulties, are less often encountered. Due to the increasingly hostile environment, drilling for natural resources becomes more challenging.

Reservoirs containing natural resources are found all over the world. Onshore reservoirs are found in Saudi Arabia, Iran and Iraq. Natural resources offshore are located below the sea floor, e.g. in the Gulf of Mexico and the Caspian Sea.

These offshore natural reservoirs have been exploited since the early 1900s. This is done by drilling rigs and oil platforms which are found on the sea bed, or alternatively by using floating rigs. Some offshore areas have limited depth and do not allow for these rigs or platforms to be placed. Another limitation for the use of rigs or platforms is ice loading. Ice loading can severely damage the installations and mitigating measures can become very costly.

A solution to this, especially on locations in shallow water depth, is the construction of an artificial island. On this island the required facilities, such as drilling rigs and processing plants, are installed. Construction of an artificial island however, results in loading of the subsoil, which in turn results in surface settlement. This in itself might not be a problem. Excessive differential settlements, however, will damage the facilities placed on top of this island. Consolidation is one of the processes which causes this settlement, and in fine grained material with low permeability this process continues for years.

Consolidation is a process in which excess pore water pressures are dissipated over time by an outflow of water. The resulting increase in effective stress generates settlements. The rate at which this happens depends, among other things, on the permeability of the soil. Permeability is soil dependent. Sand is more permeable than fine grained materials such as clay. Therefore, in clay consolidation takes significantly longer.

If construction is started during the consolidation period it might trigger differential settlements. However, in most fine grained soils it is not practical to wait till the end of consolidation which can take years. Therefore, in most situations construction is started during the process. As long as the ground level remains above sea level this is not a very big problem for the functions of the island itself.

However, the differential settlements can damage the shallow foundations on the island. In order to prevent this, an alternative foundation on piles needs to be considered.

Piles in consolidating subsoil have their own challenges. Friction between the pile and the settling subsoil will cause an extra load. The length of the pile over which the subsoil will exercise a load and the part where the pile will mobilize its bearing capacity is dependent on the relative movement between the pile and the subsoil. If the subsoil settles more than the pile an additional load from the soil on the pile is mobilized. The part where the subsoil settles less than the pile, the soil will add to the bearing capacity. This mechanism is displayed in Figure 1.

When a load is placed on the pile head it creates additional settlements, thus expanding the zone in which the pile settles more than the soil. The consequence of this is that the shear resistance in this upper layer will add to the bearing capacity of the pile.

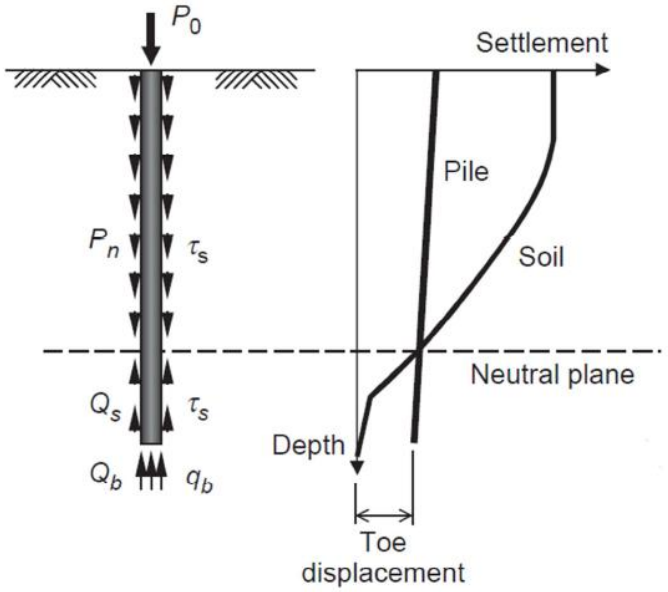

Figure 1: Differential settlement between pile and soil [Fleming *et al*, 2009]

1.2 General organization of the study

This project will be split up into two separate studies. The first part will be focused on the settlement of the soil profile. Different calculation models are selected to predict the subsoil reaction. Centrifuge tests are performed to determine the reliability of these calculation models. This should give a clear picture of the loading / support a pile will get when it is placed in this profile.

In the second part an instrumented pile will be placed in the soil profile, which will undergo a consolidation centrifuge test. The model prepared in the first part of this research can be checked and optimized with the results. Other options could be multiple piles in the soil profile, and how will these different piles influence each other.

The different research questions relate to the different phases of the study. In paragraph 1.3.1 the problem is described and the research questions will be split up into the two different phases.

1.3 Terms of Reference

The terms of reference select the boundary conditions of this research. The problem, research questions and the limitations of the study are given. These have been established at the start of the thesis.

1.3.1 Problem

The problem described in the introduction will be studied in the following way:

- Interpretation of the Site Investigations performed;

Site investigations performed at the reference project are interpreted and a 'Caspian' soil profile can be determined. Besides this general profile a 'Centrifuge' soil profile is determined, which is fitted towards the specifications of the centrifuge. A 'benchmark' situation is created to check the different calculation methods.

- Determine the most reliable calculation method for subsoil settlement;

The reaction of the 'centrifuge' and 'benchmark' soil profiles to the new loading situation should be calculated and can be checked with centrifuge measurements. From this the most accurate calculation method can be determined.

- Predict the reaction of the pile in the soil profile;

The soil profile will subject the pile to a dragload. The pile head settlement and the bearing capacity can be predicted. This can be done through different methods.

- Determine the most reliable prediction method for reaction of the pile;

The predictions performed before can be checked with centrifuge tests. The calculation method with the most reliable outcome can be determined from these tests.

1.3.2 Research Questions

The following main research question is formulated for this study:

How much differential settlement will occur between the pile head and ground level when a "floating" pile is loaded in a settling (consolidating) soil profile?

This problem can be split up into several research questions:

- How does the soil profile settle with depth?
- How to assess the level of the neutral plane?
- Can the "Caspian" soil profile be modeled in the centrifuge?
- What is the reaction of the interface between pile and soil?
- **What is the load / stress distribution along the pile shaft?**
- **Does a group of piles react differently to soil settlements then a single pile?**
- *How reliable is the outcome of the methods used in industry for modeling such problems?*

The *italic* question will be part of both the first and the second study. This question cannot be answered by the first part of the study alone. The **bold** questions only apply to the second part of the study and are not applicable in this part of the research.

1.3.3 Limitations

The following limitations have been set for this research:

- Dynamic loading will not be evaluated,
- Modeling of the problem in a Finite Element program will be done in 2D,
- Anisotropy of the soil is neglected,
- No creep will be modeled in this research,
- Only a single pile will be evaluated.

1.4 Readers manual

The first chapter gives an introduction into the problem and describes the objectives and limitations of this research.

A literature study is added in chapter 2, and has been performed on the available studies on floating pile foundations. The driving mechanism, consolidation of the subsoil, has been looked at as well. The reaction of the interface between soil and pile has been studied extensively before. The available theories, studies and literature has been listed and explained. Finally geotechnical centrifuge modeling is introduced, together with its scaling laws. The mechanisms which are scaled in this study will be listed and explained.

This research is initiated by a reference project in the Northern part of the Caspian Sea. Chapter 3 introduces the general geology of the reference project and the performed site investigations. An interpretation of the site investigation is done and from this a general soil model for the reference project has been set up. The soil model is introduced in this chapter.

Chapter 4 give the calculations which are done. Two different soil models are introduced in this chapter. A “benchmark” soil profile, which is used to examine the differences between the different models. The same is done for a “centrifuge” soil profile. This profile is largely based on the “Caspian” soil profile introduced earlier, but has been fitted to be able to test this profile in the centrifuge.

In chapter 5 the centrifuge modeling is the main focus. The test setup, preparation of the samples and execution is introduced. Some limitations of centrifuge testing are listed. Centrifuge tests have been performed on both models given in chapter 4.

The results and discussion of the calculation- and physical model tests, for the “benchmark” soil profile is presented in chapter 6. The variance in “settlement-depth”, “settlement-time” and “consolidation-time” is discussed per plot. First the calculation models are discussed. After that the result of the centrifuge tests are introduced and compared to the calculated value. Some conclusions can be drawn on which model is most reliable in predicting the settlements occurring in the centrifuge after this discussion.

The same has been done in chapter 7, but for the “centrifuge” soil profile. The results of both the calculation models compared to each other, and compared to the centrifuge results. The reliability and uncertainties of the models are discussed.

The interaction between pile and the settling soil profile is introduced in chapter 8. Shear tests on the pile-soil interface have been performed which are presented here. The shear stress which acts on the sides of the pile has been predicted with different calculation models. The neutral plane method has been used to set up a load – settlement curve for the pile head.

Finally Chapter 9 and 10 give the conclusions to this study and recommendations for further work.

1.5 Definitions

Some terms used in this report might be confusing. In other literature the terms dragload and downdrag are sometimes mixed up or miss used. Besides that the term floating pile is not clearly described in literature. The definitions used in this report are given in Table 1.

Table 1: Definitions used in this report

Floating Pile	Friction pile in a settling soil profile. In this situation both the pile and the soil will show settlements. However, due to friction along the shaft the pile will settle less than the soil and "float" in the soil profile.
Negative Skin Friction	The downward friction along the pile shaft as a result of subsoil settlement. This occurs where the surrounding subsoil settles more than the pile.
Positive Skin Friction	The upward friction along the pile shaft as a result of pile settlement. This occurs where the pile settles more than the surrounding subsoil.
Drag Load	The load transferred to a pile due to negative skin friction.
Downdrag	The downward movement of a pile due to negative skin friction and expressed in term of settlement.
Neutral Plane	The level where the settlement of the soil and the settlement of the pile is the same. The relative movement is then zero. The length of the pile above the Neutral Plane will be subjected to Negative Skin Friction. Below the Neutral Plane Positive Skin Friction will occur.

2 Literature Study

Research has been done on friction piles before. References to these research projects are given in paragraph 2.1 of this chapter.

The mechanisms influencing the behavior of friction piles can be split up into different parts. There is the driving mechanism, which is the settlement of the soil. The different approaches in modeling this soil behavior are described in paragraph 2.2.

Another aspect which will have a pronounced influence on the behavior of friction piles is the interaction between pile and soil. Research on the interface behavior between a construction element and the adjacent soil has been described in paragraph 2.3.

Lastly physical modeling in a geotechnical centrifuge is described in paragraph 2.4. The focus in this paragraph is on the scaling laws which apply for the tests in this research.

2.1 Floating Piles

Floating piles are friction piles in a settling soil profile. These piles only mobilize very limited end bearing capacity. Because the piles lack end bearing capacity, friction between the pile shaft and the soil will be activated. Whether this friction is positive or negative depends on the relative displacement between the pile and the soil. [Fellenius, 1998] already summed up several full scale tests, and has drawn conclusions from the preformed tests.

Long term full scale tests have been performed on piles in a settling soil profile [Fellenius, 2006]. Here several research projects are presented, some of which have already been presented in his earlier paper. This time the load and settlement of the pile and soil have both been presented for several locations and for a longer time period.

[Bozozuk, 1981] presented data of a full scale pile loading test, on a pile preloaded by downdrag. A pile was installed into a soft soil layer, which has been preloaded by an embankment fill. Different load schedules were planned for the pile, both static and cyclic loading was to be applied. The conclusion of the research is that cyclic loads lower than the maximum dragload does not influence the pile settlement very much. This dragload can be seen as a pre-stress that is capable of responding to cyclic and short-term live loads.

Pile Design

[Fellenius, 1984] described the loading mechanism of floating piles. He mentioned that live load and dragload do not combine and separate loading situations should be considered for the design of floating

piles. A distinction can be made between a combination of dead load and dragload and dead load combined with live load. Live loads will reduce the amount of dragload applied on the pile, but applied for a longer period of time this live load can be seen as a dead load and will add to the maximum stress in the pile. The mechanisms occurring are described in Figure 2.

Fellenius also mentions that dragload is caused by relative displacement between the pile and soil. It does not however, generate settlement itself. A floating pile will not settle more than the ground surface or even the soil settlement at the neutral plane. The neutral plane is variable though, depending on the amount of load at the pile head.

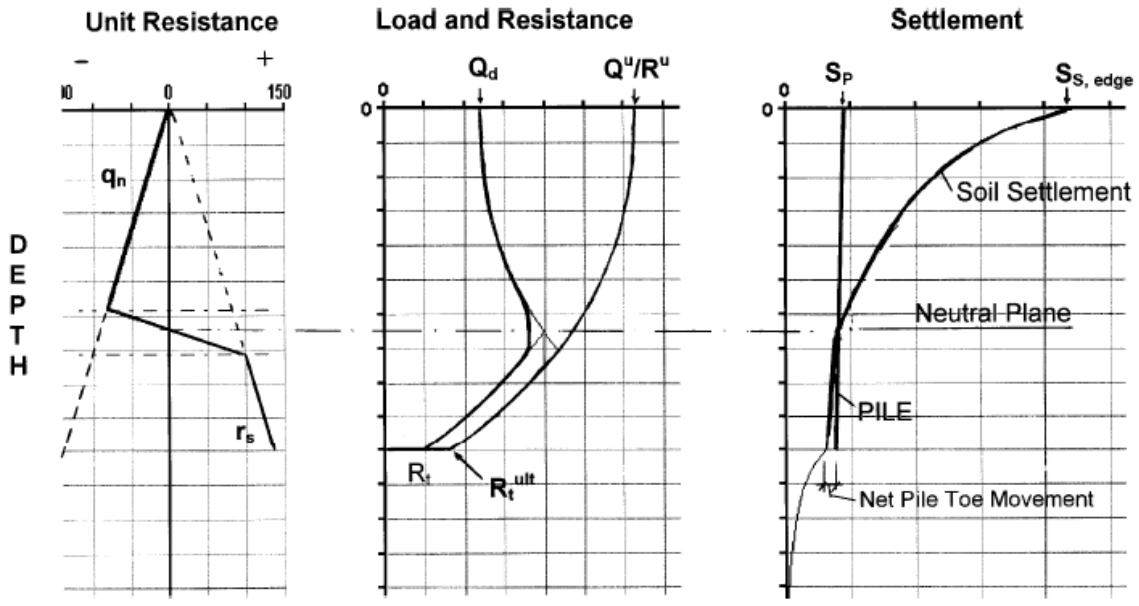

Figure 2: Neutral Plane / Transition Zone [Fellenius, 1998]

A pile design should consist of three separate aspects: Structural strength of the pile, settlement and geotechnical capacity.

2.2 Soil behavior

There are different mechanisms causing a soil profile to settle. Due to a change in stress conditions a soil body might deform due to either consolidation or creep. These two mechanisms are partly coupled, but are totally different from another.

Consolidation settlement was first discussed by [Terzaghi, 1925]. A soil body consists of soil particles, voids and water. If a soil body is completely saturated all the voids are filled with water. When a load is applied this will try to compress the body, which initially is prevented by the water. Terzaghi assumed that both the soil particles and the water will not deform. This means the void ratio should decrease to allow for deformations to occur. The groundwater located in the voids will get an overpressure and starts flowing to zones where the water has a lower pressure. The rate at which this happens depends on the permeability of the soil and the size of the load. The flow of water can be described by the flow

equation of Darcy [Terzaghi *et al*, 1996]. The equation takes into account the permeability of the soil and the gradient of pore water pressure. For this project the gradient of pore water pressure is defined by the height, width, and the soil density of a fill placed on top of the soil.

Secondary compression consists of creep. Creep is a time dependant process, rather than an increase of effective stress due to the dissipation of excess pore water pressures [Buisman, 1935]. Now a decrease in void ratio will take place by rearranging of the grain skeleton. Influences on the magnitude of creep settlement are effective stress rate and temperature [Leroueil, 1996]. In this study however, the soil is below water level and the temperature is fairly constant.

2.2.1 Theoretical Models

The most widely used and internationally accepted method has been proposed by Bjerrum in the seventh rankine lecture of 1967 [Bjerrum, 1967].

[Terzaghi, 1925] described one dimensional compression by stating that changes in a soil body are all related to changes in effective stress. His assumptions are quite reasonable, although some of them have been disproved by later laboratory tests. [Buisman, 1935] introduces the phenomenon of creep and it was [Koppejan, 1943] who combined the theories of Terzaghi and Buisman. The isotache model has been introduced by [Suklje, 1957] and relates the amount of creep settlement to the strain rate.

2.2.1.1 Bjerrum

Bjerrum specified consolidation and creep settlement with equation [1]. In this equation the consolidation has been split up into different parts. For every part there is a different parameter available. The compression (C_c) and recompression (C_r) parameters describe the settlement before and after the passing of the preconsolidation pressure respectively. Before the preconsolidation pressure the soil will be recompressed and will react stiffer. When this pressure has been reached the soil is compressed normally, and thus reacts less stiff.

$$\frac{\Delta h}{h_0} = \frac{C_r}{1+e_0}\log\left(\frac{\sigma'_p}{\sigma'_0}\right) + \frac{C_c}{1+e_0}\log\left(\frac{\sigma'}{\sigma'_p}\right) + C_\alpha \log\left(\frac{t}{t_0}\right) \qquad \textbf{[1]}$$

Besides these two parameters this equation also includes the creep influence on the settlement. The C_α parameter describes this part. As can be seen in the formula this is not influenced by the amount of effective stress, but rather by time.

These parameters can be determined with the help of oedometer tests. The settlement of the soil will be plotted versus the increase of effective vertical stress. Figure 3 and Figure 4 describe the Bjerrum compression parameters and how they are determined. The soil behavior depicted in this figures is highly idealized.

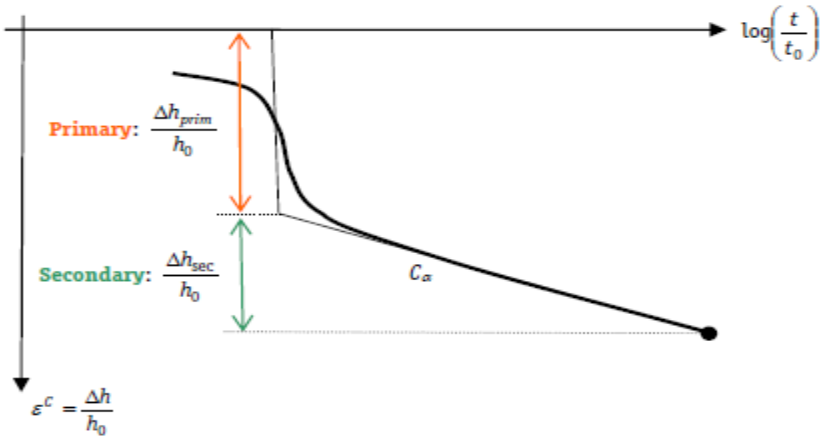

Figure 3: Soil settlement in time

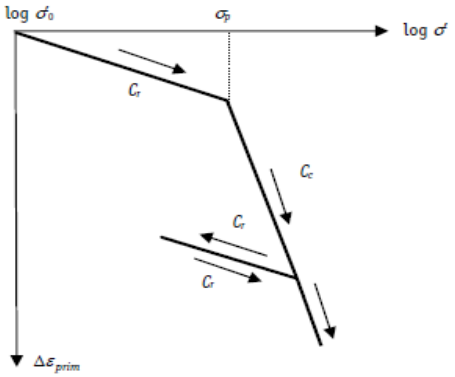

Figure 4: Description of compression parameters

2.2.1.2 Koppejan

Koppejan introduced his model for settlement calculation in 1948 [Koppejan, 1948]. It makes a distinction between primary (instantaneous) and secondary (creep) settlements. For the distinct stages different parameters are specified. Besides these parameters there are also parameters specified for unloading and reloading, so called swelling parameters.

There are different formulas used to calculate the amount of settlement. Equation [2] and [3] are used to calculate the primary settlement at stresses below and above the preconsolidation pressure respectively. Equation [4] and [5] will give the secondary settlement, again both before the preconsolidation pressure is reached and when it is exceeded. Finally equation [6] calculates the swelling which will occur after load removal.

$$\frac{\Delta h_{prim}}{h} = \frac{1}{C_p}\ln\left(\frac{\sigma'}{\sigma_0}\right) \quad [2]$$

$$\frac{\Delta h_{prim}}{h} = \frac{1}{C_p}\ln\left(\frac{\sigma_p}{\sigma_0}\right) + \frac{1}{C'_p}\ln\left(\frac{\sigma'}{\sigma_0}\right) \quad [3]$$

$$\frac{\Delta h_{sec}}{h} = \frac{1}{C_s}\log\left(1+\frac{t}{\tau_0}\right)\ln\left(\frac{\sigma'}{\sigma_0}\right) \quad [4]$$

$$\frac{\Delta h_{sec}}{h} = \frac{1}{C_s}\log\left(1+\frac{t}{\tau_0}\right)\ln\left(\frac{\sigma_p}{\sigma_0}\right) + \frac{1}{C'_s}\log\left(1+\frac{t}{\tau_0}\right)\ln\left(\frac{\sigma'}{\sigma_p}\right) \quad [5]$$

$$\frac{\Delta h_{prim}}{h} = \frac{1}{A_p}\ln\left(\frac{\sigma'}{\sigma_0}\right) + \frac{1}{A_s}\log\left(\frac{t}{\tau_0}\right)\ln\left(\frac{\sigma'}{\sigma_0}\right) \quad [6]$$

The different parameters used in the formulas of Koppejan are plotted in Figure 5.

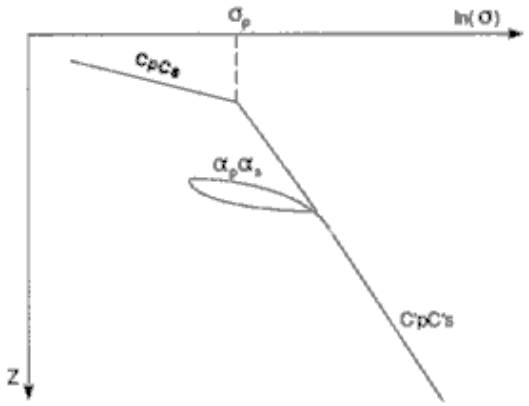

Figure 5: Koppejan Parameters

2.2.1.3 Isotache

Introduced by [Suklje, 1957] is the isotache model. This model introduces the strain rate dependency of settlements, and relates this to the mean values of void ratio and effective stress. This is done by isotachs. A set of isotachs for lacustrine chalk is presented in Figure 6. Isotaches are defined as a series of e – σ'_v plots determined from tests performed at different constant rates of strain.

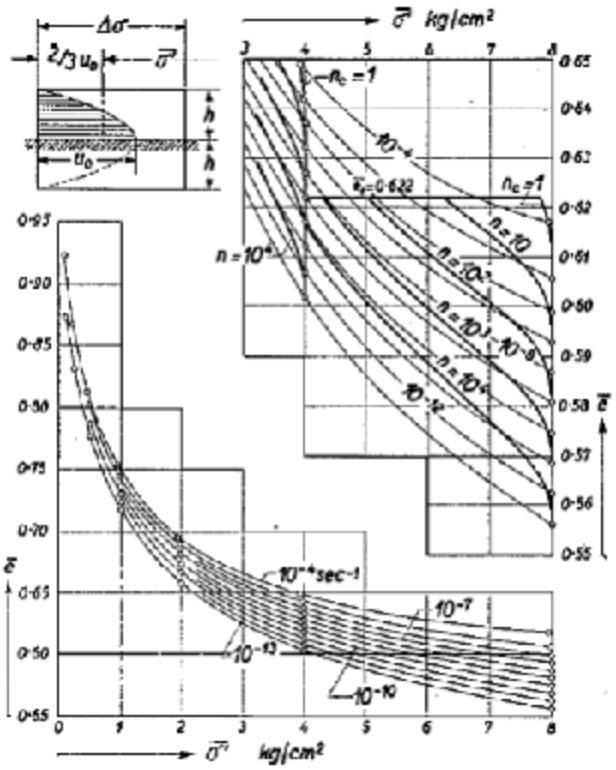

Figure 6: Isotache set for a lacustrine chalk sample [Suklje, 1957]

Later studies introduced settlement parameters connected to this isotache model [den Haan, 1994]. These parameters *a* and *b* describe the unloading and reloading behavior of the soils also specified in the earlier mentioned theories. The *c* parameter depends on the strain rate though, and determines the amount of creep settlement occurring.

2.2.2 Numerical Calculations

The previously discussed models have been implemented in a numerical framework.

Msettle and Plaxis are both able to model settlements due to loading of the soil. Advantages of these programs are that sophisticated soil profiles can be implemented easily. Calculations are based on the analytical solutions given in the paragraphs before.

2.2.2.1 Msettle v8.2

Msettle is a program developed by Deltares. This program uses analytical calculations to give a solution to the implemented geometry. As the name gives away already the program is focused on calculating the amount of settlement a certain geometry gives. Both the consolidation process and the amount of settlement can be calculated. To evaluate the consolidation process the program can use the following models:

- Terzaghi consolidation
- Darcy consolidation

To relate the changed stress conditions to an amount of settlement Msettle can use different models, the following can be chosen:

- The Bjerrum model
- The Isotache model
- The Koppejan model

2.2.2.2 Plaxis v9.02

General Information

Plaxis is a software program which uses the Finite Element Method to model soil and soil-structure interaction problems [Plaxis 2D, Reference Manual version 9.0]. It is a widely used program in the Geotechnical Engineering world. But as with every computer program, the results are dependent on the input.

Plaxis can be used to model both the amount of settlement, due to consolidation and creep, and the pile-soil interaction. The advantage is that this can be done in the same model where the Mseries needs different programs to model the settlement and the pile-soil interaction problem. The risk Plaxis poses is that if the consolidation calculation is not correct this will make the pile-soil interaction modeling be worthless as well.

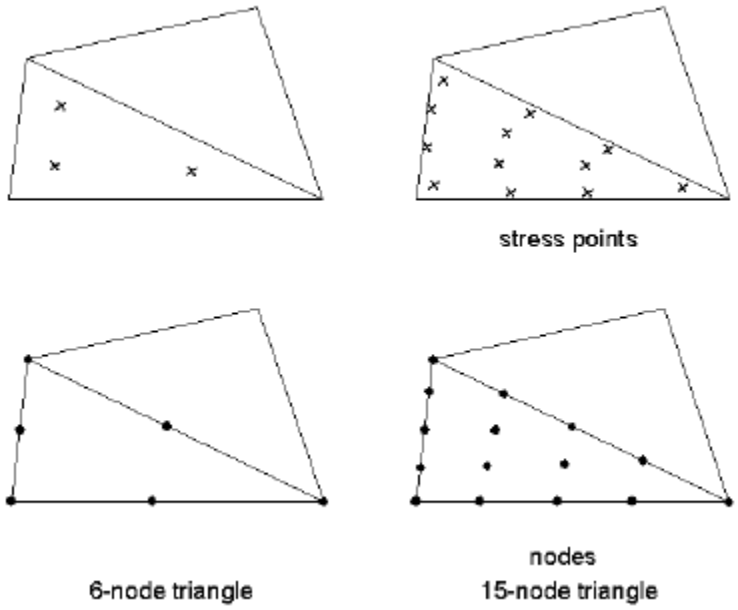

Figure 7: Elements in Plaxis

Modeling of Consolidation

Consolidation in Plaxis is modeled by the equations given by Biot's theory, this is combined with Darcy's law of fluid flow. Stresses are divided into effective stresses and pore pressures according to Terzaghi's principle. An elaborate explanation and its formulation in finite elements can be found in [Plaxis 2D, Scientific Manual Version 9.0].

Different constitutive soil models are available in Plaxis. These models represent the reaction of soil to different stress situations. Since soil is a complicated material to model, and its behavior depends on several factors, there is a large variety of models available. The models used in this thesis are described.

2.2.2.2.1 Soft Soil

In the Soft Soil model [Plaxis 2D v9.0 Material Models Manual] a logarithmic relation of strain and effective stress is implemented. Equation [7] is used to describe settlement in the primary compression zone. The deformation in unloading / reloading is assumed as elastic and behavior of the soil is predicted with equation [8].

$$\varepsilon_v - \varepsilon_v^0 = -\lambda^* \ln\left(\frac{p'}{p^0}\right) \quad \textbf{[7]}$$

$$\varepsilon_v^e - \varepsilon_v^{e0} = -\kappa^* \ln\left(\frac{p'}{p^0}\right) \quad \textbf{[8]}$$

ε_v / ε_v^e	*(elastic) volumetric strain*	*[-]*
ε_v^0 / ε_v^{e0}	*(elastic) initial volumetric strain*	*[-]*
p'	*isotropic stress*	*[kN/m2]*
P^0	*initial isotropic stress*	*[kN/m2]*
λ^*	*compression parameter*	*[-]*
κ^*	*recompression parameter*	*[-]*

The parameters lambda* and kappa* are deduced from a compression plot in “strain – ln isotropic stress” space.

Closely related to this model is the Soft Soil Creep model [Plaxis 2D v9.0 Material Models Manual]. As the name suggest, in this model creep settlements can be added as well. An extra parameter (μ*) is added which is directly related to the C_α. This parameter will describe the amount of creep settlements occurring in the time span of the performed calculation.

2.2.2.2.2 Modified Cam Clay

Besides the soft soil model, the Modified Cam Clay [Plaxis 2D v9.0 Material Models Manual] also uses a logarithmic stress – strain relation. The formulas used are slightly different as can be seen in equations [9] and [10]. The lambda and kappa parameters stand for respectively compression and recompression.

$$\mathrm{e} - \mathrm{e}^0 = -\lambda \ln\left(\frac{p'}{p^0}\right) \quad \textbf{[9]}$$

$$\mathrm{e} - \mathrm{e}^0 = -\kappa \ln\left(\frac{p'}{p^0}\right) \quad \textbf{[10]}$$

e	*void ratio*	*[-]*
e^0	*initial void ratio*	*[-]*
λ	*compression parameter*	*[-]*
κ	*recompression parameter*	*[-]*

The parameters lambda and kappa are similar to the parameters used in the soft soil model. The difference between them is that these parameters are determined in a “void ratio – ln stress” space.

2.2.2.2.3 Hardening Soil Model

The hardening soil model [Plaxis 2D v9.0 Material Models Manual] does not use a logarithmic relationship between stresses and strains. Instead the stiffness is made stress dependant with a power law using the m parameter. This parameter m can be varied to reflect the in situ soil behavior.

Pile-Soil Interaction

The interaction between the construction element and the soil is defined by their interface. The modeling of interface strength in Plaxis is a very basic way of describing the mechanism. A more thorough and fundamental approach is presented in paragraph 2.3.

In Plaxis this behavior is modeled by adding an interface to the construction element. This interface defines the amount of shear stress the soil can apply to the pile at different depths. The properties of this interface can be adjusted to suit a “realistic” behavior of the interaction. The general equation for interface strength is based upon equation [11] [Plaxis 2D v9.0 Reference Manual].

$$|\tau| \leq \sigma_n \tan \Phi_i + c_i \quad \textbf{[11]}$$

The strength of the soil can be reduced by implementing a factor R_{inter}. This factor will decrease the strength of the soil surrounding the structural element with the formulas described in equations [12] and [13]. These recalculated strength parameters are implemented into equation [11] and the interface strength can be determined.

$$c_i = R_{inter} * c_{soil} \quad \textbf{[12]}$$

$$\tan \Phi_i = R_{inter} * \tan \Phi_{soil} \quad \textbf{[13]}$$

2.2.2.3 Correlation between parameters

Settlement parameters determined from laboratory tests, such as the Bjerrum parameters, can be directly implemented or need some recalculation to support the constitutive model used. The correlation between the different parameters can be found in paragraph 4.2.3.

2.3 Pile Soil Interaction

Research done

The friction between construction elements and a soil body has been studied extensively. Several research projects have been done into this problem, both centrifuge testing [Chan, 2004] [Lam *et al*, 2008] as well as full scale testing [Fellenius, 2006] [Amini et al, 2008]. These papers present a reference situation with the soil parameters specified. After the centrifuge or full scale tests have been performed the results have been interpreted. Subsequent back calculation of α and β determines if these methods give reliable results. The parameters are discussed later in this paragraph.

2.3.1 Pile-soil Interface

The governing factor in the pile soil interaction strength is the interface between the two materials. Different physical modeling tests are done on this interface strength, both in 1g testing [Ovando-Shelley, 1994], [Sun et al., 2003] and [Mochtar and Edil, 1988] as well as Ng testing [Gorasia, 2012].

A fundamental explanation of the interface reaction is presented by [Reese, 1983]. He discusses the location of the failure plane, which is shown in Figure 8. The different influences on the interface reaction are discussed like installation effects, consolidation and roughness of the pile.

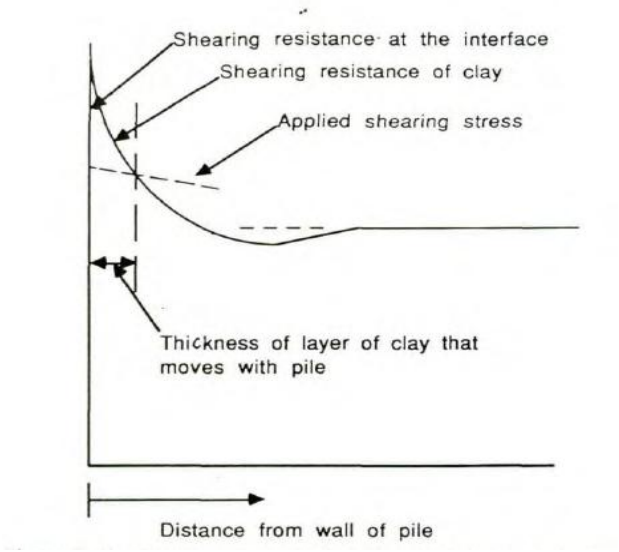

Figure 8: Conceptual curves for locating position of failure plane [Reese, 1983]

Interface behavior can also be studied in shear box tests [Ovando-Shelley, 1994] [Sun et al., 2003]. The top part of the box is filled with a soil sample and the bottom part with a representative construction material of certain roughness. This construction material can be anything, but most tests are performed on steel or concrete. The top part will be forced to move over the bottom part (thus the soil will be sheared over the construction material). Results are usually plotted together with a soil-soil shear test, this shows the loss of strength on the interface. The general trend seems to be that when the construction material has a rougher surface, the strength of the interface is higher as well.

[Mochtar and Edil, 1988] performed 1g tests on the interface between a stainless steel construction element, with varying surface roughness, and a clay sample. Different tests are performed by varying the model pile in both surface roughness and diameter, but also varying the preconsolidation pressure and effective stress of the clay sample. The results showed that the pile – clay friction angle is independent of vertical consolidation pressure or undrained shear strength. The surface roughness does influence the pile – clay friction angle clearly though, increasing up to the effective soil friction angle for rough piles.

The centrifuge tests on a model pile in kaolin clay performed by [Gorasia, 2012] study the effects of adding ribs on the pile interface, without adjusting the surface roughness of the interface. The pile head is loaded and will start displacing. Piles with different interfaces are tested and the difference between

the load – displacement reaction is measured. It can be seen that the ribs make the piles react more stiff (less displacement with the same load). The failure plane seems to be pressed into the soil by adding ribs to the piles.

2.3.2 Analytical Calculations

A generally accepted method for calculating floating piles is the neutral plane method [Fleming et al, 2009]. This method is based on the settlement of the soil surrounding the pile, and the settlement of the pile itself. The neutral plane is located where the relative displacement between the pile and the soil is zero. Above this point the friction will be negative, soil settles more than the pile. Below the neutral point the friction will turn positive. The soil will support the pile since the pile settles more than the soil. There is a transition zone where the negative friction decreases and the positive friction increases. The length of this transition zone depends on the differential settlement between the pile and the soil. The neutral plane and transition zone have been visualized in Figure 2.

Several methods have been produced to predict the amount of frictional forces the interface between the pile and soil can endure.

2.3.2.1 α-method [Total Stress Method]

The total stress method, also called the α-method, relates the undrained shear strength to friction. This is done with equation [14]. [Tomlinson, 1957] recognized a nonlinear value with a decreasing adhesion factor with increasing undrained shear strength.

$$\tau_{av} = \alpha * s_u \quad \textbf{[14]}$$

A lot of research has been done into the value of α, and which parameters influence it. Stress history, current in situ stress conditions, undrained shear strength and pile length effects have all been recognized as being an influence on the adhesion factor [Doherty and Gavin, 2011]. [Randolph and Murphy, 1985] did research into this factor, making it dependent on effective vertical stress and the undrained shear strength. This relationship has been adopted into several internationally accepted guidelines [API, 2005] [DNV, 1992].

Typical values for α in soft, slightly overconsolidated, clays are around 0.8 to 1. In stiff, overconsolidated, clays the value is typically lower and varies around 0.4 to 0.6 [Randolph and Gouvernec, 2011].

2.3.2.2 β-method [Effective Stress Method]

To avoid the uncertainties and inaccuracies of the total stress method, the effective stress method was introduced by [Burland, 1973]. This method directly translates the effective vertical stress to the friction strength as can be seen in equation [15]. The beta value is related to the friction angle and the coefficient which relates the vertical to the horizontal stress, which is shown in equation [16].

$$\tau_f = \beta * \sigma'_{v0} \quad \textbf{[15]}$$

$$\beta = K_f * \tan\delta \quad \textbf{[16]}$$

This effective stress method has been adopted for cohesionless soils in the [API, 2005] [DNV,1992] guidelines. But they are used to predict pile soil interaction problems for cohesive soils as well [Burland, 1993] [DNV, 1992] [Tomlinson and Woodward, 2008]. Research supports the use of the effective stress method in cohesive soils [Mochtar and Edil, 1988].

A problem with this method is the prediction of horizontal stresses in the soil, even before installation of the pile. Especially in overconsolidated soils this gives a lot of variation in the value of β. For soft, slightly overconsolidated, clays the β value varies between 0.8 and 1.2. The values in stiff, overconsolidated, clays are low and vary around 0.2 and 0.3 [Randolph and Gouvernec, 2011].

2.3.2.3 API

Guidelines for the calculation of axial capacity have been given by the American Petroleum Instute [API, 2005]. The preferred method for cohesive soils given in this guideline is the total stress method mentioned earlier in this report. The effective stress method is the preferred method for non cohesive soils.

CPT based methods are introduced in the latest version of the API for the prediction of shaft capacity. The UWA-05 [Schneider *et al*, 2008], the FUGRO-05 [Kolk *et al*, 2005] and the ICP-05 [Jardine *et al*, 2005] are all methods based directly on the cone penetration resistance. These methods also take length effects into account.

Besides the interface reaction also a soil reaction to axially loaded piles is given. The soil reaction will be an upper limit, since the axial capacity cannot become higher than the strength of the soil. If the interface has not failed when the maximum soil strength is reached the soil will fail and the pile will be displaced anyway. The soil reaction is modeled in a t-z curve.

2.3.3 Numerical Calculation

Besides the calculation with Plaxis the pile-soil interaction can be modeled with Mpile as well.

2.3.3.1 Mpile

Developed by Deltares, this is a software program especially focused on piles. They can either be loaded laterally or axially.

Prescribed t-z curves (for axial loading) or p-y curves (for lateral loading) can be specified for different depths of the soil. The t-z curves are soil specific and interface elements should describe the reaction of the soil accurately.

2.4 Geotechnical Centrifuge modeling and scaling

2.4.1 General

Modeling geotechnical problems in a centrifuge has several major advantages:

- Subjecting the sample to higher acceleration levels;
- Process which under 1g take years to complete are now finished in several hours;
- Stress levels are increased.

Besides the advantages there are some downsides to geotechnical modeling:

- Non uniform acceleration level over the sample;
- Conflicting scaling laws inside one test.

The technique was first recognized as useful by Edouard Philips in 1869 [Taylor, 1995] who recognized the importance of self-weight body forces in geotechnical problems. It still took until 1931 before a centrifuge test was really reported as being executed. The test was done by Philip Bucky at the Columbia University on the stability of mine roof structures. After that evidence suggests centrifuge testing being done in the USSR, but this is unclear because of the Second World War and the 'iron curtain' erupted after this.

Different centrifuges are used to model geotechnical problems [Muir Wood, 2004] and [Taylor, 1995]. The most used variant is the beam centrifuge which consists of an arm and two gondolas. The samples can be installed horizontally in the gondola. The arms will be spun around with a certain rotations per minute. The gondola will be swung outside and is placed horizontally when the rotations per minute are high enough. Normally this will be done horizontally to keep the amount of acceleration on the sample constant. If this is done vertically gravity will have an influence on the acceleration making it variable. There would be a difference in acceleration level between top and on the bottom of the sample depending on the exact geometry and acceleration level.

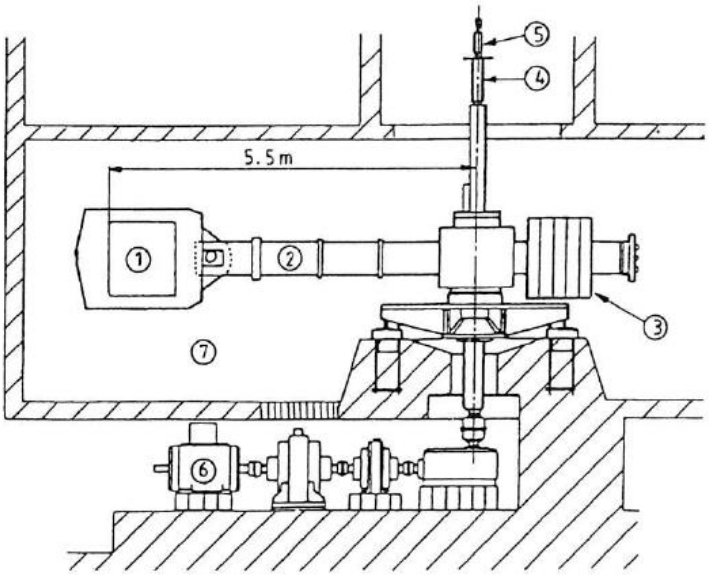

Figure 9: Overview of a beam centrifuge [Muir Wood, 2004]

Besides a beam centrifuge there is also a drum centrifuge. A drum centrifuge will spin in a channel around its axis. This means a container around its full circumference, making it very capable of modeling problems over an extended area. Drum centrifuges have some major disadvantages compared to beam centrifuges though. The radius in a beam centrifuge is smaller. The weight that needs to be activated is bigger which costs more energy. Another problem is that sample preparation, which needs to be done during flight during preparation the axis of acceleration is turned compared to the "in flight"

acceleration axis. If smaller boxes are placed in the channel this means that the sample will be installed vertically and it needs to be kept in place before the test is started.

2.4.2 Scaling

Physical model tests have the advantage over in situ tests that boundary conditions are more easily determined and controlled. Full scale tests can be done in a laboratory but are difficult in both space and cost perspective. Therefore physical model tests are usually scaled down, e.g. 1g tests or geotechnical centrifuge tests.

A geotechnical centrifuge can be used to increase the amount of acceleration imposed on a sample. By increasing the acceleration several mechanisms are scaled favorably, i.e. unit weights and therefore stresses are scaled up. [Muir Wood, 2004] and [Taylor, 1995] discussed the influence of scaling extensively and a list of scaling laws for different mechanisms is presented in Table 2. The scaling laws applicable to the problem posed in this research will be given some more attention.

2.4.2.1 Dimensions / Stress

Newtons second law dictates that force is directly related to the mass of a sample times the acceleration posed on it ($F = m*a$). Stress is force per unit area of surface ($\sigma = F / A$), therefore a linear relation between acceleration and stress can be found. By scaling up the acceleration, the stress representative in a prototype is scaled down by n times in the model [Muir Wood, 2004].

2.4.2.2 Strain

Strain is dimensionless (displacement divided by length). Both these quantities scale by n and thus strain itself does not scale.

2.4.2.3 Time (Diffusion)

The consolidation process which is a focus point in this research is a diffusion event. The scaling of this mechanism is discussed in both [Muir Wood, 2004] and [Taylor, 1995]. In both literature the scaling is subject of some debate, though the same conclusion is reached every time. The drainage length is decreased by the scaling of dimensions. Besides that also the seepage flow of water is scaled due to an increase of acceleration. This leads to a scaling of the consolidation time of $1 / N^2$, as can be found in Table 2.

Table 2: Scaling laws

quantity	scaling factor
length	$1 / n$
mass density	1
acceleration	n
stress	1
force	$1 / n^2$
strain	1
displacement	$1 / n$
time (diffusion)	$1 / n^2$
time (creep)	1

3 Soil Profile

The reference project, which initially triggered this research, is located in the Northern Caspian Sea. An overview of its geological history is given. Besides that extensive site investigation has been performed on this reference site, which is studied and a summary of this is given. Finally a reference soil model will be set up from the study of the geological history and the site investigations done.

3.1 Geology

3.1.1 General

The Caspian Sea is located in the western part of Asia. It is bordered by several countries such as Russia, Kazakhstan, Turkmenistan, Iran and Azerbaijan. The sea is the largest enclosed body of water in the world by surface, spreading an area of 371,000 km^2.

The basin has no outflows and is fueled by several fluvial systems. The largest inflow of water comes from the Volga on the north side, which contributes more than 80% of the total inflow. Other fluvial systems draining into the Caspian Sea are the Ural and Kura rivers. Due to the current inflow of fresh waters from the Volga and Ural, the northern part of the Caspian Sea has become a freshwater lake. The southern part, on the Iranian shore, is more saline due to a lack of inflow on this side [Golubev, 1998].

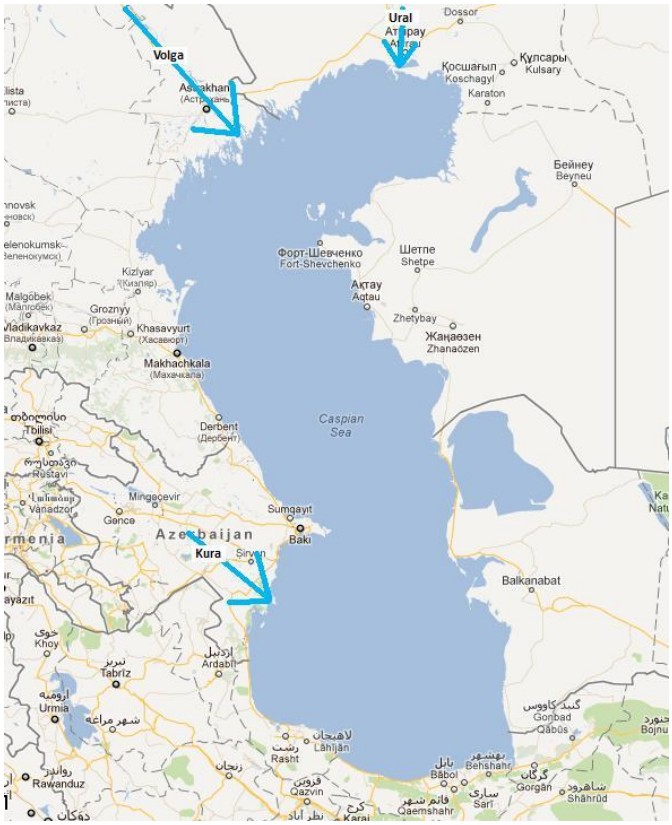

Figure 10: Location of Caspian Sea and major rivers [Google Maps]

The Caspian Sea is a structurally complex basin, which can be divided into three different parts. The northern part of the basin has a shallow water depth, an average of 5 – 6 meters with a maximum depth of 15 meters. The middle basin has an average depth of 170 meters and a maximum up to 790 meters.

The southern basin is the deepest one, with an average depth of 325 meters, maximum depth of 1,025 meters [Dolukhanov, 2009].

3.1.2 Geological History

The basin has been subjected to various sea level changes over the last decades. In more recent years a variation of water level in the Caspian Sea has been recorded of about 5 meters [Dolukhanov, 2009]. This means that some parts of the Northern area were dry and exposed to the open air. Alluvial deposits may have formed in these years and could well be encountered during a site investigation. Alluvial deposits could consist of silt or fine sands.

Different time periods which have had a large influence on the deposition pattern of the subsoil in the Caspian Sea can be found in Table 3.

Table 3: Different geological time periods [Mamedov, 1997]

Late Khazarian	110ka – 75ka	Transgression (sea level rise)
Atelyian	75ka – 32ka	Regression (sea level decrease)
Early Khavalynian	32ka – 24ka	Transgression
Yenotavian	24ka – 17ka	Regression
Late Khvalynian	17ka – 8ka	Transgression
Mangyshlak	8ka – 5ka	Regression
New Caspian	5ka – present	Transgression / Regression
ka = kiloannum (thousand years ago)		

Transgression means periods with a high mean sea level. Higher water levels will flood large areas and give the Caspian Sea the opportunity to create uniform deposits. Inside the sea itself there is a low energy zone, this will lead to deposition of small (light weight) particles. The soft soil layers in the Caspian Sea have thus been deposited during transgression periods [Mamedov, 1997].

Regression is the opposite of transgression. The mean sea level is low and the shallow sea bottom will be exposed to open air. This leads to removal of the top layers by erosion. The extend of erosion depends on the duration of the regression time period, and the environment to which the soil is exposed.

The soft soil to which this project is exposed is most probably from the time period of the “Late Khvalynian”. This is a period of transgression (deposition) followed by the “Mangyshlak” period. This is a relatively short period of regression. This means a short period of erosion for the layers formed in the “Late Khvalynian”.

3.2 Site Investigation

Extensive site investigation has been done at the reference project [Fugro, 2011]. An elaborate study has been done on the reports and the varying soil properties and parameters which come from this.

The tests performed in this site investigation are the following:

- Boreholes and CPTs;
- Laboratory tests
    - Classification testing
    - Strength testing
    - Compressibility testing
- Interface tests

3.3 "Caspian" soil profile

The tests performed in the site investigation, and the interpretation of these results can be found in Appendix A. In this paragraph the profile which is constructed from the interpretation of this site investigation is introduced.

The dimensions for the soil profile can be found in Figure 11 and Table 4. The appropriate soil properties and parameters per layer are presented in Table 5 and Table 6.

The stiffness of the different layers is calculated with the compression parameters. The rock fill introduced in the problem will cause an extra overburden pressure, and with equations [17] and [18] [Terzaghi *et al*, 1996] the settlement is calculated. With the settlement and stress increase known the stiffness of the soil can be calculated according to equations [19] and [20].

$$\Delta H_{ur} = \frac{C_r * H}{1 + e_0} \log \frac{\sigma'_{v0} + \Delta p}{\sigma'_{v0}} \qquad \text{for} \qquad \sigma'_{v0} + \Delta p \leq \sigma'_p \qquad [17]$$

$$\Delta H_c = \frac{C_c * H}{1 + e_0} \log \frac{\sigma'_{v0} + \Delta p}{\sigma'_{v0}} \qquad \text{for} \qquad \sigma'_{v0} + \Delta p > \sigma'_p \qquad [18]$$

$$E_{ur} = \frac{\Delta \sigma}{\Delta H_{ur} / H} \qquad [19]$$

$$E_{drained} = \frac{\Delta \sigma}{\Delta H_c / H} \qquad [20]$$

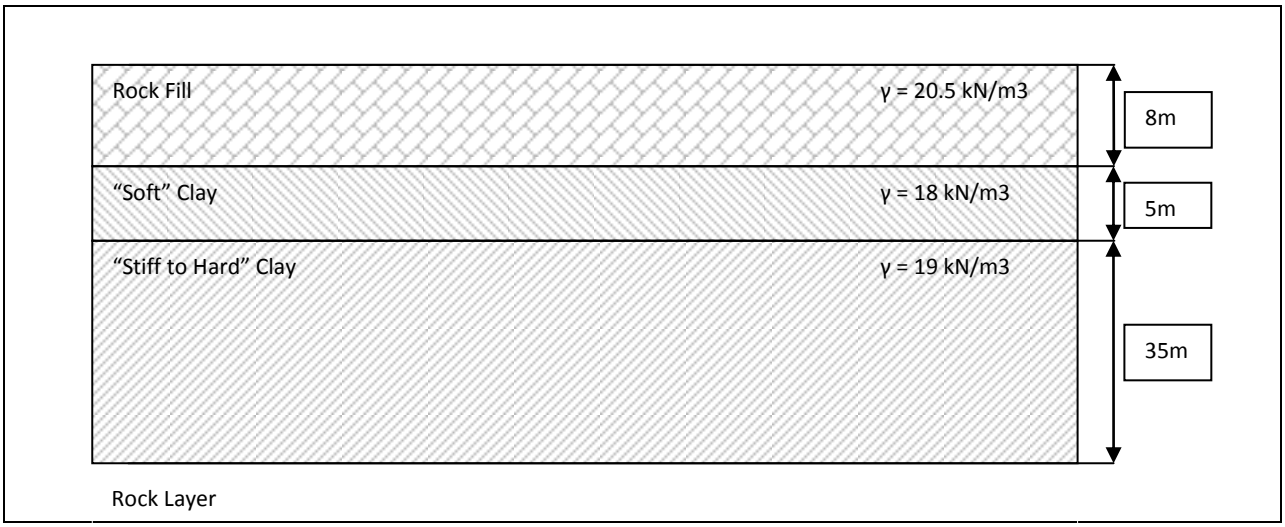

Figure 11: Soil Profile

Table 4: Dimensions of Soil Profile

	Soil Layer	Top [m + RL*]	Bottom [m + RL*]	Thickness [m]
I	Rock fill	+8	0	8
II	"Soft" Clay	0	-5	5
III - IV	"Stiff to Hard" Clay	-5	-40	35
V	Calcilutite Rock Layer	-40	-	-

*** RL = Reference Level**

Table 5: Soil properties specified for the general profile per soil layer

Layer	γ [kN/m^3]	c [kN/m^2]	ϕ [^{o}]	ν [-]	k_v [m/s]	POP [kN]	c_u [kN/m^2]
I	20.5	-	-	-	-	-	-
II	18	8	29	0.3	1.0e-8	0	15
III - IV	19	15	29	0.3	1.0e-10	400	top: 50 bottom: 200
V	-	-	-	-	-	-	

Table 6: Soil parameteres specified for the general profile per soil layer

Layer	Compression [-]	Recompression [-]	Secondary Compression [-]	Initial Void Ratio [-]	Porosity [-]	Stiffness E_{ur} [kN/m^2]	Stiffness $E_{drained}$ [kN/m^2]
I	-	-	-	-	-	-	-
II	0.34	0.08	N/A	1.00	0.50	3500	800
III – IV	0.22	0.07	N/A	0.75	0.44	13000	4000
V	-	-	-	-	-		

4 Consolidation Calculation

This chapter will present the predicted response of the consolidation of a single and multi-layer system. A one layer situation is created to check the performance of the different calculation models. This model is called the “Benchmark” soil profile.

A two layer model, based on the “Caspian” soil profile introduced in chapter 3, is set up. This two layer model will be installed in the centrifuge and will differ from this earlier specified model. This model has been named the “Centrifuge” soil profile.

4.1 Calculation Models

Calculations are done by hand, Msettle and Plaxis. The calculations will result in several plots; settlement – depth, settlement – time and consolidation – time. The settlement with depth and time are compared to the measured values in the centrifuge, and will be presented in another chapter.

The hand calculation of settlement with depth is done with the Bjerrum formula. For the consolidation in time the formula given by [Terzaghi, 1925] is used. The solution to this differential equation is given by [Verruijt, 2001] and is presented in equation [21]. Msettle is used with Darcy consolidation and the Bjerrum settlement formulas. The different constitutive models used in Plaxis are: Hardening Soil, Soft Soil and Modified Cam Clay.

$$\frac{p}{p_0} = \frac{4}{\pi}\sum_{j=1}^{\infty}\frac{(-1)^{j-1}}{2j-1}\cos\left[(2j-1)\frac{\pi}{2}\frac{z}{h}\right]exp\left[-(2j-1)^2\frac{\pi^2}{4}\frac{c_v t}{h^2}\right] \qquad \textbf{[21]}$$

The soil properties and parameters implemented into the different calculation programs, Msettle and Plaxis, have been implemented in the appendices. Appendix C shows the Msettle input for the “benchmark” profile, where Appendix D gives the input for the “centrifuge” soil profile in Msettle. Appendix E presents the Plaxis input for both profiles and all the constitutive models used.

4.2 “Benchmark” Soil Profile

A benchmark situation has been created to compare the different calculation methods to each other. Differences in results between the models can be evaluated and a model can be selected to predict the settlements in the centrifuge.

4.2.1 Geometry

The geometry used for the benchmark calculations is presented in Figure 12. As can be seen here the sample has been given a width of 100 meters, and a height of 10 meters. The amount of surcharge added on top of the sample is 100 kPa.

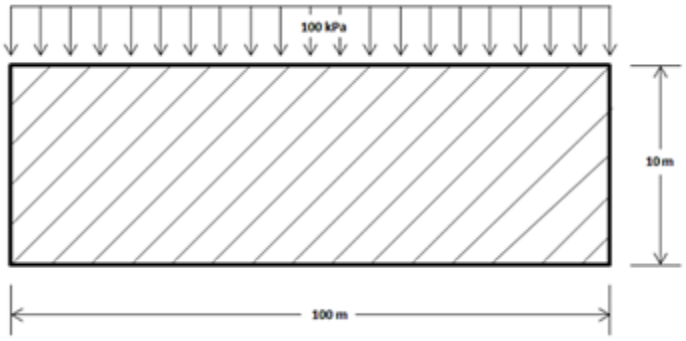

Figure 12: Geometry of benchmark situation

The side boundaries have been fixed in horizontal direction, the bottom is fixed in both horizontal and vertical direction. Besides that the sides and bottom boundaries have been made impermeable, thus drainage of excess pore pressures can only occur at the topside.

4.2.2 Properties and parameters

The soil properties and parameters which have been implemented into the different calculations can be found in Table 7.

Table 7: Soil Properties [Benchmark Situation]

	γ_{dry}	γ_{wet}	γ_{water}	ϕ	c	e_0	ν_{ur}	K_0	k_v
	[kN/m2]	**[kN/m2]**	**[kN/m2]**	**[^{0}]**	**[kN/m2]**	**[-]**	**[-]**	**[-]**	**[m/s]**
HC	18	18	10	-	-	1	-	-	3e-9
Msettle	18	18	10	-	-	1	-	-	3e-9
Pl – SS	18	18	10	29	15	1	0.2	0.515	3e-9
Pl – CC	18	18	10	29	15	1	0.2	0.570	3e-9
Pl – HS	18	18	10	29	15	1	0.2	0.515	3e-9

4.2.3 Recalculation of compression parameters

The compression parameters for the analytical calculations have been determined from different laboratory tests. These parameters are different than those required for Plaxis calculations and need to be recalculated. The parameters used in the material models are presented in Table 8.

Table 8: Compression parameters used in different methods

Method	**Compression**	**Recompression**
Hand Calc	C_c	C_r
Msettle	C_c	C_r
Plaxis		
Soft Soil	λ	κ
Modified Cam Clay	λ *	κ*
Hardening Soil	E_{50} / E_{oed}	E_{ur}

The recalculation of the one dimensional Bjerrum compression parameters into lambda and lambda* can be found in Table 9, the recompression parameters have been presented in Table 10. Table 11 shows the parameters used in the calculations. The recalculation of these parameters have been done with formulas given in [Plaxis 2D, Material Models Manual].

Table 9: Relation between compression parameters [Plaxis 2D, Material Models Manual]

	C_c	λ	λ^*
C_c	$= e / \log \sigma'_v$	$= C_c / \ln(10)$	$= C_c / (\ln(10) * (1+e_0))$
λ	$= \lambda * \ln(10)$	$= e / \ln p'$	$= \lambda / (1+e_0)$
λ^*	$= \lambda^* * (\ln(10) * (1+e_0))$	$= \lambda^* * (1+e_0)$	$= \varepsilon_v / \ln p'$

Table 10: Relation between recompression parameters [Plaxis 2D, Material Models Manual]

	C_r	κ	κ^*
C_r	$= e / \log \sigma'_v$	$= 2 * C_r / \ln(10)$	$= 2 * C_r / (\ln(10) * (1+e_0))$
κ	$= ½ * \kappa * \ln(10)$	$= e / \ln p'$	$= \kappa / (1+e_0)$
κ^*	$= ½ * \kappa^* * (\ln(10) * (1+e_0))$	$= \kappa^* * (1+e_0)$	$= \varepsilon_{vol} / \ln p'$

Table 11: Compression parameters used in calculations

	C_c		C_r
Hand Calculation	0.3		0.08
Msettle	0.3		0.08
Plaxis; Soft Soil	**λ**		**κ**
	0.1304		0.0696
Plaxis; Modified Cam Clay	**λ^***		**κ^***
	0.0652		0.0348
Plaxis; Hardening Soil	**E_{50}**	**E_{oed}**	**E_{ur}**
	[kN/m2]	[kN/m2]	[kN/m2]
	1916.67	1533.33	5175.00

The Bjerrum compression parameters are plotted in "$\varepsilon_v - \sigma'_v$" space. This means determination of these parameters is done in one dimensional space. The parameters are determined from oedometer tests, which are relatively easy and fast to perform. In this test only the vertical stress is determined (weight on top of sample). Deformations can only happen in vertical direction, as a result the volumetric strain is governed by the vertical displacement of the sample. The Cam Clay and Soft Soil parameters however are plotted in volumetric strain – mean stress space. The difference between mean stress (p') and vertical stress (σ'_v) is that the mean stress is also influenced by the horizontal stress. In the Plaxis models the change in volumetric strain is also governed by the change in horizontal strain.

Since in virgin compression the horizontal stress is increasing together with the vertical stress this does not influence the results that much in compression. In recompression though, the horizontal stresses in the soil will remain even after the preconsolidated (vertical) stress has been removed. This means that the mean stress will differ from the vertical stress and the reloading paths will differ from each other. Especially in low stress zones this influence is significant.

4.2.4 Results

Results of the calculations performed are presented and discussed in chapter 6.

4.3 "Centrifuge" Profile

The soil profile which is tested in the centrifuge has some limitations. To estimate the settlements correctly a special soil model has been set up. The soil model will predominantly be based on the height restrictions in the centrifuge. The soft clay layer has been given a height of 5 meters, but the thickness of the stiff clay layer will need to be reduced to fit the strongbox.

4.3.1 Geometry

The profile tested in the centrifuge is projected in Figure 13. This is the prototype model, which is scaled up to an acceleration level of 100 g.

The preparation of this sample is described in paragraph 5.4. It can be seen in this paragraph that the soft and stiff clay layers are actually in compression and recompression respectively.

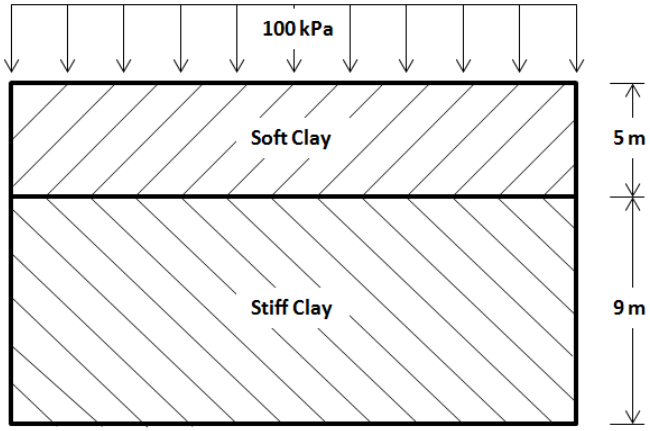

Figure 13: Geometry of "Centrifuge" Profile

4.3.2 Properties and parameters

The centrifuge tests are performed on kaolin clay. To determine the properties of this particular kind of clay several laboratory tests have been performed. These are presented in paragraph 5.7.1 and implemented in the calculations as well.

The properties which are implemented into the calculations can be found in Table 12. The compression parameters have been recalculated where this was needed. This is done through the method specified in paragraph 4.2.3.

Table 12: Soil properties and parameters in "Centrifuge" soil profile

Layer	γ [kN/m^3]	c [kN/m^2]	ϕ [°]	ν [-]	k_v [m/s]	POP [kN/m2]	Cc [-]	Cr [-]
I	20	-	-	-	-	-	-	-
II	18	8	29	0.2	3.0e-9	0	0.30	0.08
III - IV	18	15	29	0.2	3.0e-9	200	0.30	0.08
V	-	-	-	-	-	-	-	-

4.3.3 Results

Results of the calculations performed are presented and discussed in chapter 7.

5 Centrifuge Modeling

5.1 Centrifuge Specifications

The geotechnical centrifuge at the TU Delft used for consolidation is limited in its dimensions. Figure 14 shows a schematization of half of the centrifuge. The general test setup including the camera and strongbox are presented. A photo showing the real situation is added in Figure 15.

The specifications of the centrifuge are given in Table 13. The values given in the table specify the maximum, the centrifuge can also spin at lower RPM.

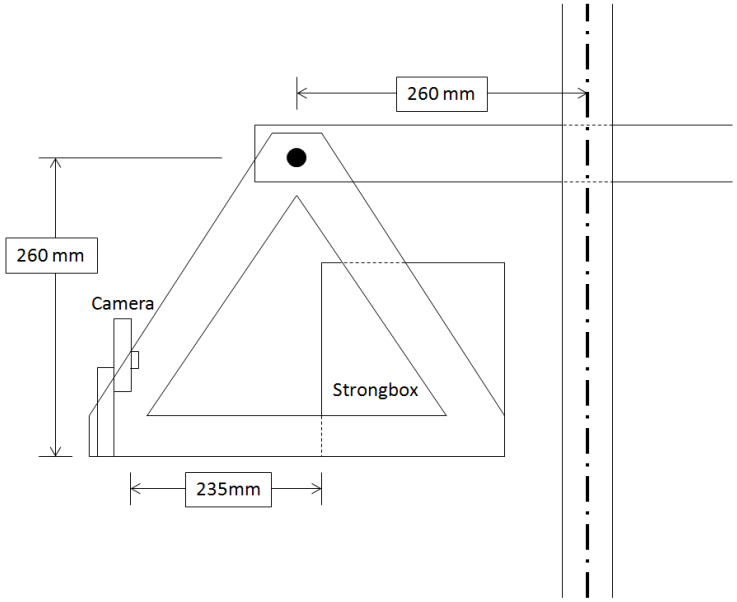

Figure 14: Schematization of the test setup

Figure 15: Picture of the Geotechnical Centrifuge

Table 13: Specifiations centrifuge and camera

Centrifuge properties		
Angular velocity	[rpm]	420
Arm length	[m]	.52
Camera properties		
Frame rate	[fps]	6
Resolution	[pixel]	2520x1940

5.1.1 Limitations

Besides many benefits of centrifuge testing there are also some limitations. Not all of these limitations have a large impact on the tests itself but are still to be considered.

5.1.1.1 G force diminishing over height

The amount of acceleration the sample is submitted to, will not be uniform over height. Since the acceleration is calculated in the following way:

$$N = \frac{\omega^2 * r}{g} \qquad [22]$$

In equation [22]; ω stands for the angular velocity, r is the arm and g is the gravitational acceleration. The angular velocity and the gravitational acceleration are constants, but the arm will vary. The distance between the top of the sample and the center point of the centrifuge will be smaller than the distance to the bottom of the sample. The arm will thus increase over the height of the sample, which means the acceleration will increase in depth.

The difference in acceleration can be seen in Table 14. The bottom of the sample is at 0.52 meter, where the top is at 0.35 meter. Figure 16 shows the vertical stresses in the depth of a profile. The vertical stresses in the model and its representative prototype, calculated with a constant acceleration of 100g, are presented. As can be seen in the graph the stresses in the model vary from the prototype sample.

Table 14: Arm length versus amount of acceleration

arm	acceleration
[m]	***[g]***
0.52	100.6
0.5	96.7
0.45	87.0
0.4	77.4
0.3	58.0

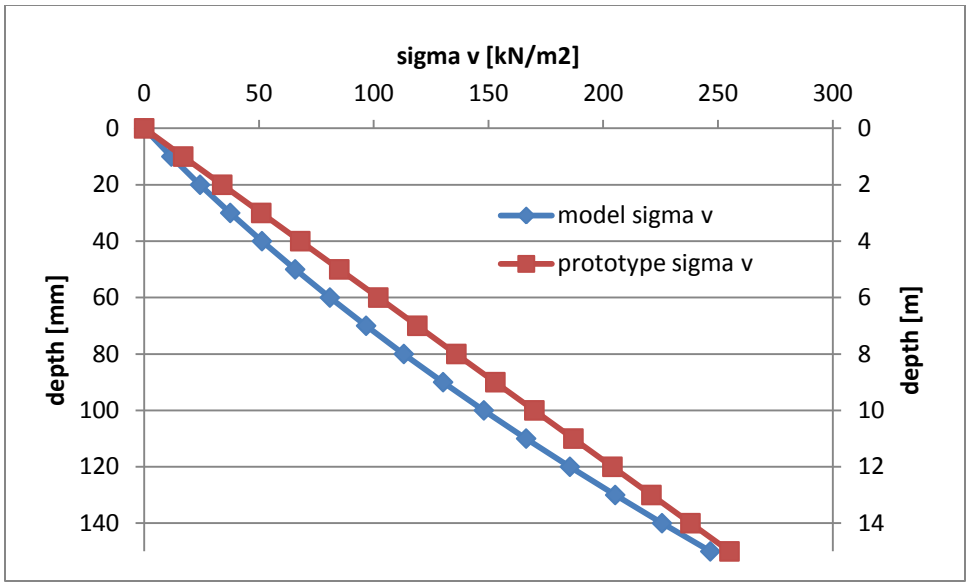

Figure 16: Vertical stresses due to own weight over depth

5.1.1.2 Soil Tested

The in situ soil cannot be imported from Kazakhstan, thus another type of clay must be used. The most used type of clay in the laboratory is kaolin clay. A powder is mixed with de-aired water to create slurry which contains only clay particles and water. Figure 17 shows the prepared slurry before it is poured into the strongbox. In Figure 18 the slurry has been poured into the strongbox and is ready to be put in the centrifuge.

The kaolin sample will be tested and its properties and parameters are determined. This outcome is compared to the in situ data, which has been tested extensively and has been presented in Appendix A.

Figure 17: Prepared Slurry

Figure 18: Strongbox ready to be tested

5.2 Strongbox Specifications

The strongboxes used for testing the clay samples are limited in height and width due to the gondola in which they are placed. Figure 19 and Figure 23 show pictures of one of the tested strongboxes, both outside the centrifuge and placed in the gondola.

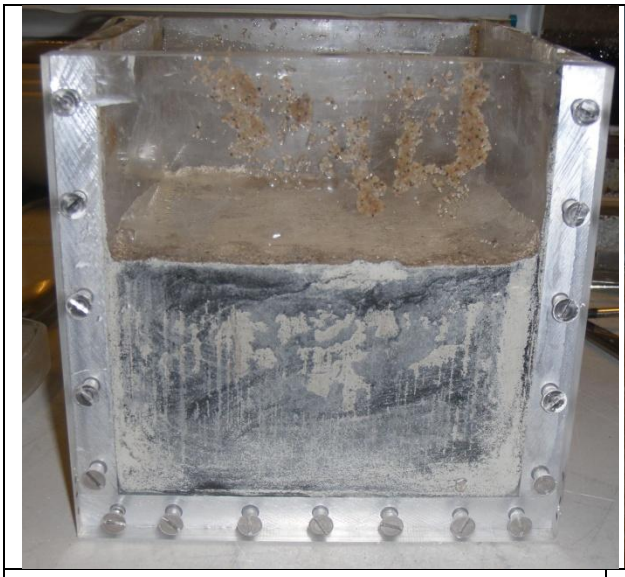

Figure 19: Side view of a strongbox

Figure 20: Strongbox placed in the centrifuge

The specifications of the strongboxes used can be found in Table 15. The strongbox is constructed of aluminium, with two sides made out of transparent Plexiglas. The transparent sides will be pointed towards the camera so measurements can be done on the clay sample inside the strongbox.

Table 15: Strongbox Specifications

		Strongbox 1	Strongbox 2
outside			
height	*[mm]*	200	200
width	*[mm]*	180	180
depth	*[mm]*	180	180
inside			
height	*[mm]*	185	185
width	*[mm]*	150	150
depth	*[mm]*	150	150
weight	*[kg]*	4.421	4.405

5.3 Test Setup

So far the specifications of the centrifuge and the strongboxes have been provided. Other parts of the test set up are:

- Camera; This camera will record the reaction of the soil to the loading.
- Laptop; The laptop will be located outside the centrifuge and is used to set up the camera and start / stop it. The captured images will be saved on this laptop.
- Router; The router is needed to provide a connection between the camera and laptop.
- Lighting; When the lit is closed the centrifuge will be dark. To get images lighting will be needed. The lighting will be attached to the gondola to create a constant lighting.

An overview of the test setup is given in Figure 21. The router and camera are placed inside the centrifuge. They are powered from a separate power supply via the slip rings on the centrifuge axis. The camera is wired to the router and mounted on one of the gondolas. The camera control is performed at a safe distance with the laptop, placed behind a brick wall. The laptop is connected to the wireless network broadcasted by the router. Through this network the images, made by the camera, are transferred to the laptop and commands are send to the camera.

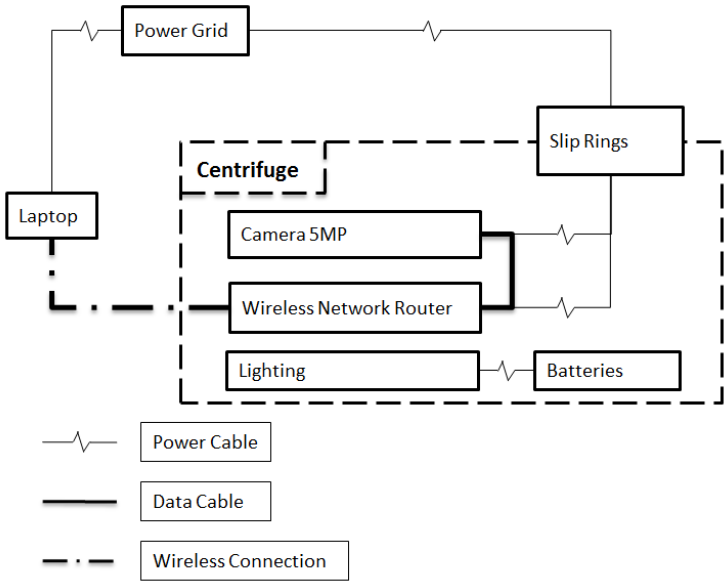

Figure 21: Overview of the Test Setup

Lighting is added in the centrifuge, but it is not connected to the power grid. The lights are powered by batteries, so they are a standalone part of the entire setup.

5.4 Sample Preparation

Before a test can be performed the sample needs to be carefully prepared. An overview on the preparation of the test samples is given in this paragraph. The dimensions of the used strongboxes can be found in paragraph 5.2.

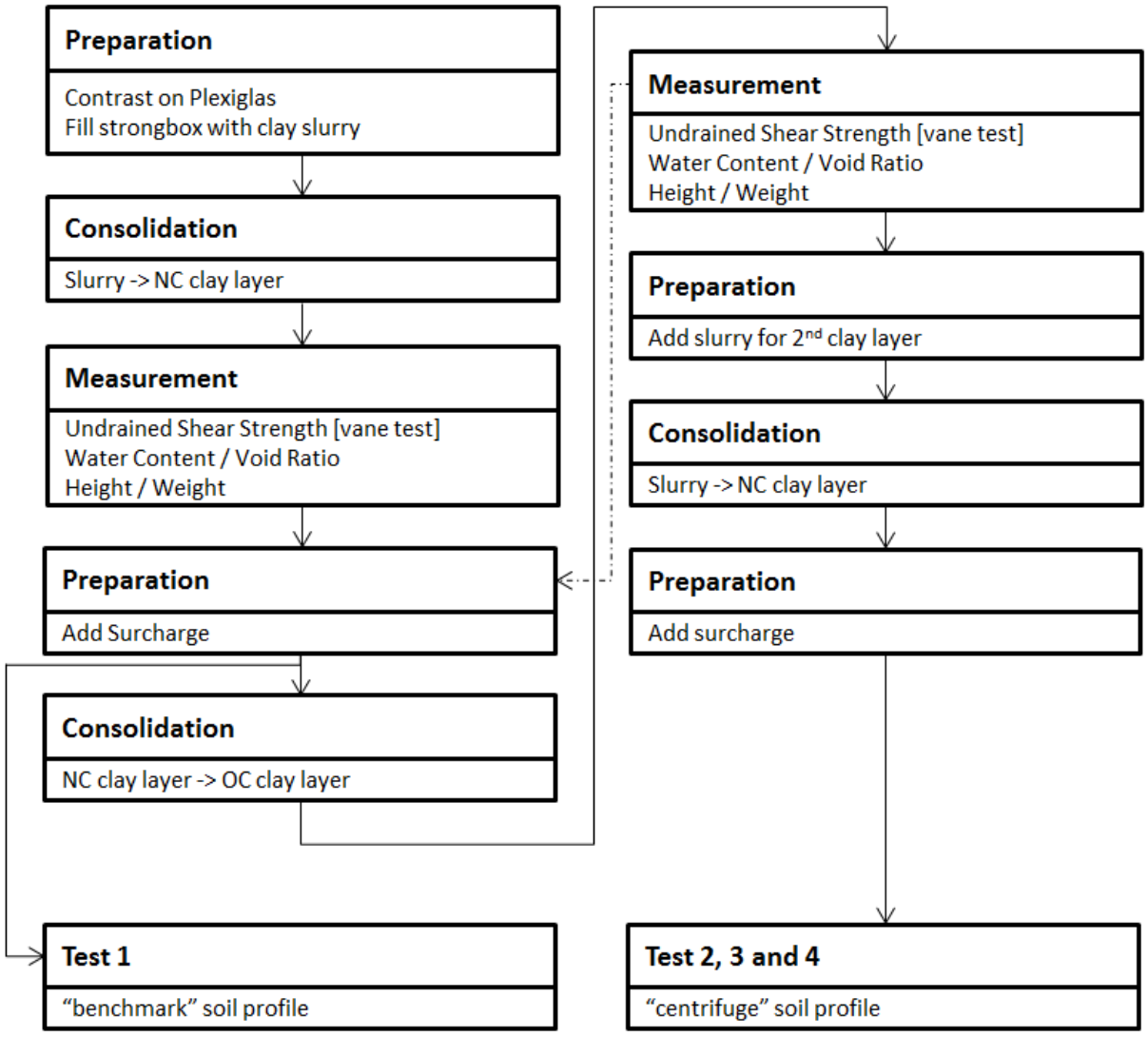

Figure 22: Test Procedure

Figure 22 shows how the sample is prepared before a test is performed. The executed tests on the "centrifuge" soil profile, which comprises of two soil layers, requires more preparation than the tests on the "benchmark" soil profile with one soil layer. The first preparation stage consists of preparing the strongbox. The contrast material, needed for capturing the displacements with the camera is added on the Plexiglas with the help of Vaseline grease. A prepared strongbox with the slurry added can be found in Figure 23.

The next step is to add a surcharge on the soil sample. This is done with weights and sand as pictured in Figure 24. This profile is tested as the "benchmark" situation. To prepare the sample for the next tests this step can be repeated several times, to reach the required Pre Overburden Pressure.

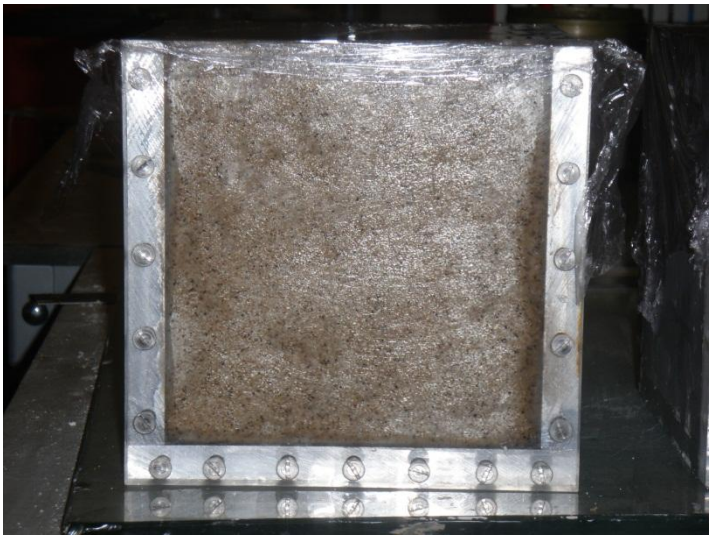

Figure 23: Strongbox with contrast and slurry

Figure 24: Sample with load

When this first layer has had its required overburden a new layer of slurry is added. The entire sample is consolidated again, to create the 2 layer system with an overconsolidated and a normally consolidated clay layer. On these samples the second set of tests can be performed.

5.5 Data capturing and processing

When the prepared sample is installed in the centrifuge the camera is started as well. The centrifuge will build up to 420 revolutions per minute, which is equivalent to about 100g acceleration in the sample. Through the laptop the camera will be set up to capture images at a predetermined time step, subsequently the images are stored on the laptop.

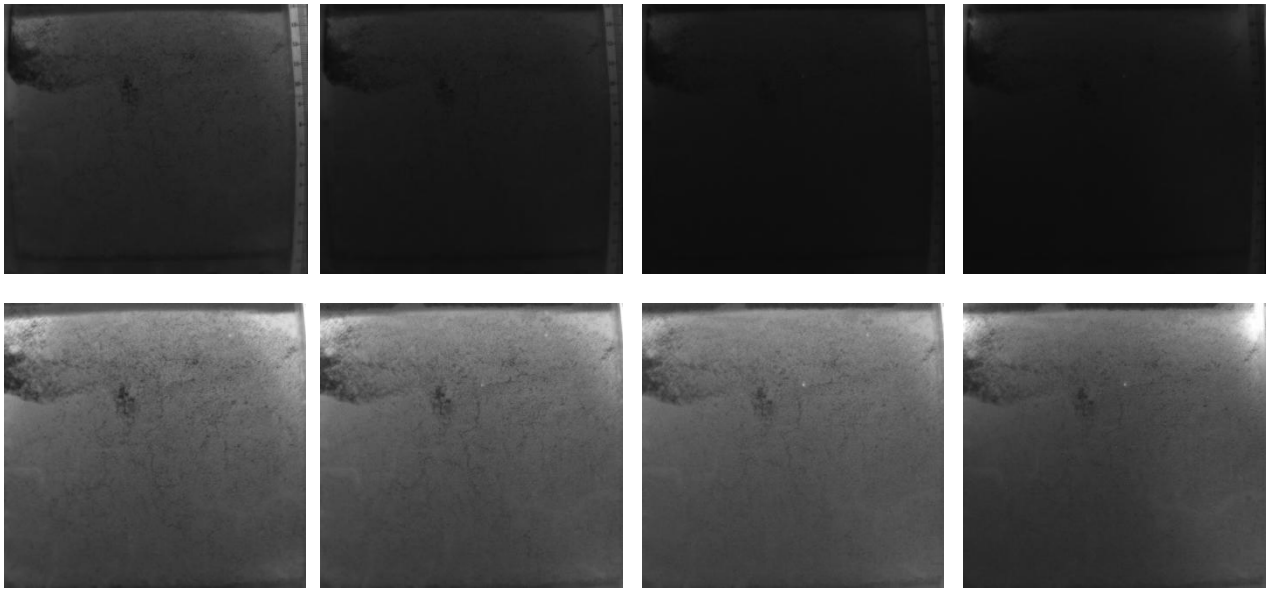

Figure 25: Pictures taken before and after processing

The images taken directly out of the centrifuge also contain parts of the strongbox, which is of no interest to this research. The images are cropped to contain only the parts of interest, e.g. the clay

sample. The contrast is adjusted so that they are ready to be analyzed. Figure 25 shows eight pictures. The top four are raw images as they are taken by the camera. Below these raw images the same pictures are added after processing.

The deformations between the images are determined with JPIV [http://www.jpiv.vennemann-online.de/] a software package for Particle Image Velocimetry (PIV). With this technique the displacements between two consecutive images can be found. Examples of the output can be found in Figure 26, which shows JPIV results of test 1. The left image is the result of a comparison between image 4 (40 minutes into the test) and image 5 (50 minutes into the test). It can be seen that the settlement is focused on the top part of the soil layer, because drainage occurs on this side. The right image is a cross-correlation of image 11 (2 hours into the test) and image 12 (3 hours into the test). Settlements penetrated deeper down in the sample, and because the interval between the images is increased the magnitude of the displacement is increased as well.

Also interesting to see in Figure 26 is the lack of contrast at some points in the sample. The contrast is not uniform over the entire clay layer and this leads to zones where particle tracking is unreliable or even impossible, leading to stray vectors in the output.

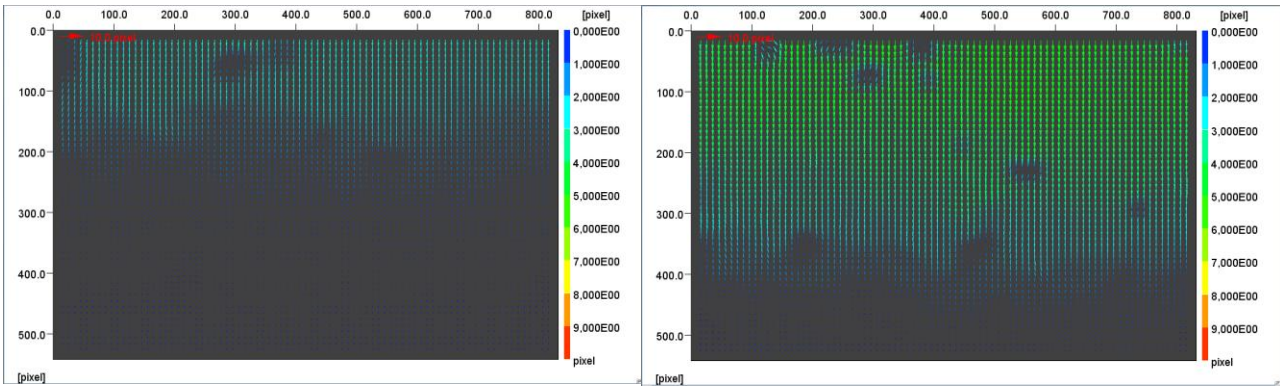

Figure 26: JPIV output

The output given by JPIV is imported into Matlab for further processing. Since JPIV gives output of settlement between 2 different images these should be summed up. By summing up the different JPIV output files the total settlement over depth can be plotted.

The JPIV output images of test 1, on the “benchmark” soil profile, have been presented in Appendix F. These images show the settlement occurring through the sample from start to the end of consolidation, where no more settlements occur.

In the presented results, six neighbouring columns of the grid in the JPIV analysis are selected, spanning an area of about 15 mm width and the total height of each sample. The different columns are averaged for the settlement readings. Zones with lack of contrast, which lead to disturbance in the measurements, are hereby smoothed.

5.6 Test Schedule and Measurements

With the data available different information on the settlement of the clay sample can be acquired. The settlement in depth will be evaluated. The settlement in time can be acquired as well. The time step between the different pictures is known, and the amount of settlement at a certain depth can be taken from the data available.

No pore pressure transducers have been installed, as a result the pore water dissipation during consolidation is not measured.

The test details of the different performed tests are presented in Table 16. Test 2 has been mentioned in this overview, but unfortunately no displacement data could be gathered from these measurements.

Table 16: Different Centrifuge Tests Performed

Soil Profile	**Test 1** "benchmark"	**Test 2** "centrifuge"	**Test 3** "centrifuge"	**Test 4** "centrifuge"
Settlement - Depth	x	-	x	x
Settlement - Time	x	-	x	x

5.7 Model tested

5.7.1 Kaolin clay

Since importing a sample of the clay located at the reference project is impossible, another type of clay is used. The clay used in the centrifuge is kaolin clay, which is made as slurry at the university. This is a purely clayey material, which does not contain sand. The properties of the clay are given in Table 17. The properties of the soil at the reference project are given as well.

Kaolin is commonly used as clay in the laboratory. Its compression parameters have been tested by [Sridharan and Venkatappa, 1973] already. The values from this research have been presented as comparison.

Table 17: Properties of Kaolin and Caspian Clay

			Kaolin	Kaolin [Sridharan, 1973]	Caspian 'NC' layer II	Caspian 'OC' layer III-IV
Unit Weight	y	[kN/m^3]	18	-	18	19
Void ratio	e0	[-]	1.7	1.5	-	-
Specific Gravity	G_s		2.6	2.59	-	-
Compression	C_c	[-]	0.30	0.305	0.34	0.22
Recompression	C_r	[-]	0.08	0.095	0.08	0.07
Shear strength	c_u	[kN/m^2]	0.1 * σ'_v	-	15	50 - 200
Liquid Limit	LL	[%]	50.5	49	-	-
Plastic Limit	PL	[%]	27.4	29	-	-
Permeability	k	[m/s]	1e-8 / 1e-9	-	1e-8	1e-10

5.7.1.1 Unit Weight

The clay slurry is poured into a strongbox, of which the dimensions are known. The height of the slurry can be measured and with this the total volume it takes can be calculated. The strongbox is weighed both before and after the slurry is added so the weight of the added slurry is known. With knowledge of the volume and weight a unit weight can be estimated. This can be done after consolidation and every load step as well. The weight of the strongbox is known and can be subtracted from the weight of the sample + the strongbox. The unit weight is expected to be increasing because of reducing void ratio / water content.

5.7.1.2 Void Ratio

The void ratio has been determined from the water content of a fully saturated specimen by drying a sample with a certain weight in the oven. All the water will be evaporated without burning the material itself. The weight of the sample before and after a test can be compared, and the amount of weight loss will represent the amount of water which has been evaporated. The voids in the sample will be completely filled with water (a fully saturated sample) and thus the amount of water evaporated can be related to the amount of voids in the sample.

The specific gravity (G_s) for kaolin clay is estimated at a value of 2.6 [http://www.galleries.com/kaolinite]. The specific gravity is calculated by dividing the weight of the soil particles to the weight of the water.

Samples have been taken after every load step in the centrifuge. The amount of surcharge is calculated beforehand (weight of surcharge + weight of the water = total stress at top of the sample. Height of the water * unit weight of water = water pressure at top of the sample. Total stress – water pressure = effective stress at top of the sample.) and the void ratio will be measured after consolidation. This

means that the effective stress a certain soil has had is known, and that the void ratio related to this can be tested. This is more or less an oedometer test and compression parameters can be related from this.

Figure 27 shows a plot of the tested void ratio versus the effective vertical stress at those points. A trendline has been added to these tests as well. The first couple of measurements show some deviation from the results. This might come from samples taken from some consolidated zones in the strongbox. The other measurements show good agreement with the trendline. This line is based on normal compression, with a parameter value of 0.30.

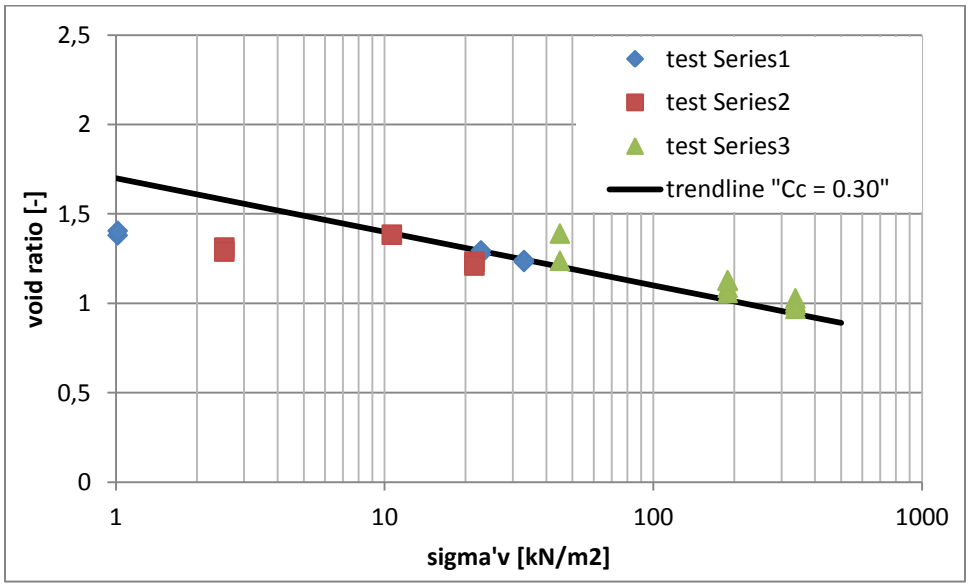

Figure 27: void ratio - effective vertical stress

With this stress dependency of the void ratio the initial void ratio can be determined, as long as the stress history of the layer is known.

5.7.1.3 Compression Parameters

The centrifuge tests in themselves are somewhat similar to oedometer tests. A one dimensional load test is performed by adding a uniform load on top of the centrifuge sample. By measuring the void ratio after every load step [paragraph 5.7.1.2] the output as with an oedometer test is a result. Plotting the results of these tests in a "e – σ'_v" graph gives an opportunity to determine the compression parameter. Since this is virgin compression, the C_c is tested.

To determine the value of the recompression parameter "real" oedometer tests have been performed. Samples which have been loaded to an effective stress of 150 kPa are placed into the oedometer. Load is added on this sample in different steps. The amount of settlement of the top plate is directly related to a loss in void ratio, since the sample is fully saturated. These values are again plotted in a "e – σ'_v" graph and, since these samples are in recompression, a value for C_r is determined.

The result of the tested samples is presented in Figure 28. The trendline added to this graph is based on a Cr of 0.08. It can be seen that after the preconsolidation pressure is passed (= +/-150 kPa) the decrease in void ratio increases. This is due to the transition from recompression to compression.

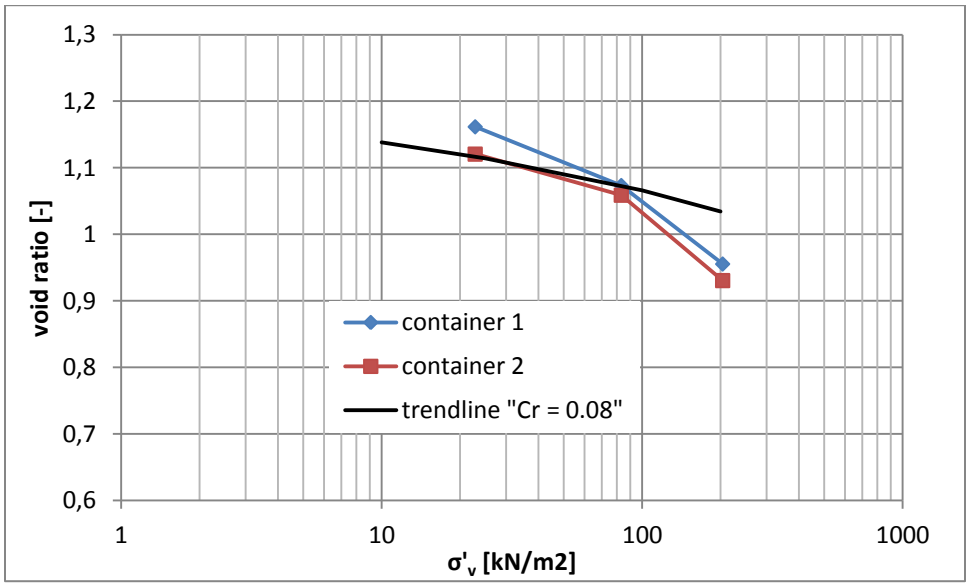

Figure 28: Results of the oedometer tests

5.7.1.4 Shear Strength

The undrained shear strength of the kaolin sample has been tested with a hand vane [BS1377: Part 7, 1990]. Figure 29 shows the results of the vane tests performed at different depths and with increasing surcharge. This leads to tests at varying effective stress levels. A trendline is drawn through this according to equation [23].

$$c_u = 0.1 * \sigma`_v \qquad [23]$$

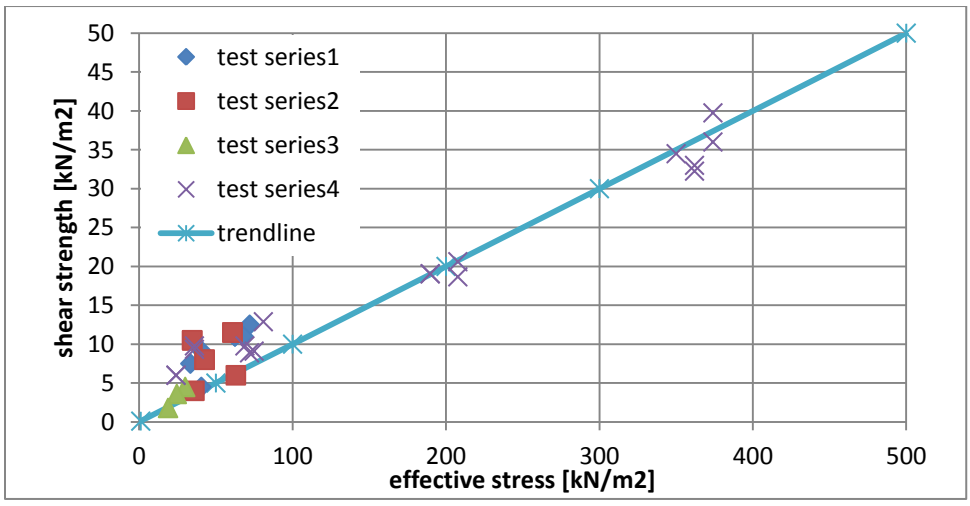

Figure 29: Relation between cu and sigma'v

5.7.1.5 Atterberg Limits

The Atterberg limits are tested to see how far a soil is away from being in a plastic or liquid state. This should be consistent for the kaolin clay used in every test. Because the samples are used several times it might be that some sand is mixed up with the clay. But because this amount is so low the influence on the Atterberg limits of the sample are negligible.

The Atterberg limits consist of a liquid limit and a plastic limit. The liquid limit has been tested with the cassagrande cup according to [BS1377: Part 2; 1990] [ASTM1995: D4318]. The plastic limit has been tested according to [BS1377: Part2; 1990]. The results are presented in Figure 30 and Table 18.

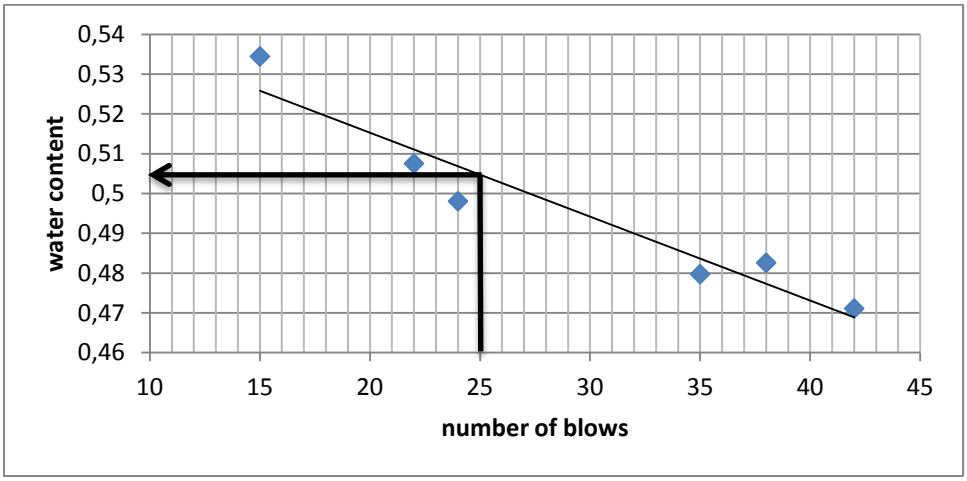

Figure 30: Results of Cassagrande Cup test

Table 18: Results of the Plastic Limit test

Sample No.	1.1	1.2	2.1	2.2
Water content [-]	0.265	0.28	0.274	0.276

The values of the plastic and liquid limits from these tests are presented in Table 17.

6 Results and Interpretation "Benchmark" Soil Profile

The results of the calculations and centrifuge tests done on the "benchmark" soil profile, introduced in paragraph 0, will be presented and discussed in this chapter. The results have been presented in different plots, divided by different paragraphs.

6.1 Settlement in Depth

The results from the calculations and physical model tests will be discussed apart from each other.

6.1.1 Calculation Model

The data is presented in Figure 31. The settlement in depth results are all plotted at the end of consolidation. The Msettle, Soft Soil and Cam Clay calculations show a comparable settlement profile. The cam clay model shows a jump in settlement at the top. This probably has to do with the low stress states at that point, leading to numerical inaccuracies for this soil model.

The Msettle and Hand Calculation give exactly the same results. This is as expected since the calculationsmethods are both based on Bjerrum settlement formulas and use the same parameters.

The soft soil model shows the same settlement profile, though it slightly underestimates the settlements. This is due to the recalculation of the settlement parameters and the difference in the model formulation.

The hardening soil model underestimates the settlements even more. Deeper down the results agree with each other, but closer to the surface the lines differentiate. The Hardening Soil model is made stress dependant with a power law, the parameter m. This parameter has already been set to 1, so it should be log stress dependant, similar to the Bjerrum parameters. Still the settlement is less, probably due to an increase in horizontal stresses and the influence of the E50 on the settlement.

It is decided that the most reliable models are the Msettle / Hand Calculation, because for these models the parameters do not need to be recalculated. The Plaxis models which fit the settlement depth plots best are the soft soil and cam clay models. The hardening soil model is influenced to much by the lateral soil stiffness, which is supposed to have no influence since this is a 1D consolidation problem.

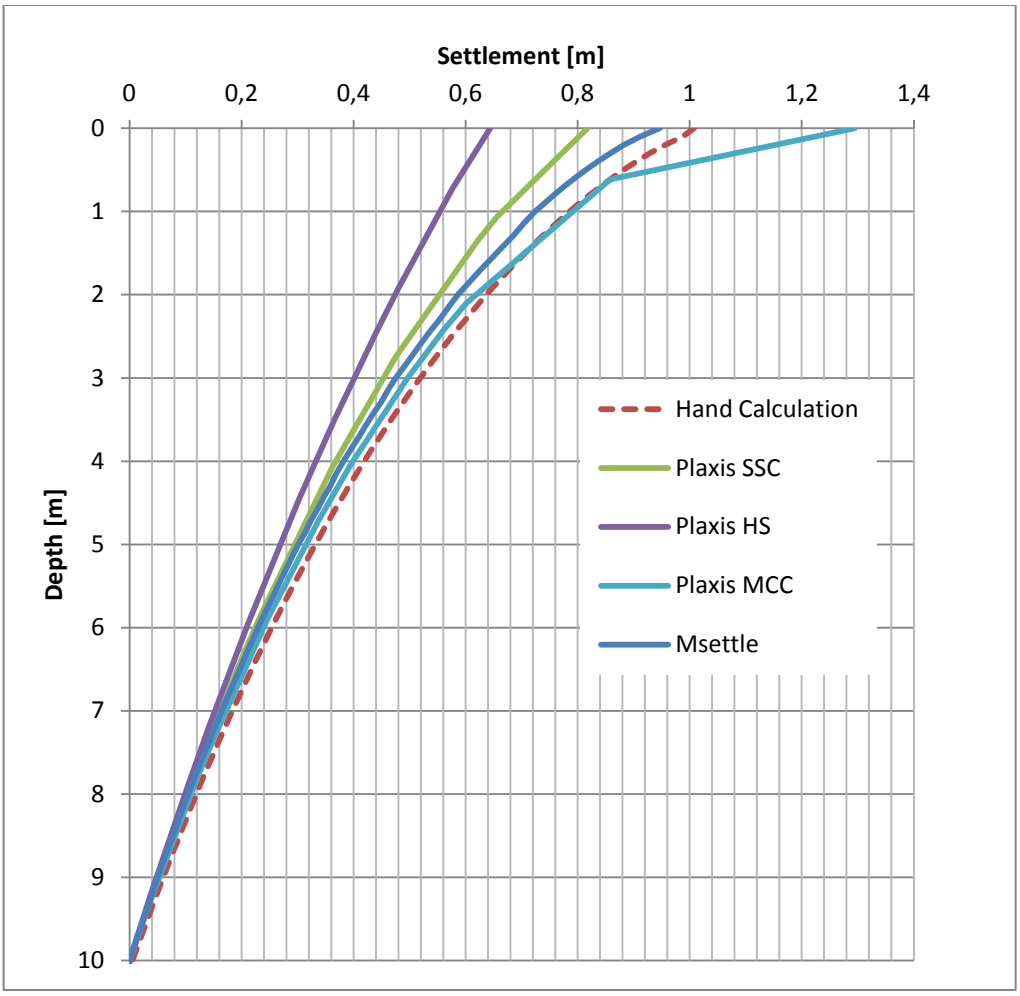

Figure 31: Calculated Settlement in depth; "benchmark" soil profile

6.1.2 Physical Model

The centrifuge test result is presented in Figure 32, together with the results of the different calculation models.

6.1.2.1 Digital compared to Manual measurements

The height of the sample ground level has been measured manually, with a caliper, both before and after the test. With these measurements the settlement of the ground level is determined. This value can be compared with the results from the camera. The trend line added in Figure 32 gives an estimation of the total settlements from the camera measurements. Table 19 shows these measurements agree quite well with each other. The camera measurements are thus quite accurate to represent settlement of the ground level.

Table 19: Measured settlements of ground level; "benchmark" soil profile

Measurement		Digital [camera]	Manual [caliper]
Settlement	**[mm]**	8.5	9

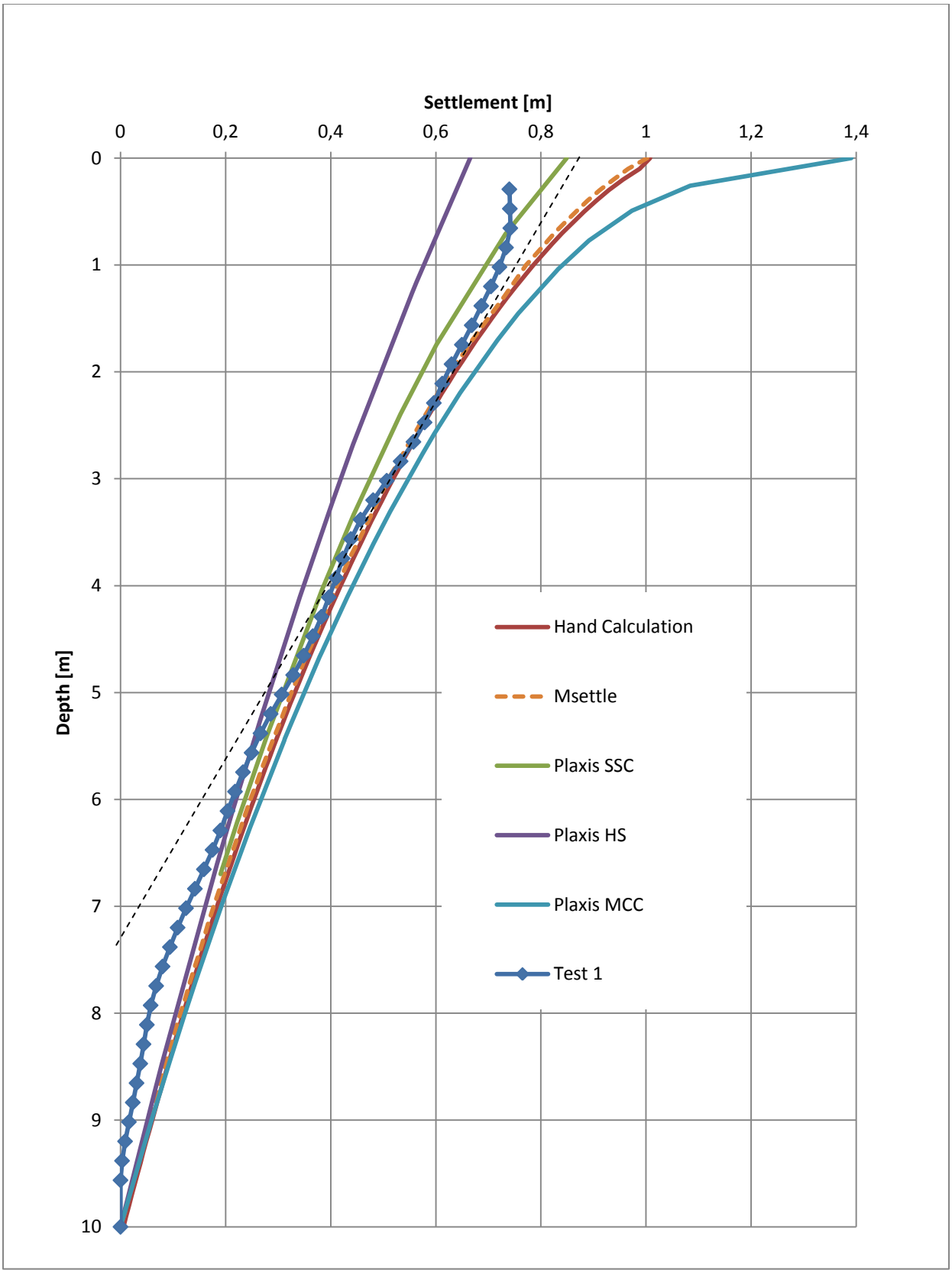

Figure 32: End of Consolidation, predicted settlements with various methods

6.1.2.2 Measurements compared to calculated results

Close to the surface the settlements of the centrifuge stay behind as can be seen in Figure 32. This has to do with the test conditions (disturbed clay at the surface, loss of contrast in the clay resulting from large deformations). The clay sample at the top is very soft and almost slurry before overburden is added. Since the sample is only consolidated under its own weight, the top side of the sample has only had no or low stresses before. Now that the sample is loaded to 100 kN/m^2 this weak layer is subjected to large deformations. At the start of the test (spinning up the centrifuge) some of the consolidation might already take place, this happens before the zero point in the actual test at 100g.
Large deformations occur at the start of the test. These deformations can be of such a magnitude that JPIV cannot track them. The measured displacements will therefore be more inaccurate near the top of the sample.
The weak layer might also be squeezed between the loading plate and the window. When the clay is squeezed out it will take the contrast material with it, leading to a loss of contrast. This loss of contrast leads to loss of correlation in the subsequent JPIV analysis of the images.

The general trend of the measured settlements agrees reasonably well with the calculations. Some parts show more settlement. This could be caused by the sand added as contrast material or the determined compression parameters might not be exact.

6.1.2.3 Correction for decrease in acceleration over depth

Mentioned before is the decrease of acceleration over the height of the sample. To correct for this a linear relationship between stress and strain is assumed. The stress level is lower higher up in the sample compared to the calculated models. The magnitude of this difference is projected in Figure 33 on the right hand side.

This difference in acceleration level, and thus stress levels, is corrected in the figure on the left. The measured settlements are multiplied by the difference in acceleration level.

The outcome of the measurements fits the calculated quite good without the correction. The corrected data shows more settlement than the calculated results. The correction done in this way is quite simplistic and might not give an accurate representation of reality.
Another cause for the deviation from the calculated values might be the contrast material (sand) which is not attached to the clay. Especially higher up in the sample, where the clay is still very soft, the sand has a higher specific density and might be pushed down through the clay.

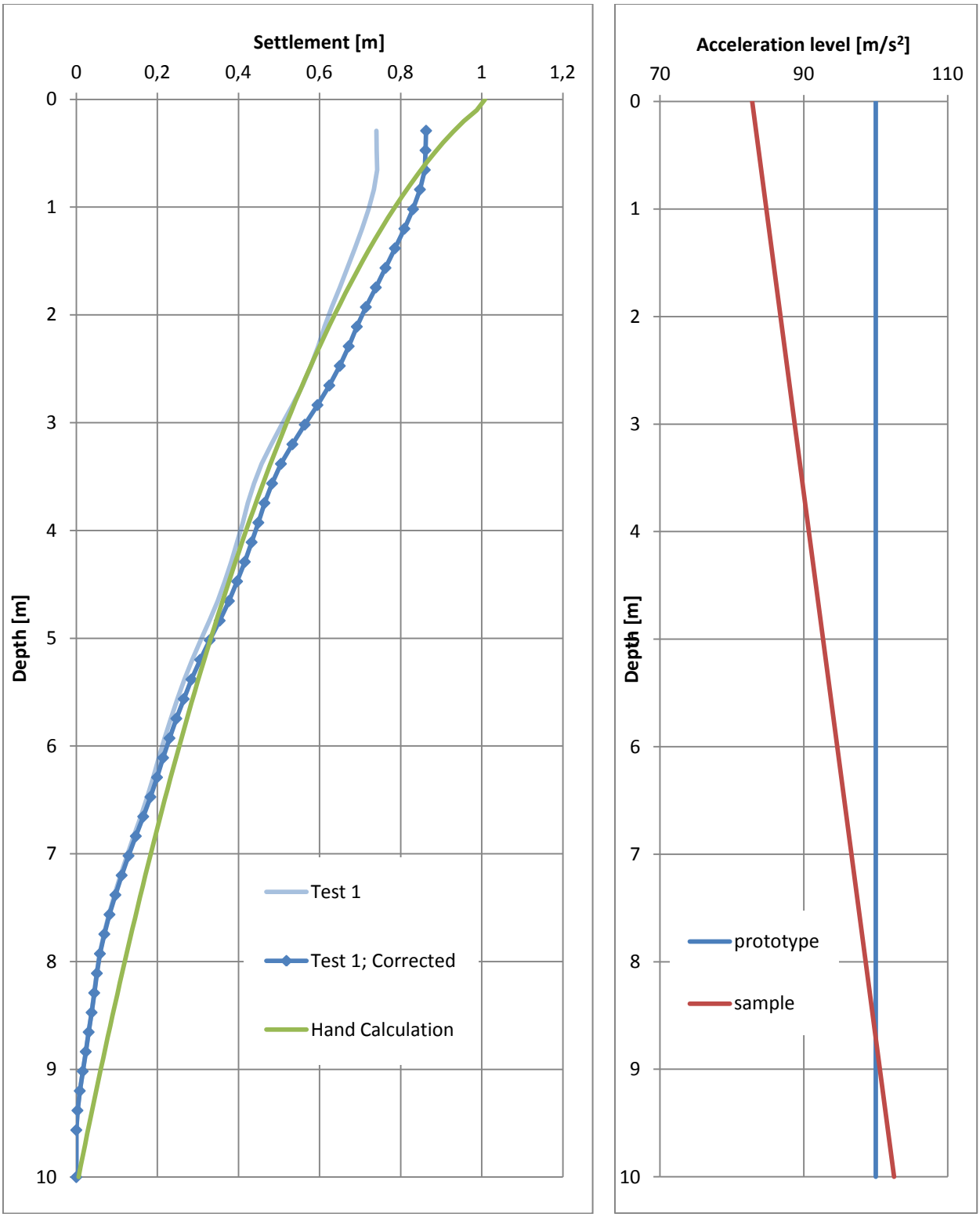

Figure 33: Measurement correction for loss of acceleration; "benchmark" soil profile

6.2 Settlement in time

6.2.1 Calculation Model

The comparison of the results for the settlement evolution in time between the calculation models and the measurements are presented in Figure 34 and Figure 37. In these “settlement in time” plots the calculated results are from Msettle and Plaxis. The Plaxis calculations have been performed with the different models described previously. A constant value for the permeability has been assumed for all the calculation models. The other parameters are all described in paragraph 4.2.2.

The calculation results show some deviation from each other. The Msettle calculation shows a bit more delay in settlements than all of the Plaxis calculations. The Plaxis models show some differences between themselves. The Hardening Soil and Soft Soil model agree quite well with each other but the Modified Cam Clay model falls in between the HS / SS models and the Msettle results. Since the settlement plotted in this figure is normalized over the total settlement at the end of consolidation, this might give a skewed image. As shown in Figure 31 the topside of the MCC model shows a jump in settlements, which influences the total amount of settlement. This influences the normalization of the plot.

The difference between Msettle and the Plaxis models can be a result of the difference in the modeling of consolidation. Besides that the difference in calculation models will add to the deviation in results.

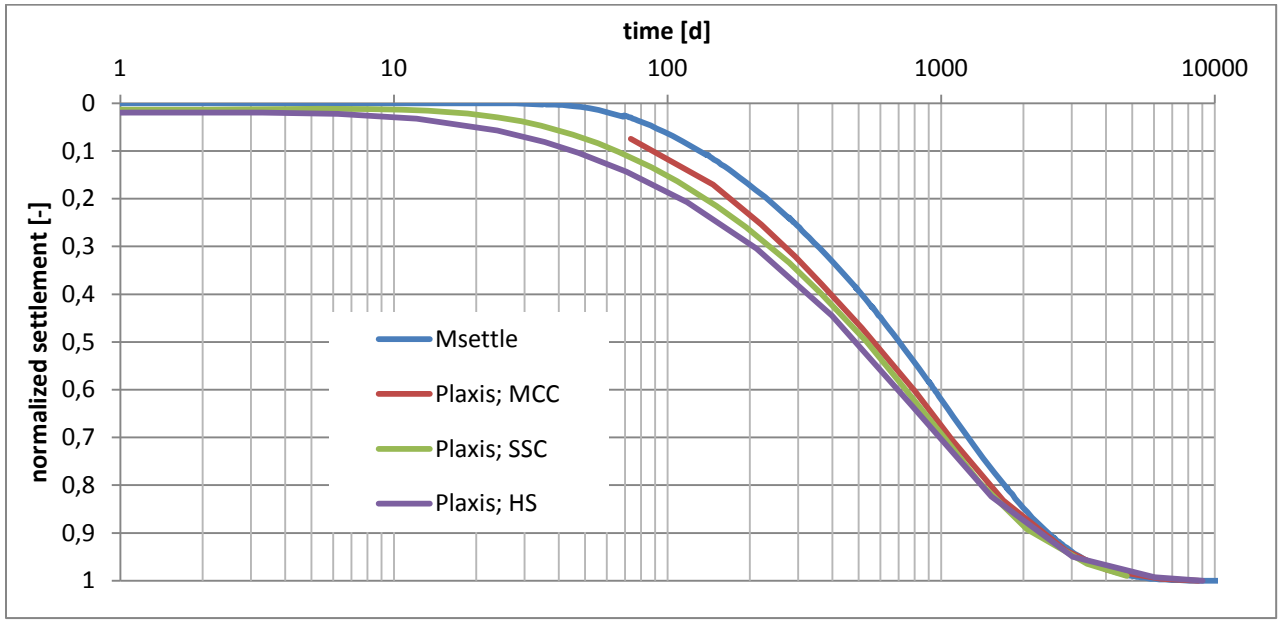

Figure 34: Calculated Settlement in time; “benchmark” soil profile

6.2.2 Physical Model

Settlement in depth at different points in time has been plotted in Figure 35 and Figure 36. In these plots the results of the centrifuge have been plotted against calculated Msettle data and Soft Soil results respectively.

The Msettle data shows a bigger difference than the Plaxis Soft Soil results but both are behind the measured data. This is expected since the implemented permeability for the calculation methods is constant and fitted to the end of the consolidation process. The permeability of the centrifuge sample converges towards this, thus has a higher permeability at the start of the test. The higher permeability leads to a faster consolidation process and combined with this an increase in settlements. The results eventually converge towards each other, since the permeability has no influence on the total amount of settlement. Expected is that in reality the permeability decreases with a loss of void ratio, this is discussed in paragraph 7.2.2.

The Plaxis Soft Soil Creep seems to predict the settlement over depth quite well. The difference between the measured and calculated data does not vary too much. The total settlement stays behind at the end of consolidation though.

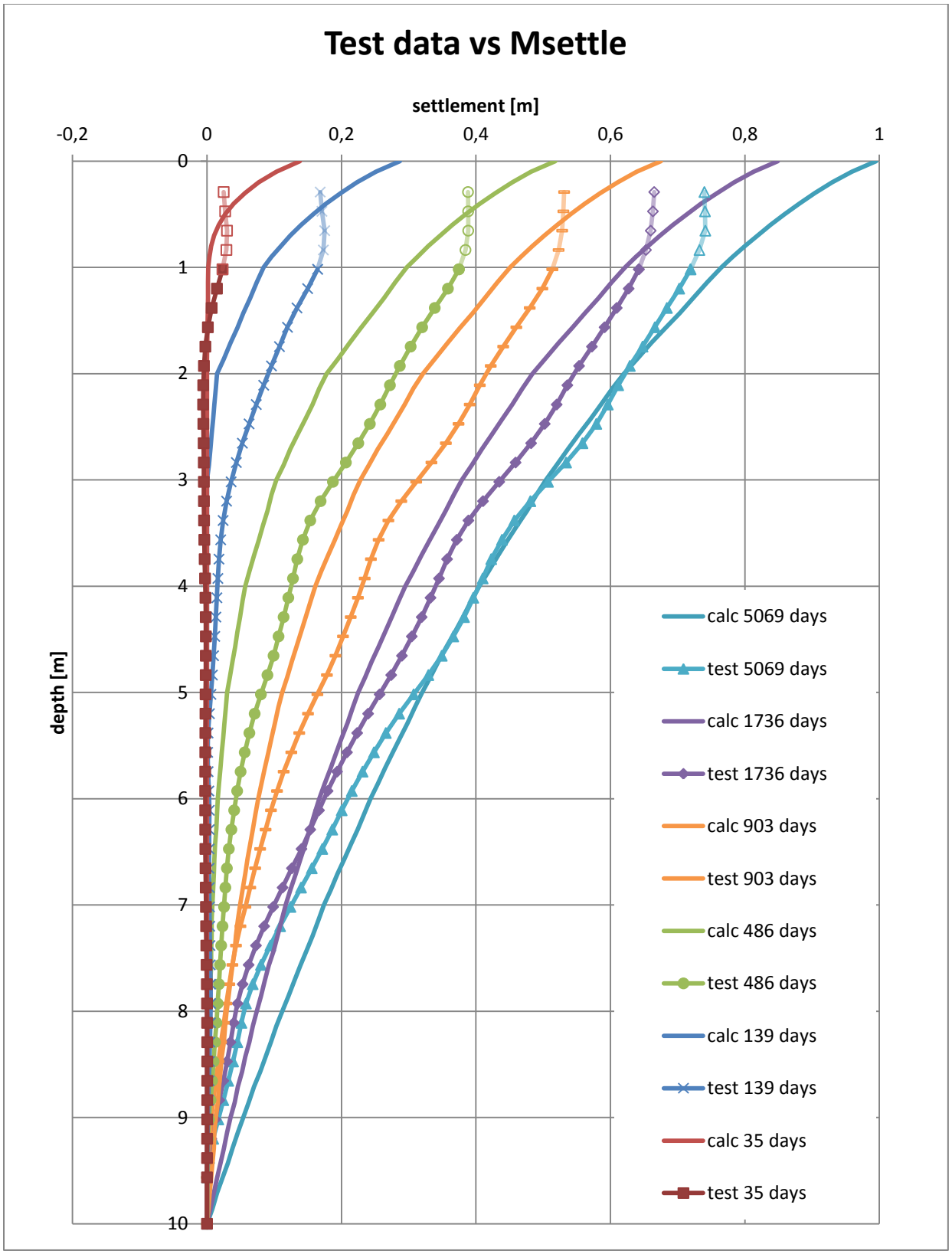

Figure 35: Settlement - depth over time; Physical test data compared with Msettle calculations

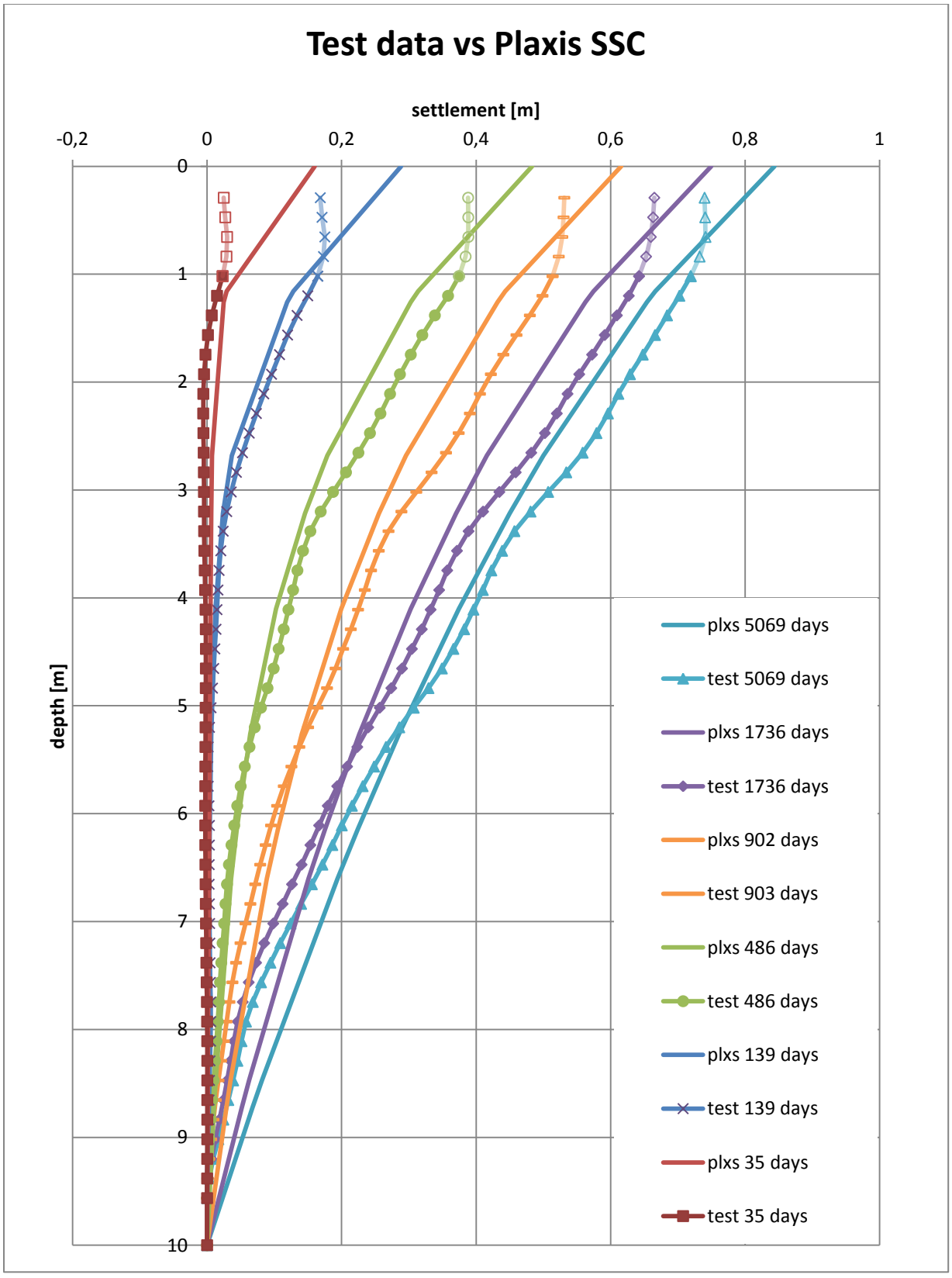

Figure 36: Settlement - depth over time; Physical test data compared with Plaxis SSC calculations

Settlement in time of the different calculation models and the centrifuge results are presented in Figure 37. This figure shows 2 different plots, representing different depths in the soil profile. Settlements start at a later stage deeper down in the profile, which is expected because drainage only occurs at the topside.

In the figure calculation results have been fitted to the outcome of the centrifuge. The parameter which determines the time dependency of the settlement is the permeability. Since this parameter is not exactly known beforehand an estimation is made. The expected value of permeability is between the 1e-8 m/s and 1e-9 m/s. The settlement-time results, as calculated with Msettle, for these values of permeability have been plotted as well.

The calculations which fit the centrifuge results best are those with a permeability of 3e-9 m/s. This value falls within the expected range. In reality the permeability will not be constant, but is expected to decrease with a loss of void ratio due to compression of the sample. The measured settlements do not fit exactly on the Msettle line [kv = 3e-9] but shows a similar trend. The settlements of the measured centrifuge results start earlier but converge toward this outcome at a later stage. This can be the consequence of the decreased permeability with a loss of void ratio in the sample. The decrease of permeability is discussed in paragraph 7.2.2.

The Plaxis calculations seem to fit the measured results exceptionally well. Both the Hardening Soil and the Soft Soil model are close to the measured results. This is remarkable because the centrifuge sample is subjected to a loss of permeability, which is not the case in the calculation models. Expected is thus that there should be a deviation in results like the Msettle calculation (settlements start at a later time but then converge towards each other).

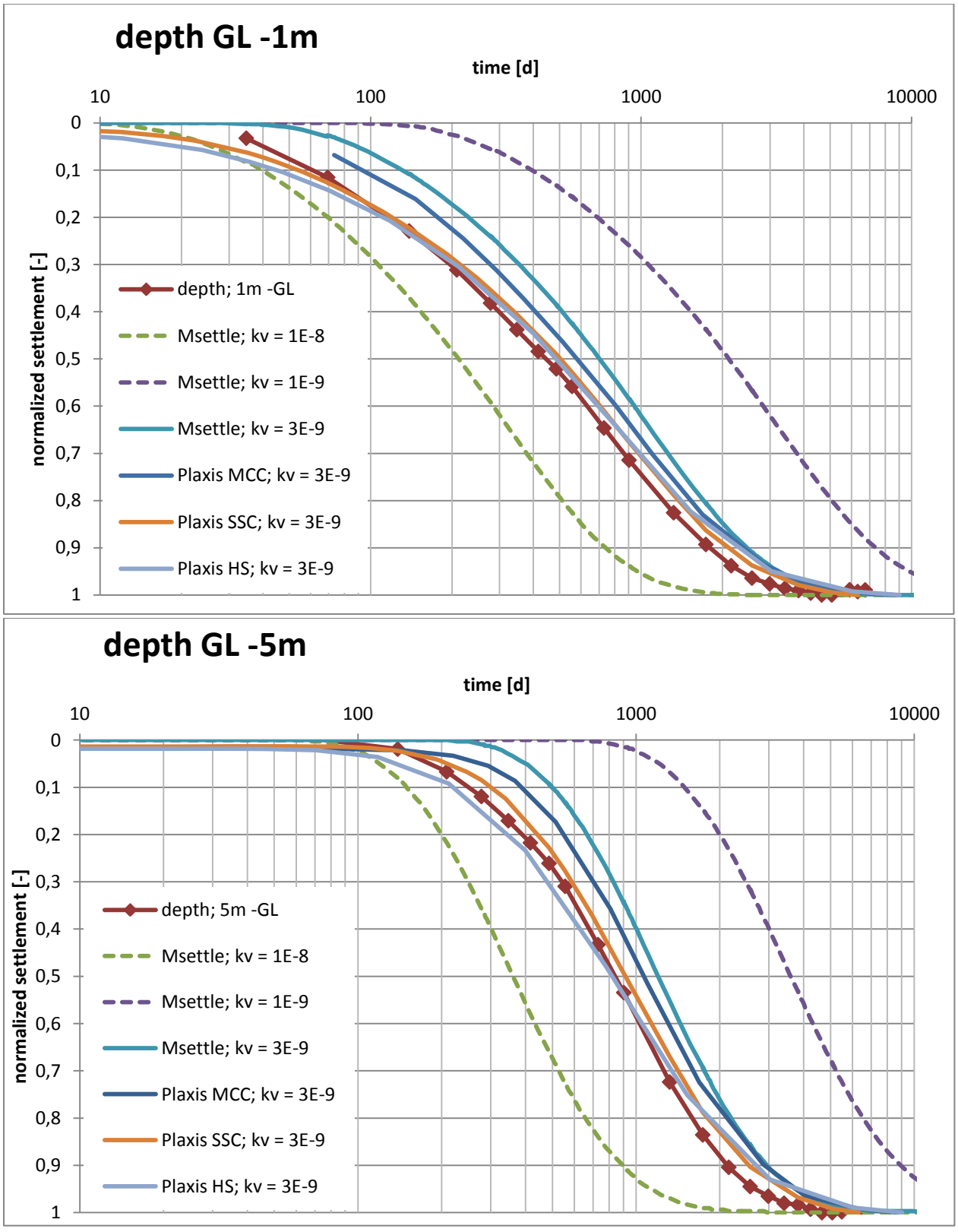

Figure 37: Time – settlement plots at different depth for the "benchmark" soil profile

6.3 Consolidation in time

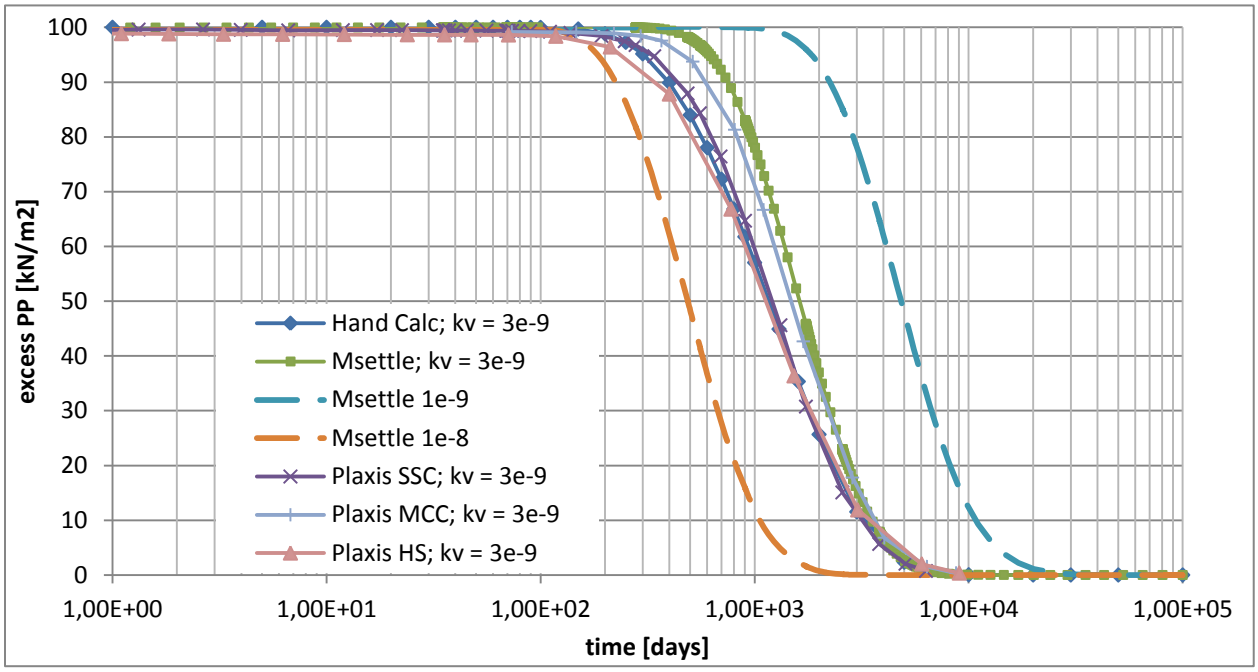

Figure 38: Calculated Consolidation in time; "benchmark" soil profile

No pore water transducers were installed in the sample. The consolidation process and its progression could therefore not be measured. The end of consolidation is assumed with the settlement time plots. These will not show any settlement after consolidation is finished, because creep is of minimal influence in the time period the tests spans.

The consolidation in time is only presented in calculations. The same models are compared again: a hand calculation, msettle, and the different plaxis models. The results are presented in Figure 38. The permeability which fitted the tests the best (kv = 3e-9 m/s) has been used to compare the results between the different calculations models. The expected values of 1e-8 and 1e-9 have been plotted as well. The results have been evaluated at the bottom of the sample. At this point the largest draining distance occurs and consolidation will take the most time.

The results seem to agree quite well. Two main differences can be seen. The Hand Calculation shows good agreement with the Plaxis Hardening Soil and Soft Soil models. Msettle seems to show more correlation with the Plaxis Modified Cam Clay model. This is the same trend which is recognized in the settlement time plots, which is logical. The settlements are triggered by consolidation and comparable trends are expected.

The difference between Msettle and the Hand Calculation is triggered by the difference in calculation methods. In Msettle Darcy consolidation is selected, where the Hand Calculation is done with the consolidation equation specified by Terzaghi. This requires a coefficient of volume compressibility as well which is gotten from the performed oedometer tests. In Msettle only a vertical permeability is specified.

The variation in results of the Plaxis models is the cause of the differences in the settlement time plots. Since the consolidation already gives differences it is obvious that settlement in time will show differences. Although the Soft Soil model converges toward the Msettle outcome as time expires, the difference at the start of consolidation is quite significant.

6.4 Revision of calculations methods

No calculation method gives an exact prediction of the centrifuge test results. The most remarkable observations from the “benchmark” soil profile centrifuge test are:

- The Msettle and Hand Calculation shows quite good correlation with the test results in a settlement – depth plot. Settlements in time show some difference, but this is expected with the assumptions made in the Msettle calculation. The influence of a decreasing permeability can clearly be seen from the physical results. This calculation method gives an accurate prediction of the subsoil reaction.
- Predictions made with the Soft Soil model give an accurate prediction of the settlements occurring in depth. The settlements show too much correlation with the centrifuge tests results, as discussed in this chapter. The results are expected but do this less pronounced than the Msettle calculation.
- The Modified Cam Clay model shows too much variation during the calculation results. The results are comparable with the Msettle results but these are deemed more reliable. Therefore this model will be left out of the scope from now on.
- The Hardening Soil model does not seem to agree with any of the other models in the settlement depth plots. It under predicts the settlements compared to the centrifuge data as well. Also the settlement time results are awkward compared to the measured data. This model will not be used in the calculations of the next models.

The Msettle, Hand Calculation and Soft Soil model in Plaxis give the most reliable results for calculating consolidation settlements in the centrifuge. These will thus be used to predict the reaction of the centrifuge soil model.

7 Results and Interpretation “Centrifuge” Soil Profile

The “centrifuge” soil profile has been presented in paragraph 4.3. The execution of the tests and the data processing has been elaborated upon in chapter 5.3

7.1 Settlement in Depth

7.1.1 Calculation Model

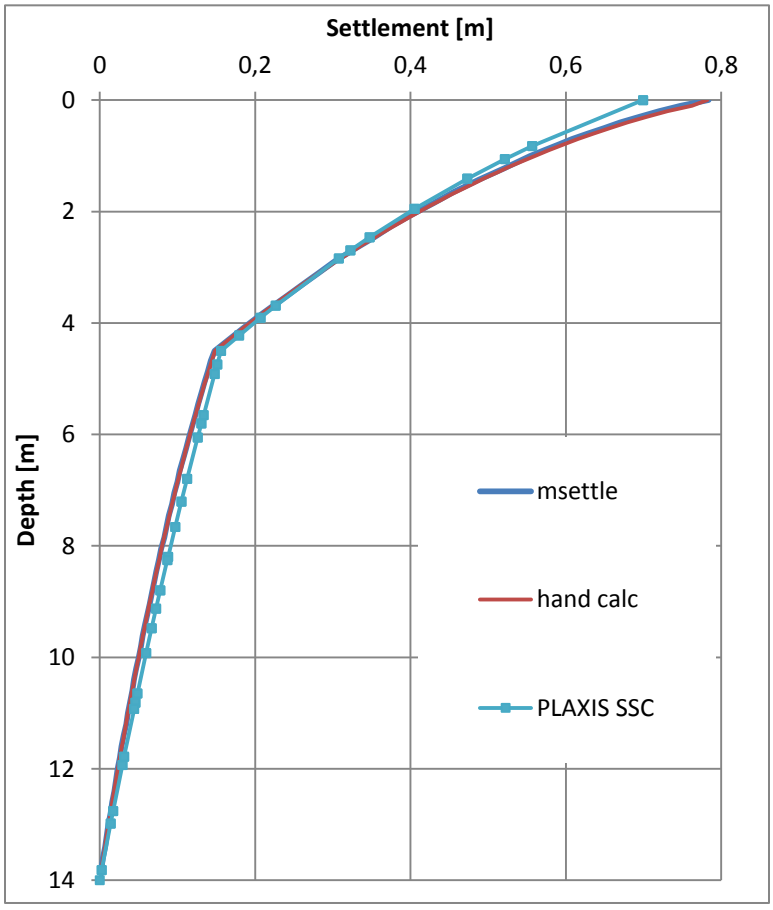

Figure 39: Calculated Settlement in Depth; “centrifuge” soil profile

The calculation data is presented in Figure 39. Compared to the “benchmark” soil profile the same differences in the varying models can be noticed. The different analytical calculations, the Hand Calculation and Msettle, show perfect agreement just as in the “benchmark” soil profile. This was expected since both calculate the settlements with the same model.

The Soft Soil model shows nearly identical results. The settlement of the soft clay layer is under predicted though. The settlement lines are nearly on top of each other, only the top 2 meters show some deviation.

7.1.2 Physical Model

The results from both centrifuge tests and the predicted response from all the numerical models are presented in Figure 40. Compared to the centrifuge test results all the calculated results give an overestimation of the settlements.

The centrifuge samples both show an increase in settlement at the interface between the overconsolidated and normally consolidated clay layers. Below four meters depth the reaction of the soil is stiff. But where the soil is in its compression state more deformation can be noticed. Just as in the calculated results the centrifuge results show a kink in the curve around the expected interface.

7.1.2.1 Digital compared to Manual measurements

Manual measurements are done both before and after the test. The ground level is measured with a caliper and settlements of the ground level are compared with the measurements done with the camera. A trend line has been drawn in Figure 40 to give an estimate of the settlements at ground level, since measurements are disturbed at the top. Table 20 shows that the (estimated) digital and manual measurements agree quite well with each other.

Table 20: Measured settlements of ground level; “centrifuge” soil profile

Measurement		Digital [camera]	Manual [caliper]
Settlement			
Test 1	**[mm]**	4.5	5
Test 2	**[mm]**	4.5	5

Both Table 19 and Table 20 show a slight underestimation of the “estimated” digital measurements compared to the manual measurements. This difference could come from the way the settlements at the top are estimated. As can be seen the trend line drawn is a straight line, where the settlement line is expected to show some curvature towards the top. This leads to slightly more settlement from the camera measurements.

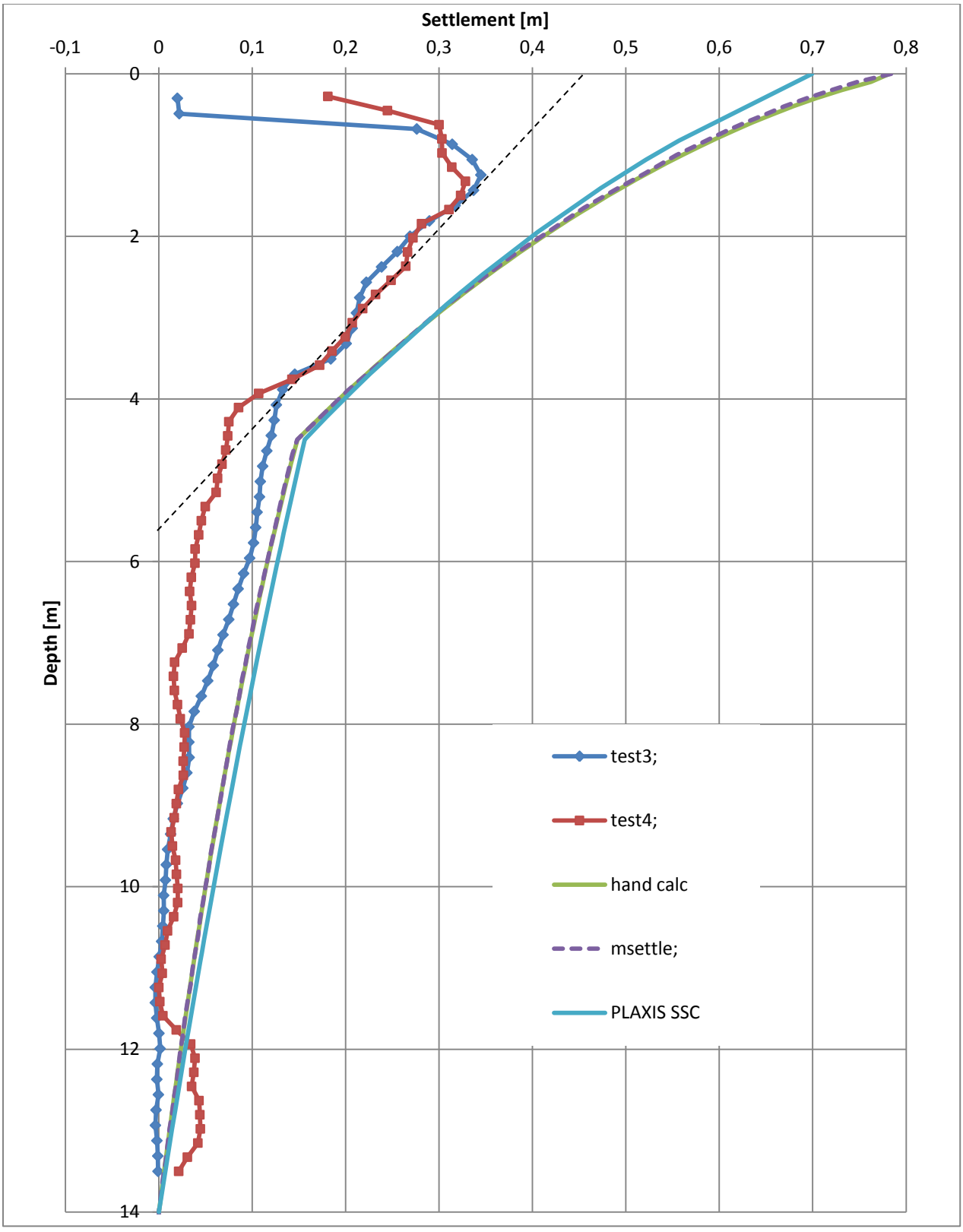

Figure 40: End of Consolidation, predicted settlements with various methods

7.1.2.2 "Wavy" settlement progression in depth

Test 4 shows some unrealistic results in the deeper "stiff" clay layer. The results deeper than 7 meters show a wavy settlement progress. This would mean compression and extension of the layer at that depth. Especially near the bottom, at 12 to 14 meters depth, a zone of compression can be seen which returns back to zero settlement higher up the sample. This behavior is highly suspect because heave would be needed to reduce the settlements.

A more likely reason for these unrealistic results is originating from the problems with the lighting inside the centrifuge. As depicted in Figure 21 the lighting is a standalone part of the test setup. The light loses intensity during the test, due to loss of battery charge. Where at the start the sample, and its added contrast material, are clearly visible this is not the case later on in the test. This is shown by Figure 25, where images at different time steps of the test are shown. Because of this the images need to be processed, which leads to an increase in contrast but also adds noise. Since the lighting is fixed above the sample the lighting gets worse over the depth of the sample. This is seen in the settlement in depth plot. Above 7 meters depth the results remain acceptable though.

A similar thing occurred in test 3. However, due to the different lighting scheme this had less impact on the test results. As a result the undulating settlement response from test 4 is not seen in test 3.

7.1.2.3 Lack of settlement measured at the top

In the top meter of both tests a drop in settlements can be noticed. Both settlement lines drop back towards zero. This is a measurement artifact from the plastic foil on the top of the strongbox. The latter prevents the water from evaporating in flight. This foil can be seen in Figure 23 and Figure 24.

As the lighting is applied above the strongbox, this is partly blocked by this foil. In this way a shade is created which falls on the top side of the sample. The contrast and lighting is already a difficult part in the research, as discussed earlier, but due to this shade a dark zone is created, which complicates cross correlation in JPIV.

7.1.2.4 Correction for decrease in acceleration over depth

Compared to the settlement predicted by the calculation models the measured results stay behind. As mentioned earlier the lighting was not optimal in both tests, which is a reason for missing or unreliable measurements deeper down in the sample. The top "soft" clay layer shows a lack of settlement as well. This can be due to the decrease of acceleration over the height of the sample. Especially at the top the acceleration levels are diverging from the 100g level assumed in the prototype calculations. Because the acceleration is lower, stress will be lower and thus stress levels stay behind the prototype level. This results in less settlement compared to this prototype profile.

Figure 41 shows this decrease of acceleration through the sample. The difference in acceleration level is added to the measured settlement. This has been done to get a better comparison between the calculated settlements and the measured values. It can be seen in the left image the corrected measurement correlate better with the calculated values.

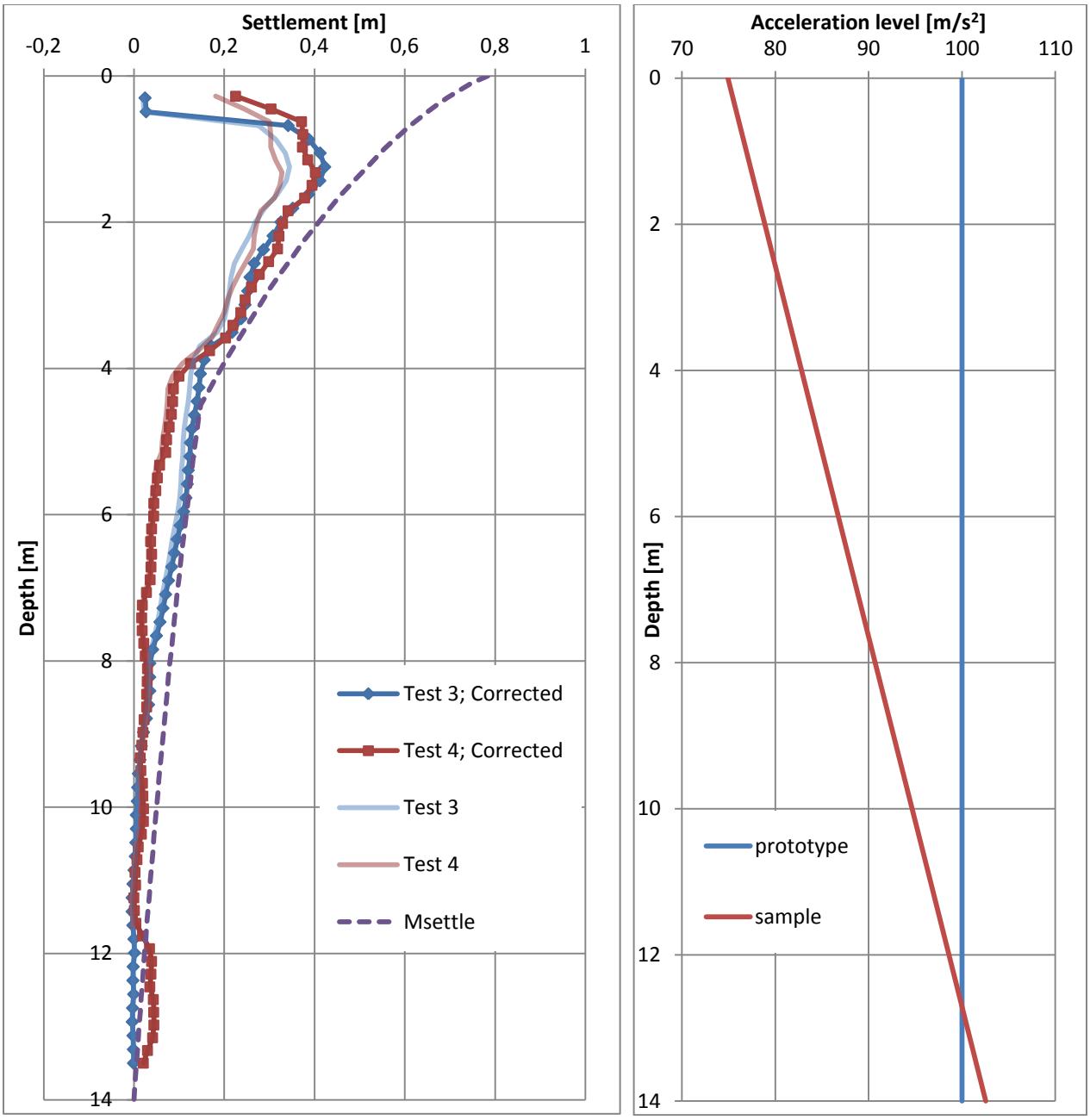

Figure 41: Measurement correction for loss of acceleration; "centrifuge" soil profile

Besides this the loading situation might deviate from the calculation model. A lower acceleration level (of 75g) has been assumed for this load, but to exactly recreate an overburden of 100 kN/m2 is nearly impossible. The overburden has been back figured with the measured data and differences of maximum 5 kN/m2 have been found. This should be negligible effect on the settlements compared to the other limitations.

7.1.2.5 Kink in settlement line at interface

The kink in the settlement line does not occur at the same point as the calculations predict. An explanation for this is related to the sample preparation. For test 3 there was a sand inclusion above the stiff clay layer. This sand was used to add contrast to the sample but did not stick to the Plexiglas very well. During consolidation of the soft clay layer the sand fell down onto the stiff clay layer. There it accumulated because the sand couldn't penetrate the stiff clay layer. The sand inclusion will react stiffer than the normally consolidated clay layer. This sand inclusion was found when the sample was dismantled, a picture of it is shown in Figure 42. Above the sand inclusion the settlements start to increase as can be seen from the results.

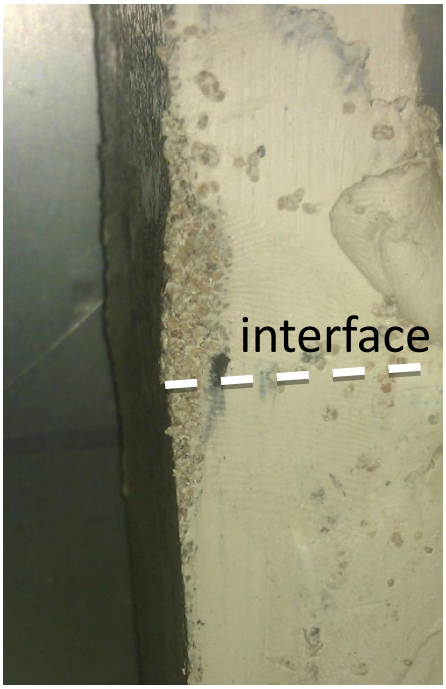

Figure 42: Sand Inclusion test 3

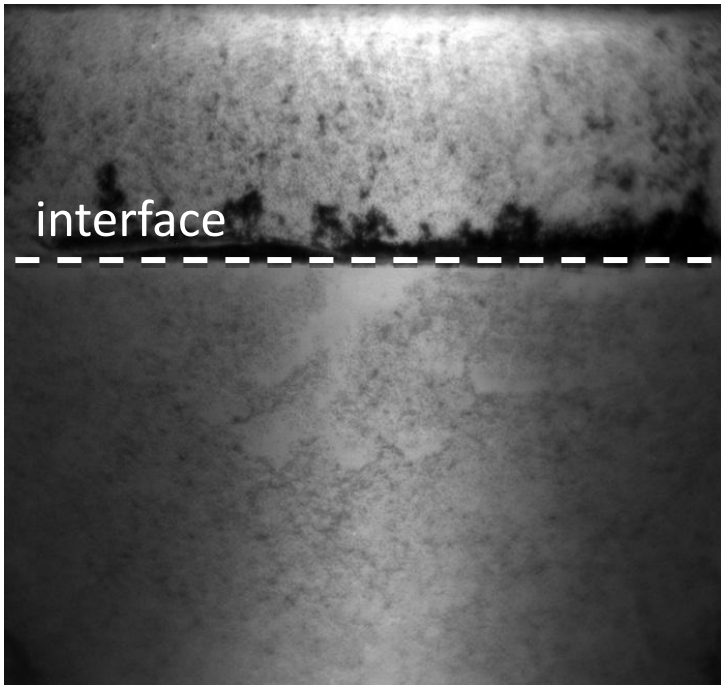

Figure 43: Processed image of test 4

In test 4 black powder was added to make sure the interface between soft and stiff clay was clearly visible. The powder created a layer in the soft clay layer where no contrast remained visible. This can be seen in Figure 43, where a processed image of test 4 is presented.

7.2 Settlement in time

7.2.1 Calculation Model

Figure 44 shows the settlement in time of the different calculation models for the "centrifuge" soil profile. The same calculation models as in paragraph 6.2.1 have been used. The permeability is kept constant for both layers, which is a simplification of reality.

A discussion on the decreasing permeability is added in paragraph 7.2.2, where the results from the calculations are compared to the physical model measurements.

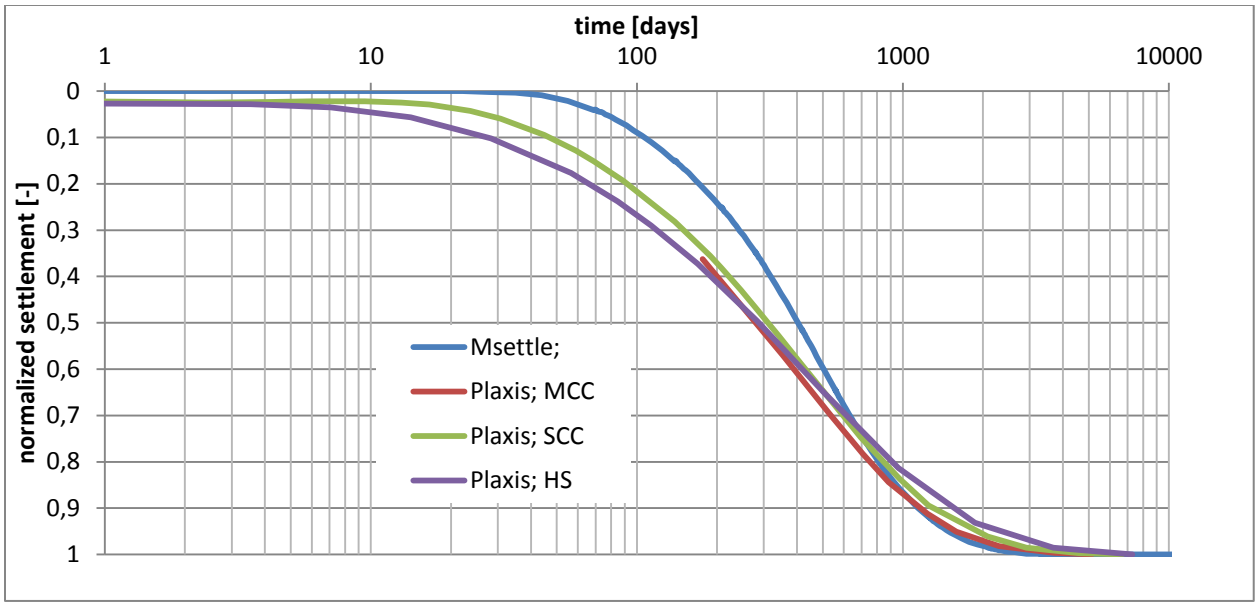

Figure 44: Calculated Settlement in time; "centrifuge" soil profile

7.2.2 Physical Model

Figure 45 and Figure 46 show results of settlement in depth at different time steps for the “centrifuge” soil profile. In Figure 45 the centrifuge test data has been plotted next to the Msettle calculation results. Figure 46 shows the same centrifuge data compared to Plaxis Soft Soil calculation results.

In Figure 45 the Msettle calculation results are staying behind on the measured values at the start of the test. This has to do with the constant permeability assumed in the calculation model. Settlements will occur earlier in the physical measurements due the higher permeability. After an equivalent of 417 days the settlements are more or less similar. The total settlements from the calculated Msettle values overestimate the measured values. Reasoning for this is discussed in paragraph 7.1.2.

Figure 46 show the different calculated values from the Soft Soil model compared to the centrifuge test results. In this figure the calculated values seem to agree quite good with the measured data at the start of the test. The reaction of the overconsolidated layer is predicted quite well. The total settlements are over predicted again, just as the Msettle data does. This different in total settlement is discussed before.

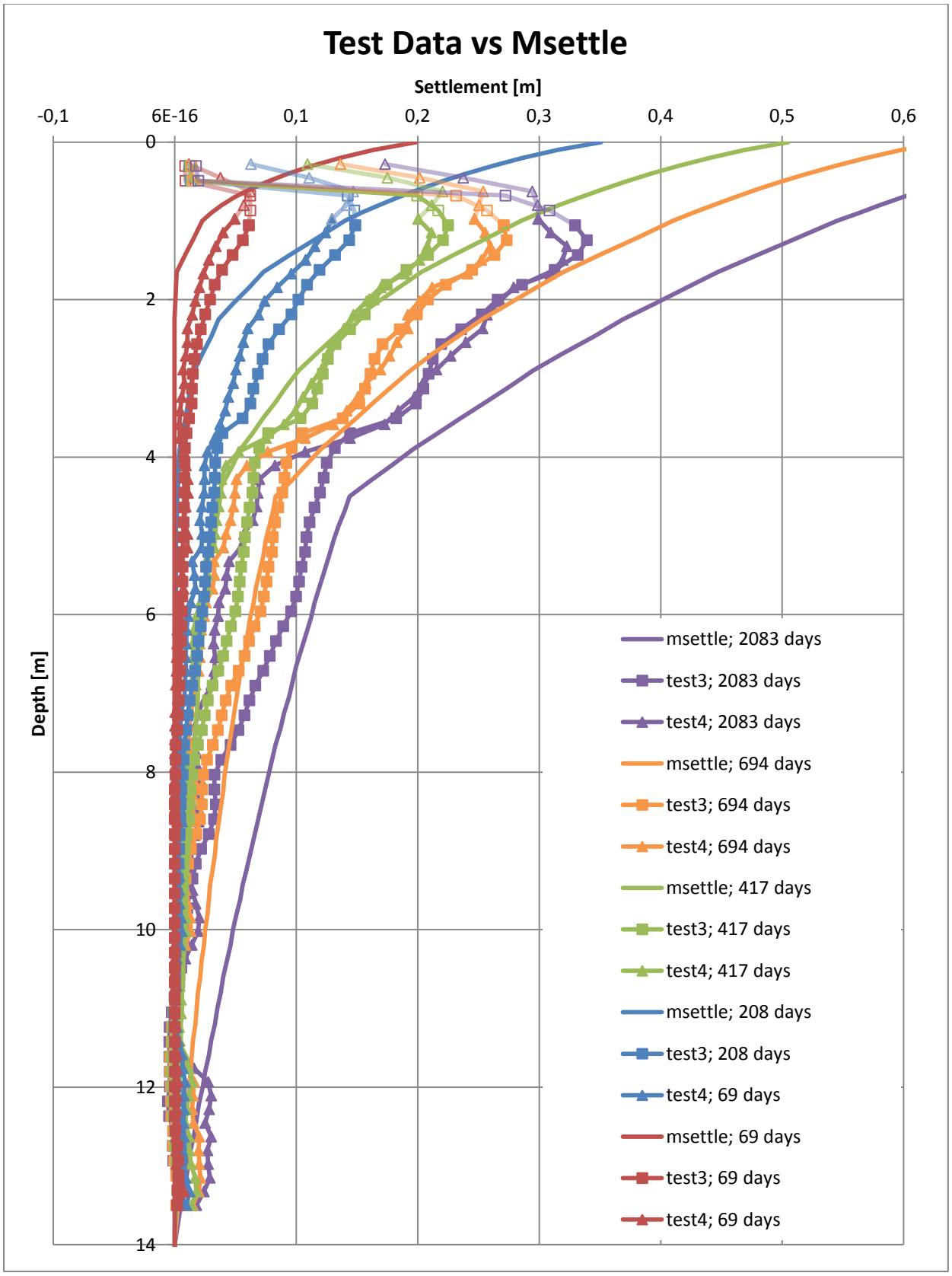

Figure 45: Settlement - depth over time; Physical test data compared with Msettle calculations

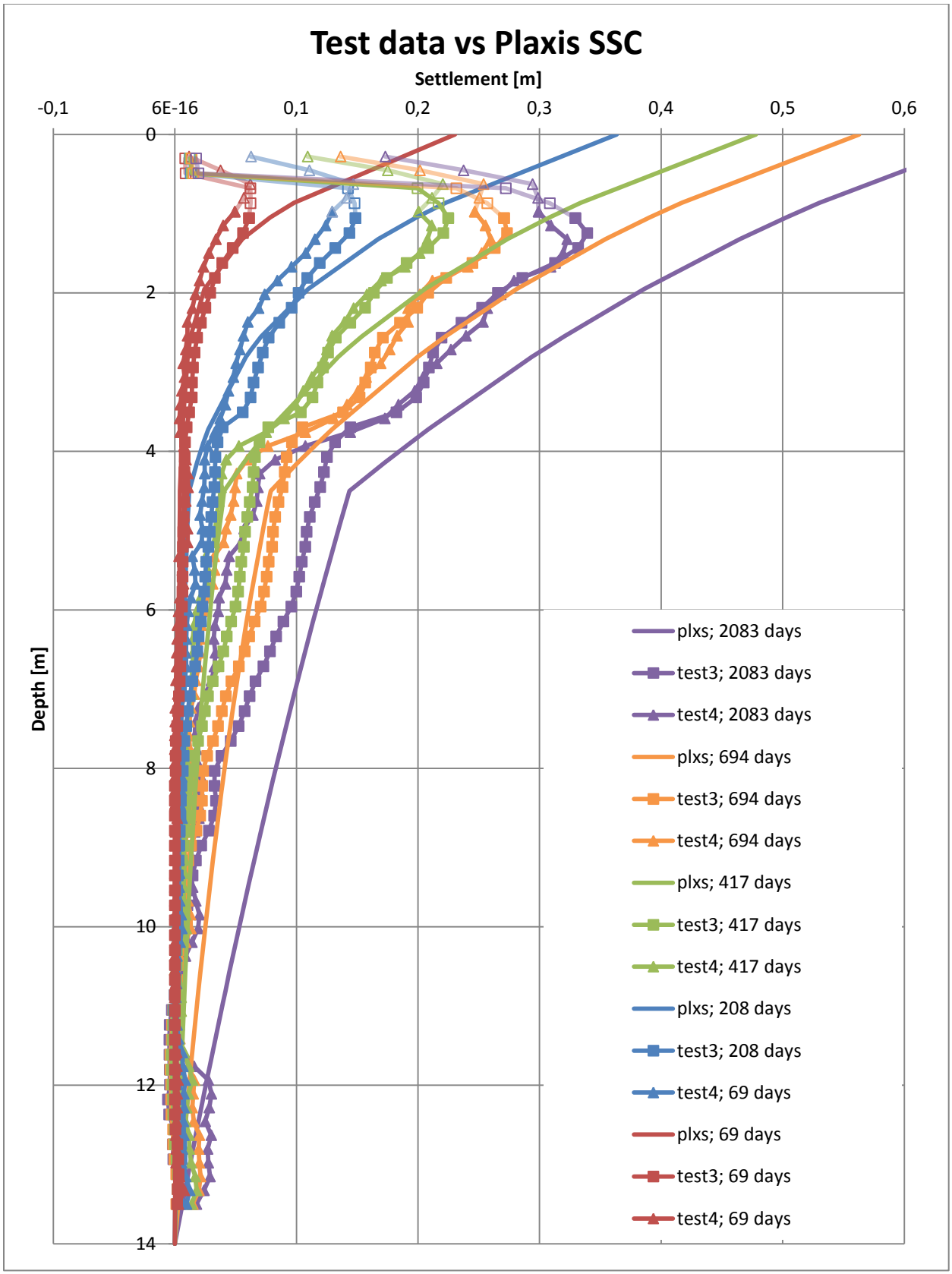

Figure 46 Settlement - depth over time; Physical test data compared with Plaxis SSC calculations

7.2.2.1 Decrease of permeability

[Al Tabbaa and Muir Wood, 1987] did research on the relationship of void ratio and permeability of kaolin clay. Tests on the permeability are done in both the vertical and the horizontal direction. These relationships are presented in equation [24] and [25]. With these equations the decrease in permeability for the sample tested in this research is calculated and plotted in Figure 47.

$$k_v = 0.53 * e^{3.16} * 10^{-9} \ [\mathrm{m/s}] \quad [24]$$

$$k_h = 1.49 * e^{2.03} * 10^{-9} \ [\mathrm{m/s}] \quad [25]$$

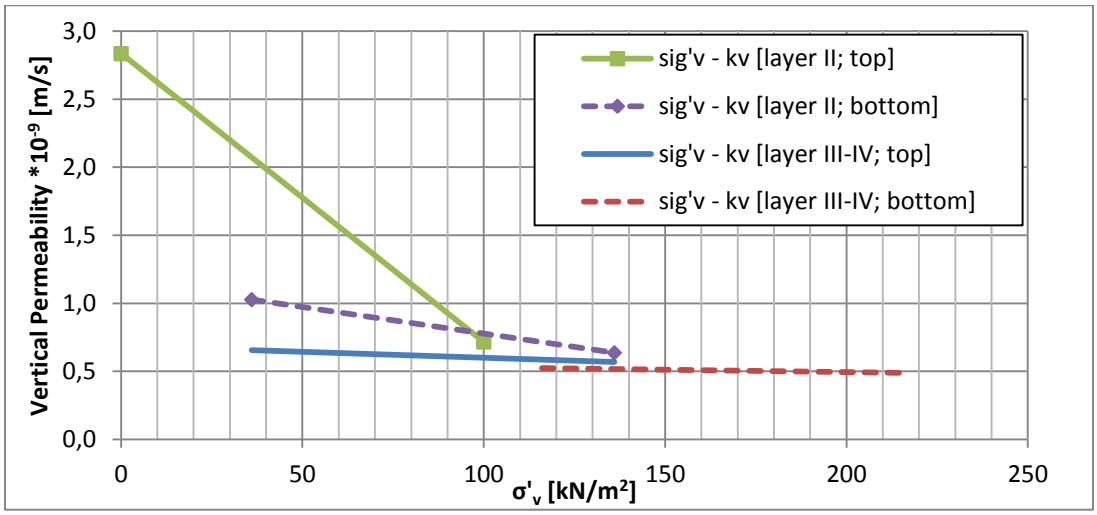

Figure 47: Permeability - Vertical pressure plot

From Figure 47 it can be seen that for the normally consolidated clay layer the decrease in permeability is severe. The top of the normally consolidated layer starts from the initial void ratio (e_0) and is compressed due to the overburden pressure applied. The consequence is a large decrease in void ratio an together with this a pronounced decrease in permeability. This has to do with the more pronounced decrease in void ratio in normal compression. On the interface the difference is noticeable as well. The bottom of the NC clay shows more decrease in permeability than the top of the OC clay layer. For the overconsolidated clay layer the decrease in void ratio is nearly negligible, the lines in the figure are nearly horizontal.

The total values for permeability do not seem to agree with the measured values though. The normally consolidated sample would have a permeability of 3e-9 m/s without any overburden. This is not the case for these tests. This can be seen from the fitted calculations in Figure 37 and Figure 48. Here the permeability of 3e-9 m/s looks like the value which is reached after compression of the clay layers.

7.2.2.2 Settlement time plots at different depths

Settlement plotted in time has been presented in Figure 48. Msettle calculations with varying permeability have been plotted against the measurements done during the two centrifuge tests. The settlements at a depth of 1 meter have been compared to each other, since the measurements in the centrifuge sample are not reliable above this point.

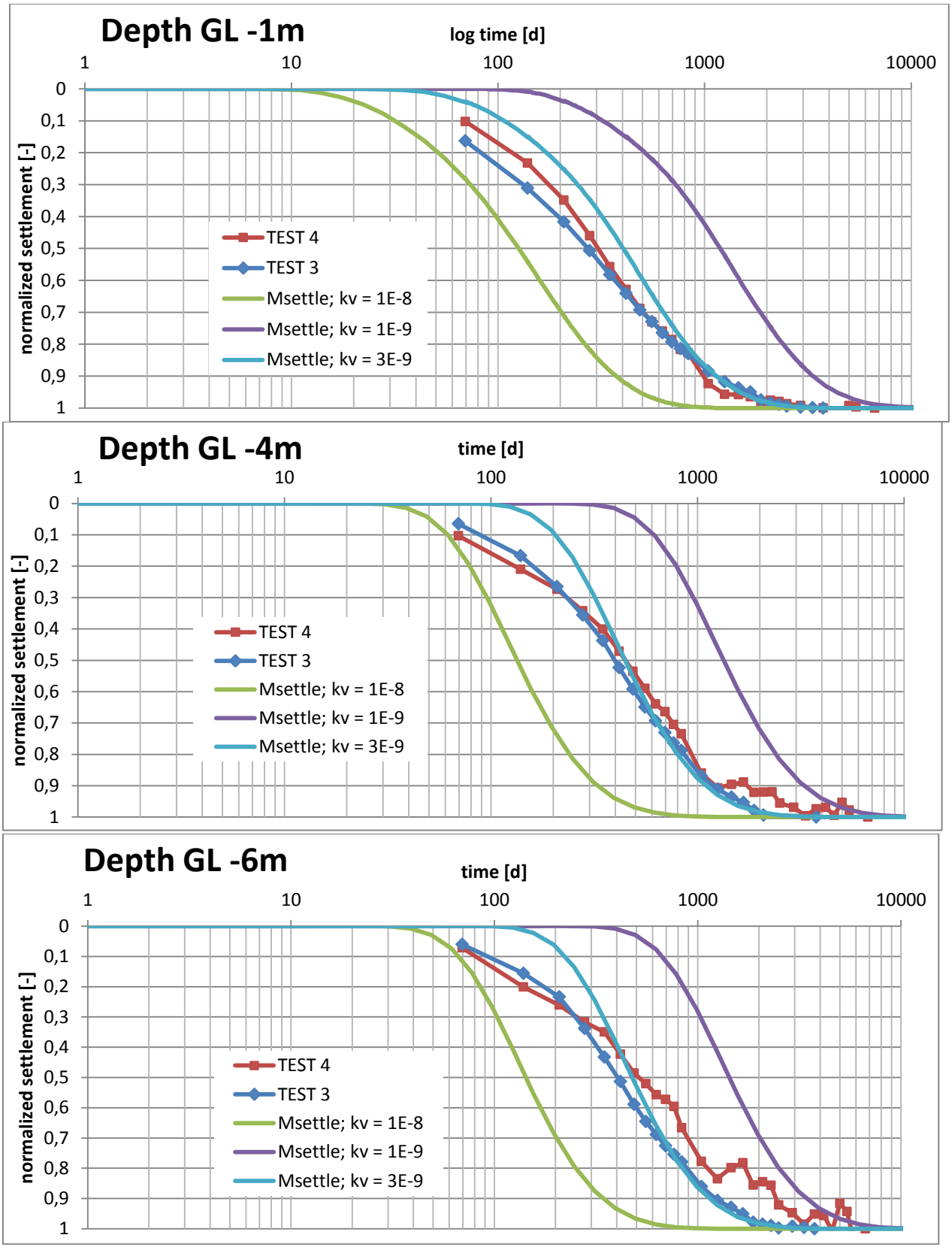

Figure 48: Time - Settlement plots at different depths for the "centrifuge" soil profile

The measurements seem to converge towards the calculation of the settlement with a permeability of 3e-9 m/s. The first measured step is after an equivalent of 70 days, as a result the lines start when some settlement has already taken place. The consolidation process starts earlier than the calculated line (of k_v = 3e-9 m/s), this can be due to higher permeability at the start or the startup of the centrifuge. Because the measurements are started when the centrifuge reaches 100g some consolidation has already taken place before the zero point.

The measurements at a depth of 4 meters and 6 meters below ground level are representative for the stiff, overconsolidated clay layer. 4 meters depth is the bottom of the soft clay layer, near the interface. Expected is that the permeability of this layer is rather constant. Thus the settlement in time measurements should agree with the calculated values better than the earlier discussed graphs. Both plots seem to show this behavior quite well. The measured values look similar to the calculated values with a permeability of 3e-9 m/s, especially after an equivalent of 300 days (45 minutes into the test). The start shows some deviation though, where this is coming from is not known exactly.
The normalization of the plot might be a cause for this. Because the total settlement of the stiff clay layer is small, a small disturbance might already show settlements in this plot. The camera might have moved during the starting up of the centrifuge. This leads to 'movement' of the sample between the first image (zero point) and the second image.

7.2.2.3 Noise in measurements

A point of attention is the accuracy of the measurements in time. Deeper down the measurements become less reliable as discussed in paragraph 7.1.2. The lighting gets less intense with time due to a loss of battery charge. This can be seen in the plots projected in Figure 48, especially from the data of test 4.

The decrease of light can be seen in both time and depth. At the top, 1 meter below ground level, the measurements still seem to be quite accurate. Though deeper down, 4 meters and 6 meters below ground level, the measurements show a lot of inaccuracy later on in the test. Because of the different lighting scheme in test 4 it is more severe in this test than in test 3. Test 3 is therefore deemed more reliable than test 4.

7.2.2.4 Settlement of NC layer

The settlement between 1 meter depth and 4 meters depth is purely compression of the normally consolidated clay layer. If the values from these layers are subtracted from each other than the compression of this clay layer is left. The values this gives can be compared to the measurements from test 1, which is also done on a normally consolidated sample. The settlement values from test 1 between a depth 1 meter and 5 meters are used to compare with.

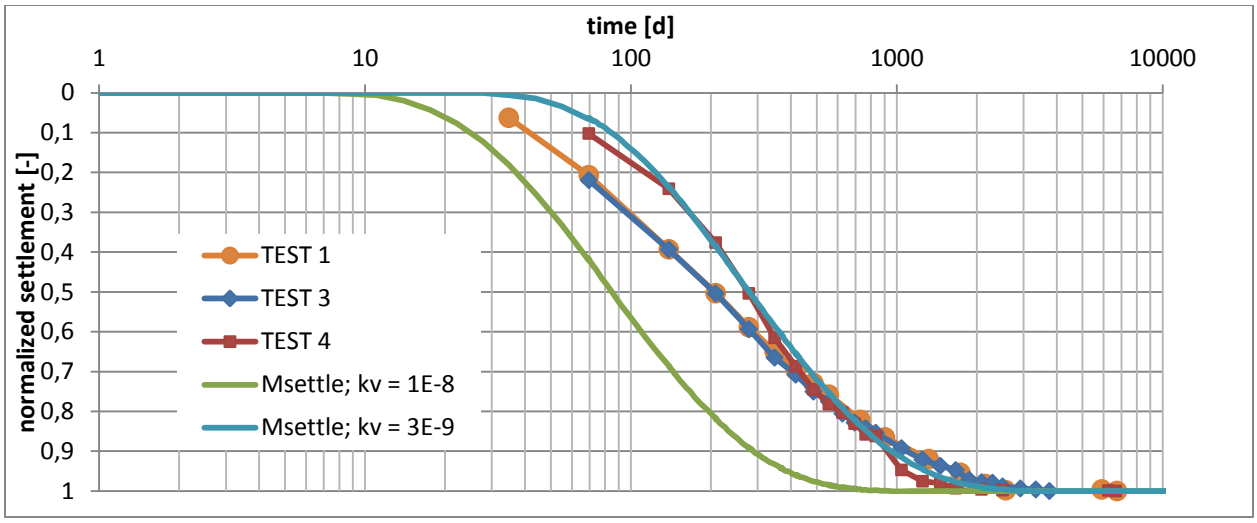

Figure 49: Settlement in time, top part

Figure 49 shows these compared values. Test 1 and 3 agree very well with each other, as can be seen from the graph. Test 4 does not show a very good agreement. This test is influenced by the noise, from the measurement taken at a depth of 4 meters, as explained earlier. The settlement lines show a decrease in permeability as expected, starting settlements ahead of the calculated constant permeability line and converging to it.

7.3 Consolidation in time

Consolidation in time has not been measured in the centrifuge. The permeability is a large uncertainty in the test, and it is hard to give a prediction on this. The only way to get a feel for the permeability is to fit the measured settlement time values to a calculated value. Since this profile consists of 2 different layers, with most likely 2 different values for permeability, it is very hard to give an estimate for the permeability.

Calculations on the consolidation have been done though, with a constant permeability. The results from these calculations are presented in Figure 50. The results plotted in this graph are calculated at the bottom of the sample. The hand calculation has been done with the method introduced in paragraph 4.1. Again the permeability has been assumed constant for all calculation models. The variation in permeability is discussed earlier, but a value for this variation is difficult to assume and the question remains how well this would reflect reality.

As discussed earlier the permeability of the OC clay layer will not change much. This is because the void ratio will not decrease a lot in recompression, because the structure of the clay has already been formed for these stress levels. The large changes in void ratio for the NC clay layer will influence the permeability quite severe though. This can be seen in the measurements as well. The soft layer shows a pronounced decrease in permeability, where the stiff clay layer has this less explicit.

The magnitude of this decrease in permeability might be predicted with the relation given by [Al Tabbaa and Muir Wood, 1987], as discussed earlier in this chapter. The magnitudes of permeability predicted by this relationship between void ratio and permeability seems to be off though.

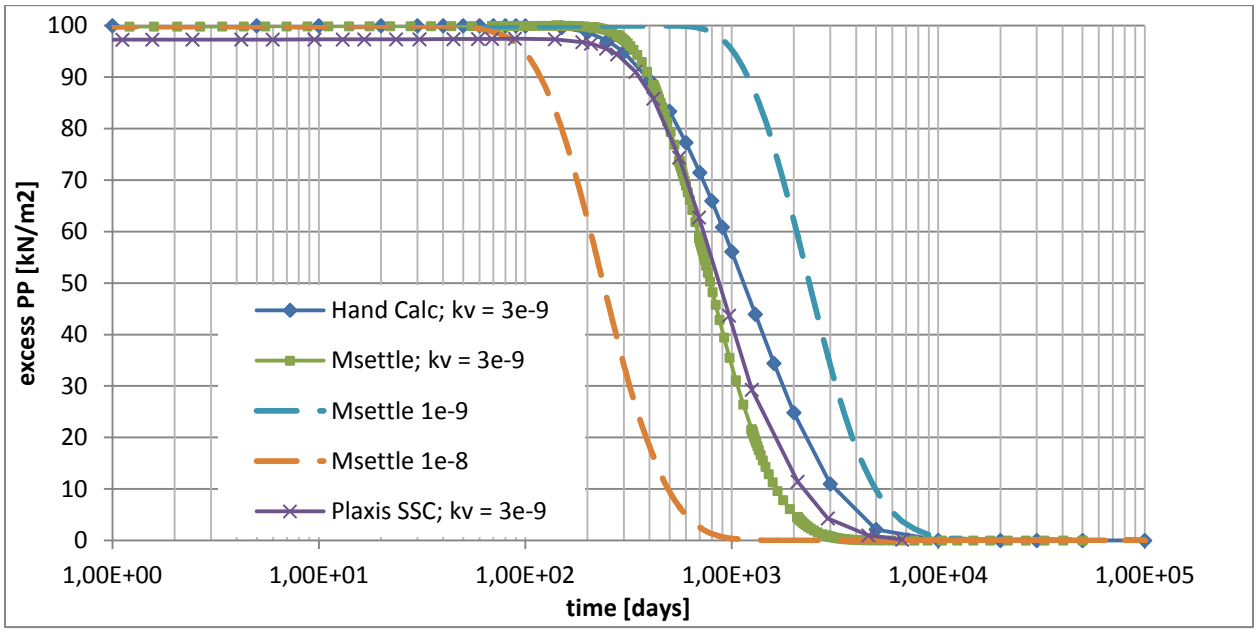

Figure 50: Calculated Consolidation in time at the bottom of the sample; "centrifuge" soil profile

It can be seen from the settlement versus depth plots at different time steps, presented in Figure 45 and Figure 46, that at the start of the consolidation process the predictions are acceptable or even behind the settlements in the centrifuge. This means that the consolidation in the top layer of the centrifuge sample is proceeding faster than in the prediction models. That would suggest that the permeability of the real sample is higher than implemented in the calculation models.

7.4 Conclusion

When the different calculation models are compared to the results from the centrifuge tests the following conclusion can be drawn. The Msettle / Hand Calculation give the most accurate predictions for the soil reaction in the centrifuge. Both the settlement – depth plots and in time these calculation methods give quite good predictions. The differences between the results can be explained, and have to do with inaccuracies in the parameters implemented.

The different Plaxis models which are used to predict the soil reaction give some uncertainties. The recalculation of compression parameters is one of the main things. Especially in recompression, where horizontal stresses influence the isotropic stress, this will give deviations from the Msettle results. The model in Plaxis which is most accurate is the Soft Soil model. This gives the best overall performance, both settlement – depth and settlement – time. From now on the Soft Soil (Creep) model will be used to predict the subsoil reaction. The Cam Clay model gives a big jump in settlements at the top part, but still gives quite good predictions. The Hardening Soil model is influenced by the E50 which will make it react much stiffer than the other models.

8 Pile Soil Interaction

8.1 Model

First the assumptions on which the calculations are done are given. After this the calculations and its results are given.

8.1.1 Reaction of subsoil

As discussed in chapter 7 the advised models are Msettle with Bjerrum compression parameters and Darcy consolidation. The constitutive model best used in Plaxis is the Soft Soil or the Soft Soil Creep model.

With these models the reaction of the subsoil to its new loading situation is calculated. The settlement and stresses on the pile in this subsoil is calculated in this chapter. This is done for the centrifuge soil profile.

8.1.2 Pile

The pile implemented in the calculation is circular, with a diameter of 1 meter. This diameter is a value often encountered in offshore environments. It is assumed as a solid pile, which means only friction on the outer shaft is mobilized. In the centrifuge tests, to be performed in the next study, a solid pile made out of aluminium is most likely to be used. The prediction can thus be checked in this next study.

The length is assumed at 10 meters. This means the pile will not be resting on the bottom of the sample and is still in the deforming soil profile.

8.1.3 Building stages

The calculations have been kept very basic. The same is done with the building stages and the loading of the pile. With the placement of the fill the pile will be placed as well. This means that without any load the pile will be subdued to the full displacement of the soil.

After the end of consolidation, and thus full settlement of the soil profile, the pile is loaded. The load is increased every step and the displacement of the pile head is studied. Since the pile is assumed as infinitely stiff the settlement of the neutral plane is the same as the settlement of the pile head.

8.2 Shear Box Test

Direct shear box tests are performed to get a view of the interaction of the interface between the pile and soil. The test setup, procedure and results are presented in Appendix G. A short summation of the performed tests and results is given in Table 21.

Table 21: Results Direct Shear Box tests

		Test 1	Test 2
Sample Diameter	*[mm]*	75	75
Sample Height	*[mm]*	25	25
Surcharge	*[kg]*	2	2
	[kN/m2]	45	45
Shearing rate	*[mm/min]*	0.0024	0.0024
Peak shear stress	*[kN/m2]*	20.0	18.8
Peak friction angle	*[deg]*	23.8	22.6
Residual shear stress	*[kN/m2]*	15.0	15.5
Residual friction angle	*[deg]*	18.4	19.0

8.3 Analytical Calculations

With the interface strength known the pile soil interaction problem can be calculated. This is done through 2 simple analytical methods already introduced in paragraph 2.3.2.

8.3.1 α-method (total stress method)

The [API, 2005] guidelines give internationally accepted methods for the design of piles. In this guideline equations [26], [27] and [28] are used for the design of skin friction in cohesive soils. Designing the end bearing of a pile in cohesive soil is described by equation [29].

$$f_s = \alpha * s_u \quad [26]$$

$$\boldsymbol{\alpha = 0.5\left(\frac{s_u}{\sigma'_{v0}}\right)^{-0.5}} \quad \text{for} \quad \boldsymbol{\left(\frac{s_u}{\sigma'_{v0}}\right) \leq 1} \quad [27]$$

$$\boldsymbol{\alpha = 0.5\left(\frac{s_u}{\sigma'_{v0}}\right)^{-0.25}} \quad \text{for} \quad \boldsymbol{\left(\frac{s_u}{\sigma'_{v0}}\right) > 1} \quad [28]$$

$$\boldsymbol{q = 9s_u} \quad [29]$$

s_u	:	undrained shear strength	[kN/m^2]
σ'_{v0}	:	effective vertical stress	[kN/m^2]
f_s	:	skin friction	[kN/m^2]
q	:	end bearing capacity	[kN/m^2]

The subsoil reaction has been calculated with Msettle. The settlement at the end of consolidation has been calculated and a pile has been implemented into this. The pile is assumed as infinitely stiff, thus no elastic shortening will occur in the pile. Therefore the displacement of the neutral plane is the same as the displacement of the pile head.

8.3.2 β-method (effective stress method)

The β-method is given for cohesionless soils in the [API, 2005]. Several papers [Burland, 1973], [Mochtar and Edil, 1988] [Doherty and Gavin, 2011] use this method to predict the pile-soil interaction for cohesive soils. Therefore this calculation method has been used to predict the settlement and stresses along the pile. Equations [30] and [31] are used in this calculation method.

$$f_s = \beta * \sigma'_v \quad \textbf{[30]}$$

$$\beta = K_0 * \tan \delta \quad \textbf{[31]}$$

σ'_v	:	effective vertical stress	[kN/m^2]
K_0	:	earth pressure coefficient	[-]
δ	:	interface friction angle	[^{0}]

8.4 Load Settlement Curves

With the friction along the pile soil interfaces known the neutral plane can be determined for different loads. With an increase of the dead load on the pile, it will be pressed more into the soil and thereby pull the neutral plane upwards. With the neutral plane closer to the top of the pile, the zone of positive friction is increased and thus the bearing capacity of the pile. Examples of these plots for both the total stress and effective stress method can be found in Appendix H.

In Figure 51 the load displacement curves of both methods have been projected. The pile in this calculation is assumed infinitely stiff. The settlement of the neutral plane is thus the settlement of the pile head. It can be seen that the alpha method give a higher stiffness to the pile than the beta method. The P_{max} for the alpha method is estimated higher as well.

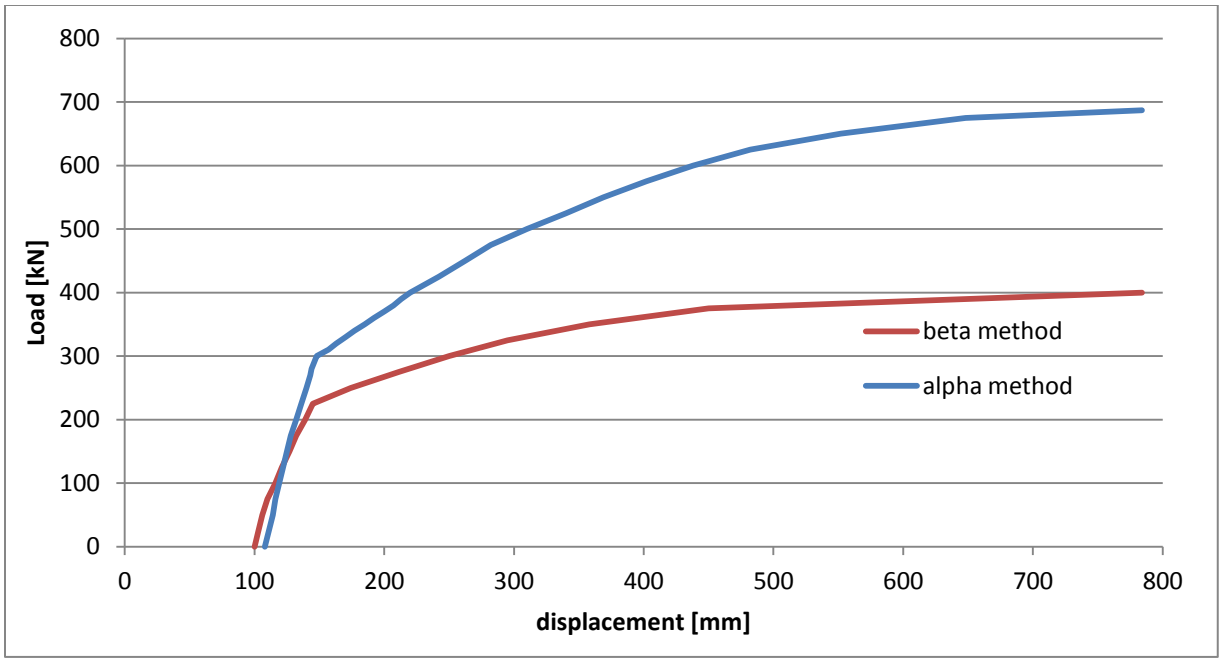

Figure 51: Load Displacement curves for the alpha and the beta method

The decrease of stiffness which can be seen in both methods is due to the neutral plane passing from the stiff clay layer into the soft clay layer.

8.5 Comparing different models

The results of the α- and β method vary by approximately 300 kN when full shaft friction is activated. This is nearly 75% of the total strength calculated with the β method, which is high. The calculated values for α are taken from the API guidelines. Expected is that there is some safety in these calculated values. The values for β are calculated with the interface friction angle which is tested, and an estimated earth pressure coefficient.

Since the values for α are calculated from guidelines it would be expected that there is some safety in here. Still the shaft capacity for this method is much higher than the calculated values for the effective stress method.

The effective stress method gives an underestimation of the shaft capacity compared to the total stress method. Especially in the overconsolidated soil, where the estimated earth pressure coefficient gives an underestimation of the horizontal stresses. Since in overconsolidated soils the horizontal stresses remain even after the overburden has been removed the calculated horizontal stresses will be an underestimation of reality.

8.6 Discussion

Several simplifications are done to make a quick calculation of the piles. First of all the end bearing effects have not been applied in this calculation. This end bearing will add to the stiffness and bearing capacity of the pile. The positive friction graph will be moved away from the pile, and thus the neutral plane is moved deeper into the soil. The forces at the bottom of the pile will add to the total bearing capacity. The height of this end bearing capacity and its mobilization can be assumed from guidelines.

The pile has been wished into place for this research, ignoring installation effects. The pile will be driven into the soil, which will create disturbance of this soil. In normally consolidated or slightly Over Consolidated soils this will lead to an increase in pore water pressures, and thus a decrease of effective stresses due to compaction of the soil skeleton [Randolph and Gouvernec, 2011].
In highly overconsolidated soils this can lead to dilation effects. Disturbing the compacted soil skeleton and leading to an increase in void ratio with the consequence of a decrease in pore water pressures [Randolph and Gouvernec, 2011]. These leads to an increase in effective stress and thus shear strength during installation. If these effects play an important role in clays should be studied more extensively.

The time effects on the shaft friction due to consolidation. The dissipation of pore water pressures leads to an increase in effective stress. Combined with this the shear strength of the soil and the pile-soil interface will increase. The influence of this over the length of the pile has not been reviewed in this research.

Time of installation is important because of the above named problem. Besides the time of installation there is the time of loading. Especially deeper along the pile shaft excess pore pressures exist long after the overburden has been placed. This is the zone where bearing capacity is mobilized by the pile, and this will thus be lower when consolidation is still in progress.

In the total and effective stress method there is no influence of peak and residual strength. In these methods the interface friction is fully mobilized when even the smallest relative displacements occur. Especially near the neutral plane, where relative displacements between pile and soil are small, this has an influence. The t-z curves do model this behavior and therefore give a more accurate representation of the soil strength. The calculations for the effective stress methods are performed with the residual friction angle. Along most parts of the interface the displacements are of such a magnitude that the residual strength is reached, and this is deemed a more reliable value.

Plugging of the pile has been assumed for the calculation performed. Since in the centrifuge a solid aluminium pile will be used, this plugged situation is a reasonable assumption. If plugging really occurs in the real situation, with large diameter steel tubular piles, should be examined.

9 Conclusions

Recreating a two layer soil profile, where one layer contains stiff clay and the other soft, can be done in the centrifuge. Calculation methods have been benchmarked to the results of the centrifuge tests. These predictions give an accurate representation of the settlement in the physical model. Settlement in depth is most accurately described by the program Msettle, which uses Bjerrum settlement and Darcy's consolidation equation, and Plaxis, using the constitutive Soft Soil model. The settlements in the centrifuge are predicted with an accuracy of about ten percent.

The settlement in time seems to be described accurately as well. The permeability, which has a dominant role on settlement in time, and its decrease in loss of void ratio are not precisely known before the test. Calculations are done with a constant permeability. As expected the centrifuge results seem to diverge from a higher permeability (1e-8 m/s), and converge towards a calculated settlement line with a lower permeability (3e-9 m/s). The "settlement in time" lines are calculated with Msettle and give a good image of the decrease in permeability during the test.

The progression of settlement in depth, during the test, can be measured accurately from the centrifuge. Again this is influenced by the decreasing permeability of the centrifuge sample, but the differences which occur are expected beforehand. The settlements, especially at the top of the sample, occur earlier than the calculated values which have been given a constant permeability. Later on in the test the calculated values converge towards the measured values.

The measured compression parameters agree well with the values found in the literature. These compression parameters are tested in an oedometer test, and are given in a one dimensional stress space. Recalculation of the compression parameters into isotropic stress dependant parameters does not give the same settlement predictions. The used relationships given in the Plaxis 2D Material Models manual do not seem to give an accurate relation.

The initial void ratio is tested from the normally consolidated clay sample, after being consolidated for one day in the centrifuge. This value does show some deviation from the values in literature. The measured undrained shear strength is strongly dependent on the stress history the soil has been subdued to.

The performed direct shear box tests show that the peak friction is mobilized at displacements of about one millimeter. Further shearing led to the residual friction which meant a decrease in shear stress of about 20%. Both samples tested in the shear box showed the same behavior and reaction to shearing, a deviation in results of about 5% was noticed.

10 Recommendations and Further Study

To gain more insight in the reaction of friction piles in a settling soil profile, the following research steps are recommended:

1. A more extensive investigation on the recompression behavior of the used test soil. In the current work only two oedometer tests have been performed on a sample which has been consolidated to a certain pressure in the geotechnical centrifuge. More load steps in recompression and tests on different samples are advised.
2. The sample illumination in the centrifuge should be significantly improved. Battery powered ligths gave problems for tests over a prolonged period. As discussed in the report the loss of battery charge leads to an error in measurements. In future tests the lighting should be connected to a more stable power source (i.e. the power grid), so that a decrease of light intensity will not occur. The latter will increase the reliability of the measurements.
3. The permeability and the evolution of permeability during compressesion of the used kaolin clay should be studied in more detail. Therefore, the current assumptions for the permeability can be validated, as permeability tests can be easily performed in the centrifuge.
4. A more thorough research into the interface friction angle between the soil and the pile, e.g. with direct shear box tests, should be considered. In addition to the in this research performed drained tests at one overburden pressure several more tests with varying overburden pressures can give a better overview on the friction angle and adhesion on the interface.
5. Only two formulas for the values for α and β have been used in this research, one for both factors. However, many different formulas have been suggested to predict the values for α and β. These could be investigated using Mpile, with t-z curves tested from the shear box, or in Plaxis and compared to future model tests.
6. With an instrumented model pile in a settling soil profile these different calculation models can be validated.
    a. Distinction should be made between end bearing capacity and shaft friction. This can be done with a separate load cell at the pile base.
    b. Differential settlement between the pile and soil can be examined as well. The pile is infinitely stiff and soil settlements can be measured in the same way as done in this research.

    c. Settlement of the neutral plane can be assessed by assuming the pile as infinitely stiff as well. The settlement of the pile head, which can easily be measured, is the same as the neutral plane. Continuous measurements of the load-settlement response of the pile head during loading should give a good image of the neutral plane.
    d. Variations in building phases can be investigated. The pile can be installed at different stages in the test. The loading scheme of the pile therefore is varied as well.
7. Time dependant behavior of the interface reaction. Due to an increase of effective stress with the dissipation of pore water pressures the shaft friction will increase. The effect of this over the depth of the pile deserves some more research.
8. Creep has been neglected in this study. Since creep is a purely time dependent process, this is not scaled in the centrifuge. The magnitude of creep settlements can be monitored in a oedometer tests. The effect of different stress levels might be tested as well. The amount of creep settlements over depth of the soil sample and its influence on the pile-soil interaction should be studied more extensively.
9. Effects of installation of the pile should be studied more extensively. A lot of research has been done into these effects. Does the normally consolidated clay show a higher increase in water pressures, and does dilation occur in highly overconsolidated clays are points of attention in this.
10. By increasing the surface roughness of the pile the interface friction angle is increased. This will increase the shaft friction along the pile-soil interface. The influence of this surface roughness can be studied in both the direct shear box and on the model pile in the centrifuge. The smooth pile can be used as a base and different surface roughness can be compared to this.
11. Testing on field samples is a valuable addition to this study. Since kaolin is a pure clay sample which does not show the same reaction as clay from the field. Effects like anisotropy and lateral loading occur in field conditions and should be considered.

11 References

Al-Tabbaa, A., Muir Wood, D., 1987. *Some measurements of the permeability of kaolin*, Geotechnique, Vol. 37, No. 4, pp. 499 – 503

American Petroleum Institute, 2005. *Recommended Practice for Planning, Designing and Constructing Fixed Offshore Platforms – Working Stress Design – Errata and Supplement 2 (October 2005),* API RP 2A-WSD

American Society for Testing and Materials, 1995. *ASTM D4318-10 Standard Test Methods for Liquid Limit, Plastic Limit and Plasticity Index of Soils*

American Society for Testing and Materials, 1998. *ASTM D3080-98 Standard Test Method for Direct Shear Test of Soils Under Consolidated Drained Conditions*

Amini, A., Fellenius, B.H., Sabbagh, M., Naesgaard, E., Buehler, M., 2008. *Pile loading tests at Golden Ears Bridge*, 61st Canadian Geotechnical Conference, 8 p.

Bjerrum, L., 1967. *7th Rankine Lecture: Engineering Geology of Norwegian Normally-Consolidated Marine Clays as related to Settlements of Buildings*, Geotechnique 17, pp. 81 – 118

Bozozuk, M., 1981. *Bearing Capacity of Pile Preloaded by Downdrag*, 10th International Conference on Soil Mechanics and Foundation Engineering

Brinkgreve, R.B.J., Broere, W., Waterman, D., 2008. *Plaxis 2D Reference Manual Version 9.0*, Plaxis bv, ISBN-13 978-90-76016-06-1

Brinkgreve, R.B.J., Broere, W., Waterman, D., 2008. *Plaxis 2D Material Models Manual Version 9.0*, Plaxis bv, ISBN-13 978-90-76016-06-1

Brinkgreve, R.B.J., Broere, W., Waterman, D., 2008. *Plaxis 2D Scientific Manual Version 9.0*, Plaxis bv, ISBN-13 978-90-76016-06-1

British Standard, 1990. *BS 1377, part 2, Methodsof test for soils for Civil Engineering purposes. Classification tests*

British Standard, 1990. *BS 1377, part 7, Methods of test for soils for Civil Engineering purposes. Shear strength tests (total stress)*

Burland, J.P., 1973. *Shaft friction of piles in clay – a simple fundamental approach*, Ground Engineering, Vol. 6, No. 3, pp. 30 – 38

Chan, S.H., 2004. *Negative Skin Friction on Piles in Consolidating Ground,* Mphil Thesis, Hong Kong University of Science and Technology

Deltares, 2009. *Msettle Version 8.2: Embankment Design and Soil Settlment Prediction,* ISBN 978-90-810136-4-2

Den Haan, E.J., 1994. *Vertical Compression of Soils,* Delft University Press, ISBN 90-407-1062-7

Det Norkse Veritas, 1992. *Foundations,* Classification Notes, No. 30.4

Doherty, P., Gavin, K., 2011. *The Shaft Capacity of Displacement Piles in Clay: A State of the Art Review,* International Journal of Geotechnical and Geological Engineering, Vol. 29, No. 4, pp. 389 – 410

Dolukhanov, P.M., Chepalyga, A.L., Shkatova, V.K.., Lavrentiev, N.V., 2009. *Late Quaternary Caspian: Sea-Levels, Environments and Human Settlement,* The Open Geography Journal, Vol. 2, pp. 1 – 15

Fellenius, B.H., 1984. *Negative Skin Friction and Settlement of Piles*, Second International Seminar on Pile Foundations, 12 p.

Fellenius, B.H., 1998. *Recent Advances in the Design of Piles for Axial Loads, Dragloads, Downdrag and Settlement*, ASCE and Port of NY&NJ Seminar

Fellenius, B.H., 2006. *Results from long-term measurement in piles of drag load and downdarg*, Canadian Geotechnical Journal, Vol. 43, No.4, pp. 409 – 430

Fleming, K., Weltman, A., Randolph, M., Elson, K., 2009. *Piling Engineering*, *3rd edition,* Taylor & Francis, ISBN13 978-0-415-26646-8

Fugro, 2011. *Geotechnical Report Investigation Data, Caspian Sea Kazakhstan,* Shell Development Kashagan B.V.

Golubev, G.N., 1998. *Environmental policy-making for sustainable development of the Caspian Sea area*, Central Eurasian water crisis: Caspian, Aral and Dead Seas, pp. 91 – 104, ISBN 92-808-0925-3

Gorasia, R.J., McNamara, A.M., 2012. *Higher shear capacity ribbed piles,* Proceedings of the 2nd European conference on Physical Modelling in Geotechnics

Jardine, R.J., Chow, F.C., Overy, R., Standing, J., 2005. *ICP design methods for driven piles in sands and clays*, Thomas Telford, ISBN 0 7277 3272 2

Keverling Buisman, A.S., 1936. *Results of long duration settlement tests*, Proceedings of the 1st international Conference on Soil Mechanics and Foundation Engineering, pp. 103 – 107

Kolk, H.J., Baaijens, A.E., Senders, M., 2005. *Design criteria for pipe piles in silica sands,* Proceeding of the International Symposium on Frontiers in Offshore Geotechnics, pp 711 – 716

Koppejan, A.W., 1948. *A formula combining the Terzaghi load-compression relationship and the Buisman secular time effect*, Proceedings of the 2nd International Conference on Soil Mechanics and Foundation Engineering, pp. 32 – 37

Lam, S.Y., Ng, C.W.W., Leung, C.F., Chan, S.H., 2008. *Centrifuge and numerical modeling of axial load effects on piles in consolidating ground*, Canadian Geotechnical Journal, Vol. 46, No. 1, pp. 10 – 24

Leroueil, S., 1996. *Compressibility of Clays: Fundamental and Practical Aspects*, Journal of Geotechnical Engineering, Vol. 122, No. 7, pp. 534 – 543

Mamedov, A.V., 1997. *The Late Pleistocene – Holocene history of the Caspian Sea*, Quaternary International, Vol. 41 – 42, pp. 161 – 166

Mesri, G., 1985. *Settlement Analysis of Embankments on Soft Clays,* Journal of Geotechnical Engineering, Vol. 111, No. 4, pp. 441 – 464

Mochtar, I.B., Edil, T.B., 1988. *Shaft Resistance of Model Pile in Clay*, Journal of Geotechnical Engineering, Vol. 114, No. 11, pp. 1227 – 1244

Muir Wood, D., 2004. *Geotechnical Modelling*, Taylor & Francis, ISBN 978-0-203-47797-7

Ovando-Shelley, E., 1994. *Direct shear tests on Mexico City clay with reference to friction pile behavior*, Geotechnical end Geological Engineering, Vol. 13, No. 1, pp. 1 – 16

Price, D.G., de Freitas, M.H. (ED), 2009. *Engineering Geology - Principle and Practices,* Springer-Verlag Berlin Heidelberg, ISBN 978-3-540-29249-2

Randolph, M.F., Murphy, B.S., 1985. *Shaft capacity of driven piles in clay*, Proceedings of the 17th annual offshore technology conference, pp. 371 – 378

Randolph, M.F, Gouvernec, S., 2011. *Offshore Geotechnical Engineering,* Spon Press, ISBN 978-0-415-47744-4

Reese, C.L., 1990. *The action of soft clay along friction piles: bay mud revisited*, http://www.vulcanhammer.org/

Schneider, J.A., Xu, X., Lehane, B.M., 2008. *Database assessment of CPT design methods for axial capacity of driven piles in siliceous sands,* Journal of Geotechnical en Geoenvironmental Engineering, Vol. 134, No. 9, pp. 1227 – 1244

Sridharan, A., Venkatappa Rao, G., 1973. *Mechanisms controlling volume change of saturated clays and the role of the the effective stress concept*, Geotechnique, Vol. 23, No. 3, pp. 359 – 382

Suklje, L., 1957. *The analysis of the consolidation process by the isotaches method*, Proceedings of the 4th International Conference of Soil Mechanics and Foundation Engineering, pp. 200 – 206

Sun, D.A., Matsuoka, H., Morichi, K., Tanaka, Y., Yamamoto, H., 2003. *Frictional behaviour between clay and steel by direct shear type apparatus,* Chapter 30 of Deformation Characteristics of Geomaterials, Swets & Zeitlinger, pp. 239 – 245, ISBN 978-90-5809-604-3

Taylor, R.N. (ED.), 1995. *Geotechnical Centrifuge Technology*, Blackie, ISBN 0-7514-0032-7

Terzaghi, K., 1925. *Erdbaumechanik auf bodenphysikalischer Grundlage*, Leipzig und Wien, Franz Deuticke

Terzaghi, K., Peck, R.B. (ED.), Mesri, G. (ED.), 1996. *Soil Mechanics in Engineering Practice, 3rd edition*, John Wiley & Sons, ISBN 978-0-471-08658-4

Tomlinson, M.J., 1957. *The adhesion of piles driven in clay soils,* Proceedings of the 4th international conference on soil mechanics and foundation engineering, London

Tomlinson, M. J., Woodward, J., 2008. *Pile Design and Construction Practice, 5th edition,* Taylor & Francis, ISBN 978-0-415-38582-2

Venneman, JPIV program, http://www.jpiv.venneman-online.de/

Verruijt, A., 2001. *Soil Mechanics*, Delft University of Technology

APPENDICES

APPENDIX A

Site Investigation; Interpretation

Extensive site investigation (SI) consisting of boreholes and CPTs have been done at the location of the reference project. During the soil exploration samples are retrieved from different depths in the subsoil. These samples have been tested in the laboratory to obtain the different hydraulical and mechanical properties.

11.1.1 Boreholes and CPTs

The SI has been done to get an overview of the different layers in the subsoil located at the project site. The tests are done to a specified depth, or until a bottom rock layer is encountered. The risk of damage or safety is increased if in these situations drilling would continue in the rock layer.

Soil exploration has been done in a large area of the Caspian Sea [Fugro, 2011]. Selected is the data which is focused on an area around the reference project. The boreholes are alternated with CPTs at varying depths. From the CPTs the cone resistance of the soil is measured. Various mechanical material properties can be correlated from this, such as unit weight and undrained shear strength.

Samples are taken by percussion sampling and piston sampling. The percussion sampling is done by dropping a weight on the sampler, which is than hammered into the soil. This is a very common way to get “disturbed” samples from the soil [Price, 2009]. Piston sampling works like the name indicates. A sampler is pushed into the soil and a soil samples will be taken out of the subsoil. The samples are taken at regular intervals.

11.1.2 Laboratory tests

Different laboratory tests have been done on the retrieved samples. Soil properties like: compressibility, permeability, unit weight, friction angle and cohesion have been tested. Several testing methods have been used to tests these properties.

11.1.2.1 Classification testing

Classification tests are done to give values for the following properties:

- Unit weight
- Density (void ratio)
- Water content
- Particle size analysis
- Atterberg limits

With the unit weight of the different layers the in situ total stress can be calculated. By subtracting the water pressure from this the current effective stress can be determined. The initial void ratio is used in other tests like the oedometer test.

The other properties are used to classify the soil. Atterberg limits are used for clay layers, which are the main focus of this study. The water content is used in the calculation of the unit weight. The particle size analysis gives the distribution of soils in a certain sample (mainly clay / silt or sand).

11.1.2.2 Strength testing

Strength testing comprises of:

- Pocket penetrometer
- Torvane
- Triaxial tests
    - Unconsolidated Undrained (UU)
    - Consolidated Undrained (CU)
    - Consolidated Drained (CD)

Soil properties like cohesion (c'), friction angle (ϕ'), undrained cohesion (c_u) and stiffness (E) are determined in these tests. The pocket penetrometer and torvane tests are used to investigate the c_u, which are related to the CPT data as well. The values given by the penetrometer and torvane are used to check these values and the measured property seems to agree.

From the triaxial tests the other properties can be calculated. Depending on the form of the test (UU, CU or CD) the drained or undrained properties of the tested sample can be determined. The drained cohesion and friction angle can be determined with an undrained triaxial test as well. The tests will describe a failure envelope in "shear stress – axial stress" space, from this failure envelope the drained strength properties can be determined [Verruijt, 2011].

11.1.2.3 Compressibility testing

Compressibility testing has been done on multiple samples.

- Oedometer tests

From these tests the compression parameters are determined. The results of the oedometer tests are presented primarily in "void ratio – vertical effective stress" diagrams and a few "settlement – time" graphs are attached in Appendix B. The different compression parameters can be determined from these diagrams, and are also presented in the site investigation reports. C_c, C_r are related to the "void ratio – stress" graphs and C_α has been determined from the "settlement – time" graph. The preconsolidation pressure is determined with the graphical "Casagrande" construction [Terzaghi et al, 1996].

Besides the compressibility properties of the soil the hydraulic conductivity has been tested in the oedometer tests. With the coefficient of consolidation (c_v) and the compressibility coefficient (m_v), which are properties that can be calculated from the oedometer test results, the hydraulic conductivity (k_v) is calculated. This is done with equation [32], given by [Terzaghi et al, 1996].

$$c_v = \frac{k_v}{\gamma_w} * m_v \qquad \textbf{[32]}$$

11.1.3 Interface testing

Besides the soil exploration and property testing of the soil, interface tests have been done as well. Interface tests describe the behavior of surface between the soil and another material, like concrete, steel or plastic. Since the interface between the pile and the soil is of great importance for this research, these tests are very useful.

The interface tests that have been done are focused on pipelines. Stress conditions are low in this situation because of the shallow depth of pipelines, which are close to the soil surface. The tests performed are varied with different types of soils and construction material. The soils are clay and sand, the construction material is concrete and plastic with a smooth and rough surface.

Results of the different tests can be found in Figure 52. The different series describe a series of tests with a certain material;

- Series 1; Sand
- Series 2; Soft Clay
- Series 3; Stiff Clay

Series	Interface	Stresses [kPa]		Coefficient of Friction μ [-]
		Normal	Shear	
1	Smooth	10	5	0.50
		20	9	0.45
		40	20	0.50
	Rough	10	9	0.90
		20	16	0.80
		40.5	31	0.78
	Concrete	10	11	1.10
		20	18	0.90
		40	31	0.78
	Soil-Soil	10	8	0.80
		20	17	0.85
		39.5	31	0.78
2	Smooth	10	9	0.90
		20	11	0.55
		40	17	0.42
	Rough	10	11	1.10
		20	16	0.80
		40	26	0.65
	Concrete	10	13	1.30
		20	20	1.00
		40	25	0.62
	Soil-Soil	10	6	0.60
		20	12	0.60
		40	21	0.53
3	Smooth	10	6	0.60
		20	10	0.50
		40	17	0.42
	Rough	10	8	0.80
		20	12	0.60
		39.5	21	0.53
	Concrete	10	10	1.00
		20	15	0.75
		40	21	0.53
	Soil-Soil	10	7	0.70
		20	14	0.70
		40	22	0.55

Figure 52: Results Shear Tests

As can be seen the shear strength of the interface between soil and rough plastic / concrete is higher than the soil – soil shear strength. This does not seem logical, if the soil does not fail on the interface it will fail on the soil – soil interface which describes an upperbound of the interface strength. An explanation for these results can be that in a shear box, the failure surface is forced in a certain place (the plane between the upper and lower part of the box). This means that the strength is purely focused on the interface, where in situ the soil would fail elsewhere.

11.2 Ground Model

From the site investigation done at the reference location a ground model has been set up. The subsoil has been split up in several “general” soil layers. Soil properties have been obtained for these different layers as well. These properties are based on the laboratory tests done on the retrieved samples.

The first clay layer encountered is a “soft” layer. This layer will cause the most settlement but is not very thick. A “firm to stiff” clay layer is located close to the surface. This layer has a varying thickness but is always more than 15 meters thick. Somewhat deeper beneath this layer there is a “very stiff to hard” clay layer. This layer is again varying in thickness but is normally present with a thickness of about 15 to

20 meters. Below these soft soil layers a rock layer is present. This rock layer is assumed to be incompressible and impermeable.

The chosen dimensions for the model profile are given in Table 22. The parameters presented in Table 23 and Table 24 are derived from several site investigations. How these parameters are derived can be found in Paragraph 11.2.1. An image of the subsoil profile can be found in the main report.

Table 22: Dimensions of Soil Profile

	Soil Layer	Top [m + RL*]	Bottom [m + RL*]	Thickness [m]
I	Rock fill	+8	0	8
II	"Soft" Clay	0	-1 (-0.5 to -2.0)	1 (0.5 to 2)
III	"Stiff" Clay	-1 (-0.5 to -2.0)	-20 (-15 to -25)	19 (14 to 24)
IV	"Hard" Clay	-20 (-15 to -25)	-40 (-35 to -45)	20 (10 to 30)
V	Calcilutite Rock Layer	-40 (-35 to -45)	-	-

* RL = Reference Level

Table 23: Soil properties per soil layer, determined from the Site Investigation

Layer	γ [kN/m^3]	c [kN/m^2]	ϕ [kN/m^2]	c_u [kN/m^2]		Initial Void Ratio [-]	Porosity [-]
I	20.5	-	-	-		-	-
II	18	8	29	15		1.00	0.50
III	18.5	15	29	top: bottom:	35 120	0.80 (0.60 – 1.00)	0.44
IV	19.5	15	29	top: bottom:	140 230	0.70 (0.50 – 0.90)	0.41
V	-	-	-			-	-

Table 24: Soil parameters per soil layer, determined from the Site Investigation

	Bjerrum Compression Parameters				
Layer	**Compression** C_c [-]	**Recompression** C_r [-]	**Secondary Compression** C_α [-]	k_v [m/s]	**POP** [kN]
I	-	-	-	-	-
II	0.34 (0.19 – 0.58)	0.08 (0.05 – 0.17)	0.008 (0.007 – 0.009)	1.0e-8	0
III	0.34 (0.19 – 0.58)	0.07 (0.05 – 0.17)	0.008 (0.007 – 0.009)	1.0e-10	400
IV	0.22 (0.13 – 0.32)	0.06 (0.03 – 0.10)	0.008 (0.007 – 0.009)	1.0e-10	500
V	-	-	-	-	-

11.2.1 Derivation of Parameters

The parameters given earlier in this chapter are based on several site investigations. A reference location has been chosen, and the site investigations done in the perimeter of this reference location have been used to determine the parameters.

11.2.1.1 Unit Weight

The borehole logs in Appendix B contain data on the unit weight of each layer, plotted against depth. The unit weight seems fairly constant per layer. The mean value for the unit weight of each clay layer has been taken and is presented in Table 23.

11.2.1.2 Cohesion and friction angle

The cohesion and friction angle describe the drained strength of the soil. Since the lifetime of the facilities build upon this soil will exceed the consolidation time, at some point a drained situation will occur. These parameters can be calculated from triaxial tests done in the site investigation.

Consolidated Undrained (CU) triaxial tests are performed with pore pressure measurements. These tests give a stress path in “p’-q” space. For tests with multiple shearing stages a failure envelope can be derived and cohesion and friction angle can be determined. Samples from different depths have been tested and the values have been presented in the site investigation. The mean values have been taken for the layers in the model and are presented in Table 23.

Since no CU triaxial tests are available for layer II the parameters are based on engineering judgment and experience with normally consolidated clay layers.

11.2.1.3 Hydraulic conductivity

Hydraulic conductivity has been tested during the oedometer tests performed on several samples. This parameter is assumed constant in horizontal and vertical direction. This assumption is supported by the process in which the soil layers have been deposited. The clay layers present in the reference project are thick marine clay deposits, in which the horizontal and vertical hydraulic conductivity will not vary a lot [Terzaghi et al, 1996].

In Figure 53 hydraulic conductivity has been plotted versus depth. These values have been tested in an oedometer test, at different pressures placed on top of the sample. Since the value of permeability is calculated from the compressibility of the soil, these measurements have a large scatter and are not very reliable. The value of the hydraulic conductivity has been taken constant for the deeper clay layers. The top “soft” clay layer has a higher hydraulic conductivity as can be seen in the figure.

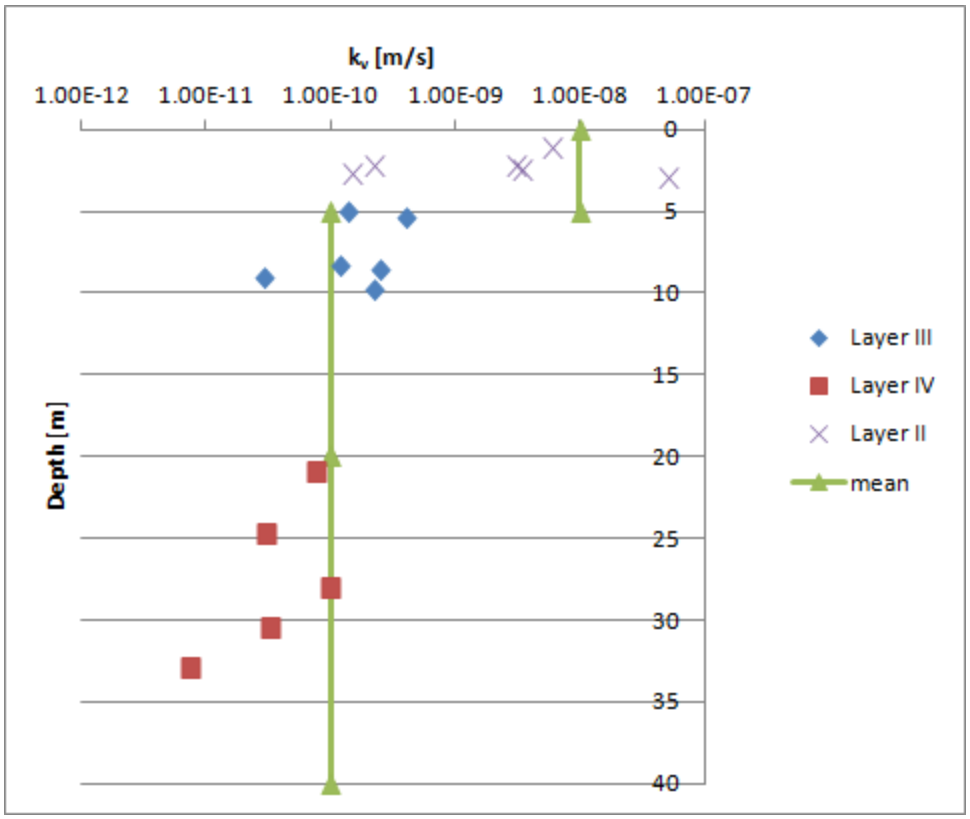

Figure 53: Permeability in depth

11.2.1.4 Compression parameters

The samples, taken from different depths, have been tested in an oedometer apparatus for their compression parameters. The tested values for the parameters have been plotted versus depth in Figure 54. The data has been split up in values describing layer III and IV. Mean values for both layers have also been plotted in the graph. For the recompression parameter the same has been done.

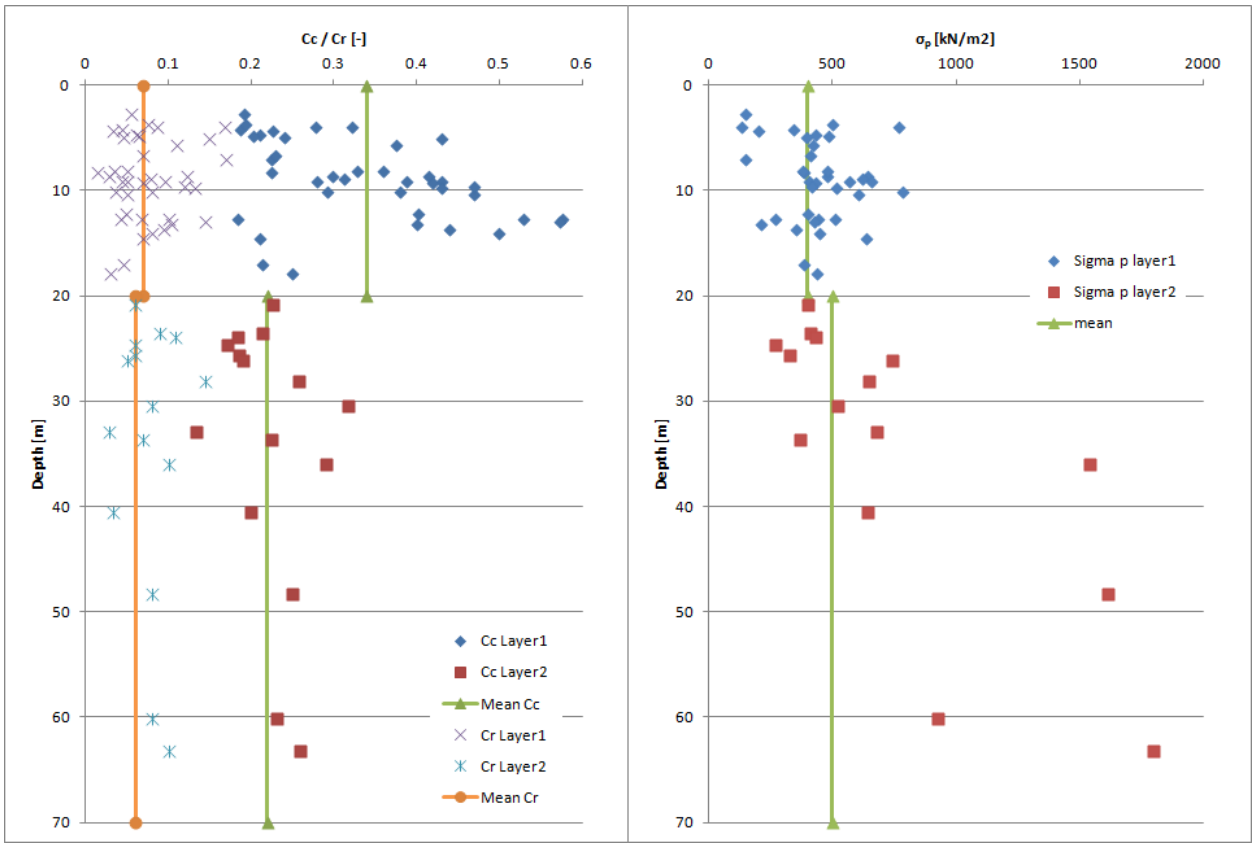

Figure 54: Compression parameters and preconsolidation pressure plotted in depth

Besides the compression and recompression parameters, there is the secondary compression parameter which describes the amount of creep settlement which will occur. This parameter is, in contrary to the C_c and C_r, based on a settlement / log time scale. In the performed site investigation data is available from the oedometer tests. The settlement / time graphs have been presented for several samples from different depths, and graphs are plotted for every load step. The values for C_α for every load step and sample can be found in Table 25. A settlement time plot from one of the oedometer tests can be found in Appendix B.

Table 25: Values for secondary compression parameter

Sample Depth [m]	Load Step 1	2	3	4	5	6	7
-4	0.0147	0.0071	0.0057	0.0115	0.0101	0.0101	0.0183
-10.35	0.0019	0.0061	0.0081	0.0141	0.0464	0.0414	0.0322
-26.15	0.0020	0.0061	0.0047	0.0072	0.0101	0.0115	0.0126
-36	0.0069	0.0061	0.0085	0.0120	0.0178	0.0187	0.0222
-48.3	0.0019	0.0051	0.0057	0.0065	0.0212	0.0234	0.0201
-63.17	0.0068	0.0081	0.0038	0.0094	0.0182	0.0185	0.0081

The values seem to be increasing with load step. This means that secondary compression becomes larger when the applied load on top of the sample is increased. The depth of the sample does not seem to influence the magnitude of the C_α value very much. The shaded values represent the value corresponding to the current vertical pressure, and the mean of this value has been chosen as the secondary compression parameter in the model presented in Table 25.

11.2.1.5 Over consolidation

A soil is considered over consolidated when it has been loaded with a higher pressure than it currently is experiencing. This can either be caused by a pre-overburden pressure or by ageing.

In geological history soil profile can change due to sedimentation and erosion. Some of the above laying soil can be eroded away and thus unloading the soil layers deeper down. Another common way of creating over consolidated layers is glaciers. These thick walls of ice where active in ice ages long past, and have since been melted. Overconsolidation can also occur without an actual load on top of it.

Ageing of a soil layer can cause a "apparent" pre consolidation as well. This is caused by creep settlement, but can also be caused by cementation of the soil skeleton.

The different ways to describe over consolidation is the Pre Overburden Pressure (POP) or Over Consolidation Ratio (OCR). Both are displayed in Figure 55. The OCR is preferred if overconsolidation is caused by ageing, a POP is considered more appropriate when a large overburden is the cause [Deltares, 2009].

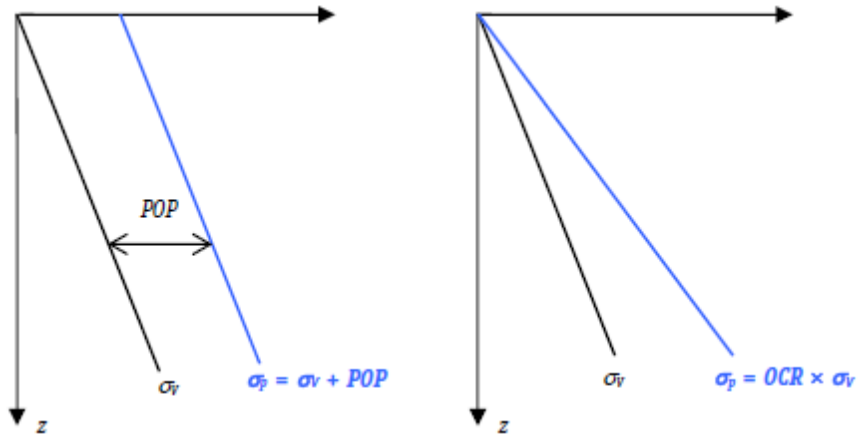

Figure 55: Difference between POP and OCR [Deltares, 2009]

These can be tested with oedometer tests or triaxial tests. Samples from different depths have been taken and tested for the value of σ_p. Figure 54 shows the different preconsoldation pressure values tested over depth. The values have been split up into layers III and IV again, showing a difference in mean σ_p for these clay layers.

The soft clay layer at the top of the sample has been deposited recently and does not seem to have sustained an overburden pressure. This means that the current in situ stresses are the highest pressure this soil has undergone.

11.2.1.6 Void ratio

The void ratio has been obtained for the oedometer samples. A plot has been made of the different void ratios tested, at different depths. The mean has also been plotted, which is presented in Table 23.

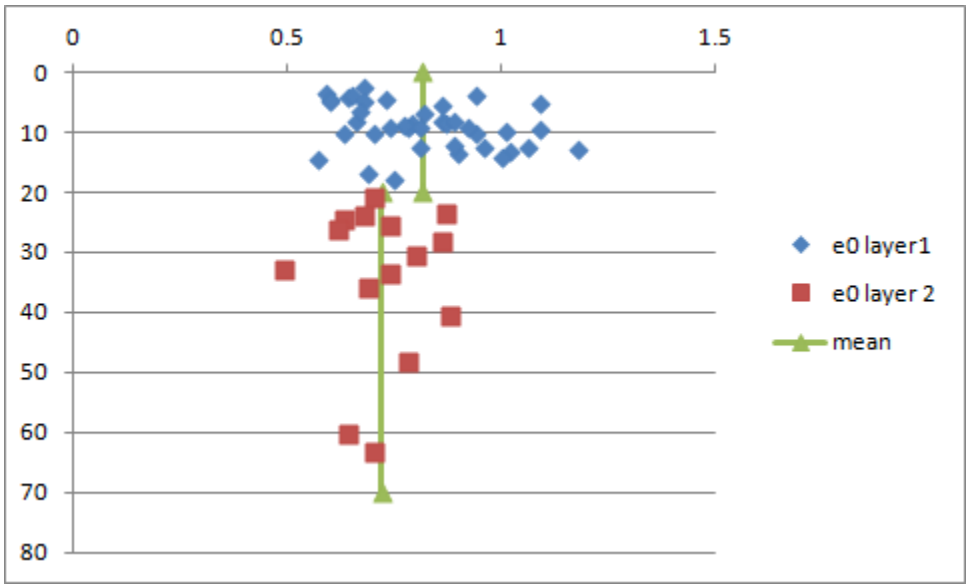

Figure 56: Void Ratio vs depth

11.2.1.7 Undrained Shear Strength

The undrained shear strength of the subsoil has been tested in several ways. A correlation between cone resistance has been made, so a nearly continues image is created in the borehole logs added in Appendix B. Besides the correlation with the CPT data there are some laboratory and insitu tests done like the torvane, pocket penetrometer and triaxial tests. The values from these tests are also plotted in the borehole logs.

For the different clay layers a plot is created for the value of this parameter. The values presented in Figure 56 are correlated from the borehole logs. The slope is calculated and the data has been extrapolated to the right depth.

APPENDIX B

Site Investigation; Data

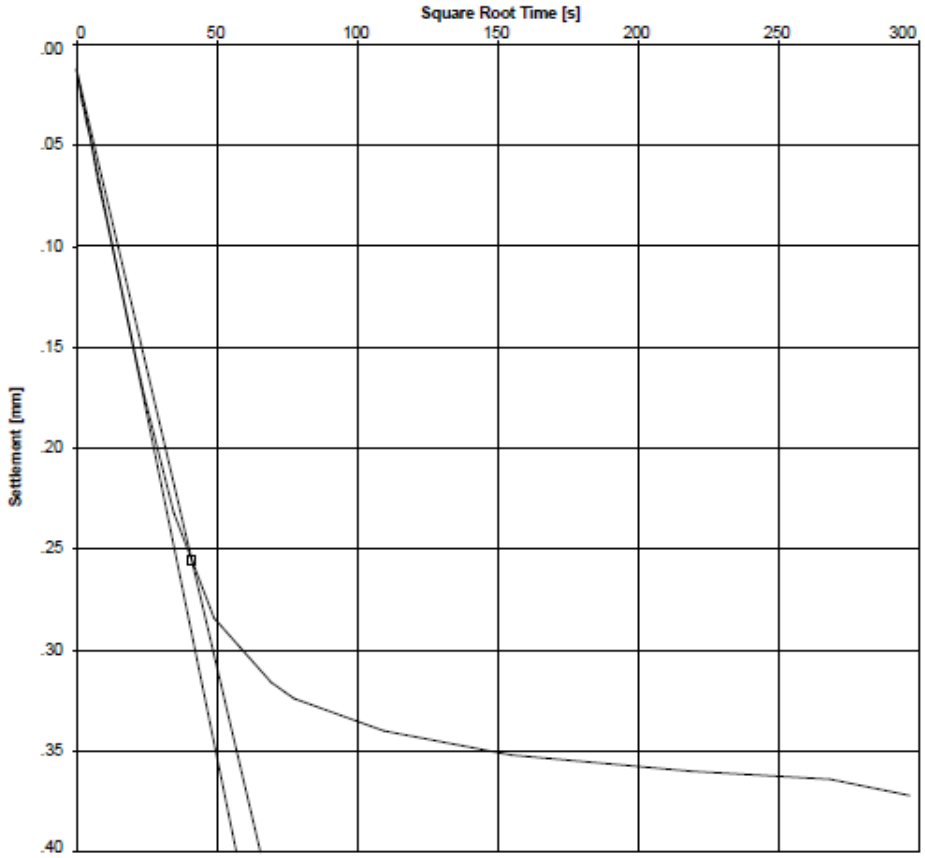

Borehole : U_B_02
Sample : 2 WAX A
Depth : 10.35 m
Soil type : CLAY

Test stage : 3
Stress P : 300. kPa
Stress dP : 150. kPa
Height : 18.608 mm

Consolidation		50	90	%
H	=	.135	.243	mm
H100	=	.270	.270	mm
t	=	398	1689	s
c_v	=	4.3E-08	4.3E-08	m^2/s
m_v	=	9.7E-02	9.7E-02	m^2/MN
k_v	=	4.1E-11	4.1E-11	m/s

OEDOMETER TEST RESULTS

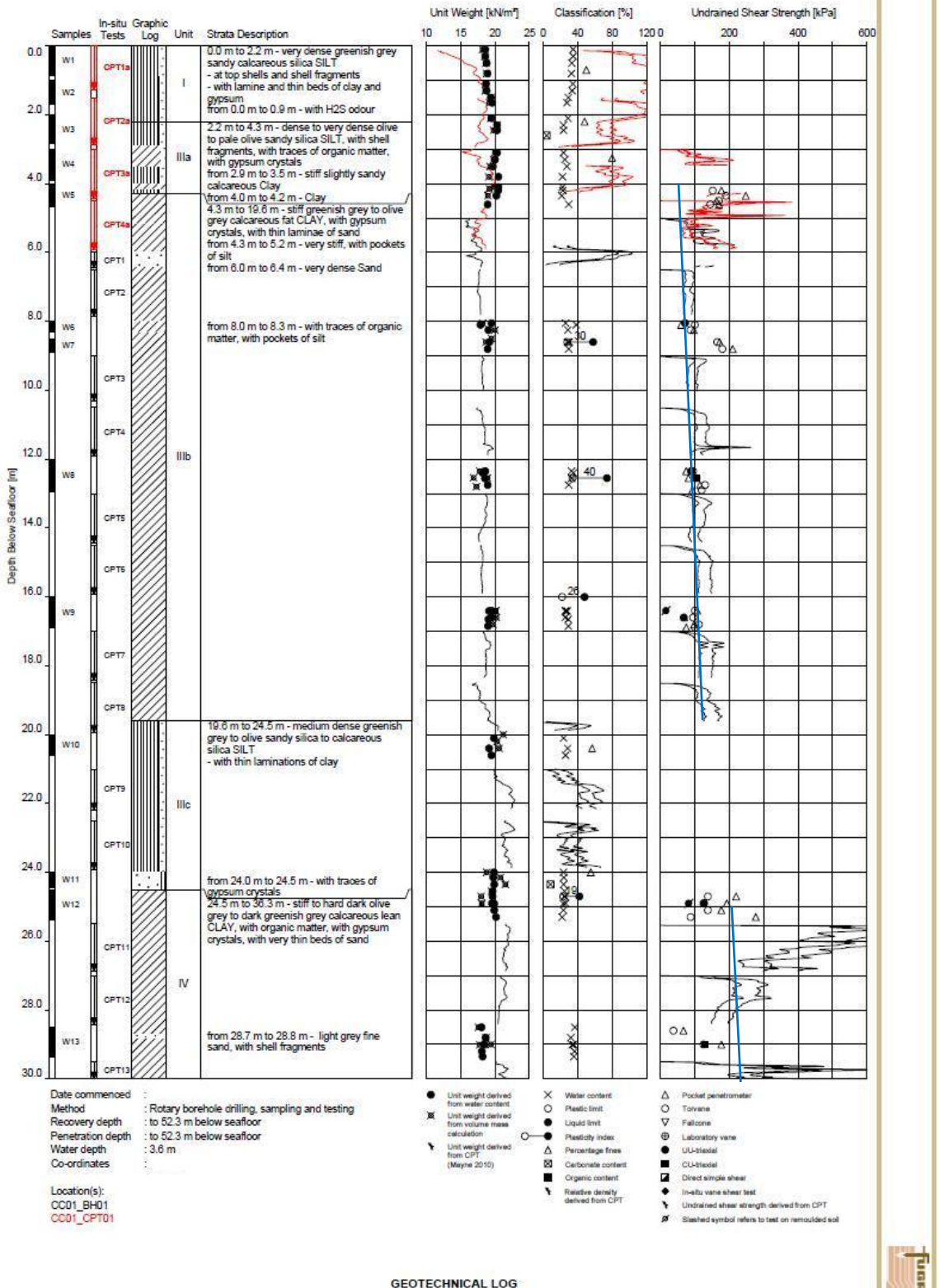

GEOTECHNICAL LOG

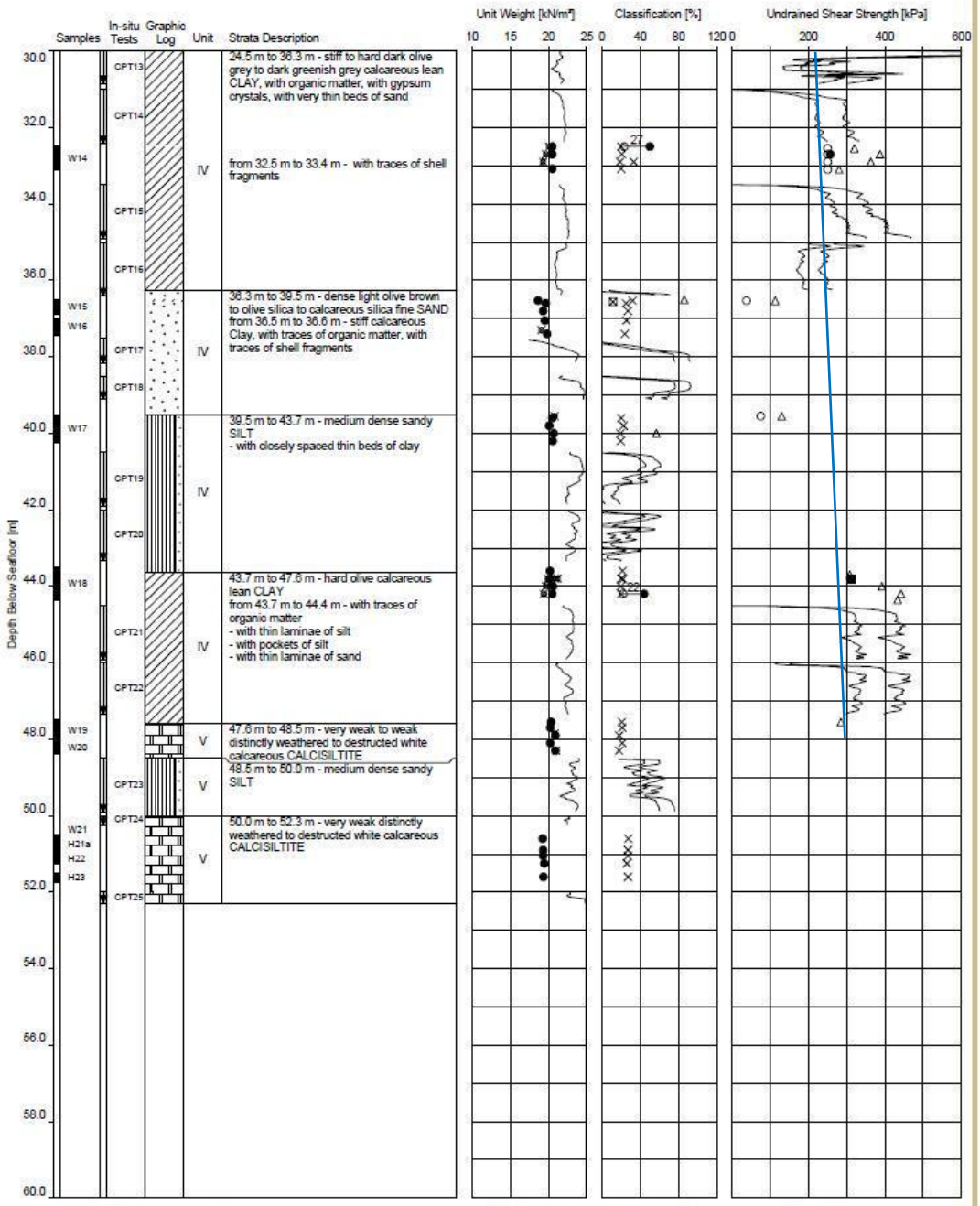
Samples
In-situ Tests
Graphic Log
Unit
Strata Description
Unit Weight [kN/m³]
Classification [%]
Undrained Shear Strength [kPa]
Depth Below Seafloor [m]
24.5 m to 36.3 m - stiff to hard dark olive grey to dark greenish grey calcareous lean CLAY, with organic matter, with gypsum crystals, with very thin beds of sand
from 32.6 m to 33.4 m - with traces of shell fragments
36.3 m to 39.5 m - dense light olive brown to olive silica to calcareous silica fine SAND from 36.5 m to 36.6 m - stiff calcareous Clay, with traces of organic matter, with traces of shell fragments
39.5 m to 43.7 m - medium dense sandy SILT
- with closely spaced thin beds of clay
43.7 m to 47.6 m - hard olive calcareous lean CLAY
from 43.7 m to 44.4 m - with traces of organic matter
- with thin laminae of silt
- with pockets of silt
- with thin laminae of sand
47.6 m to 48.5 m - very weak to weak distinctly weathered to destructed white calcareous CALCISILTITE
48.5 m to 50.0 m - medium dense sandy SILT
50.0 m to 52.3 m - very weak distinctly weathered to destructed white calcareous CALCISILTITE
Date commenced :
Method : Rotary borehole drilling, sampling and testing
Recovery depth : to 52.3 m below seafloor
Penetration depth : to 52.3 m below seafloor
Water depth : 3.6 m
Co-ordinates :
Location(s):
CC01_BH01
CC01_CPT01
GEOTECHNICAL LOG

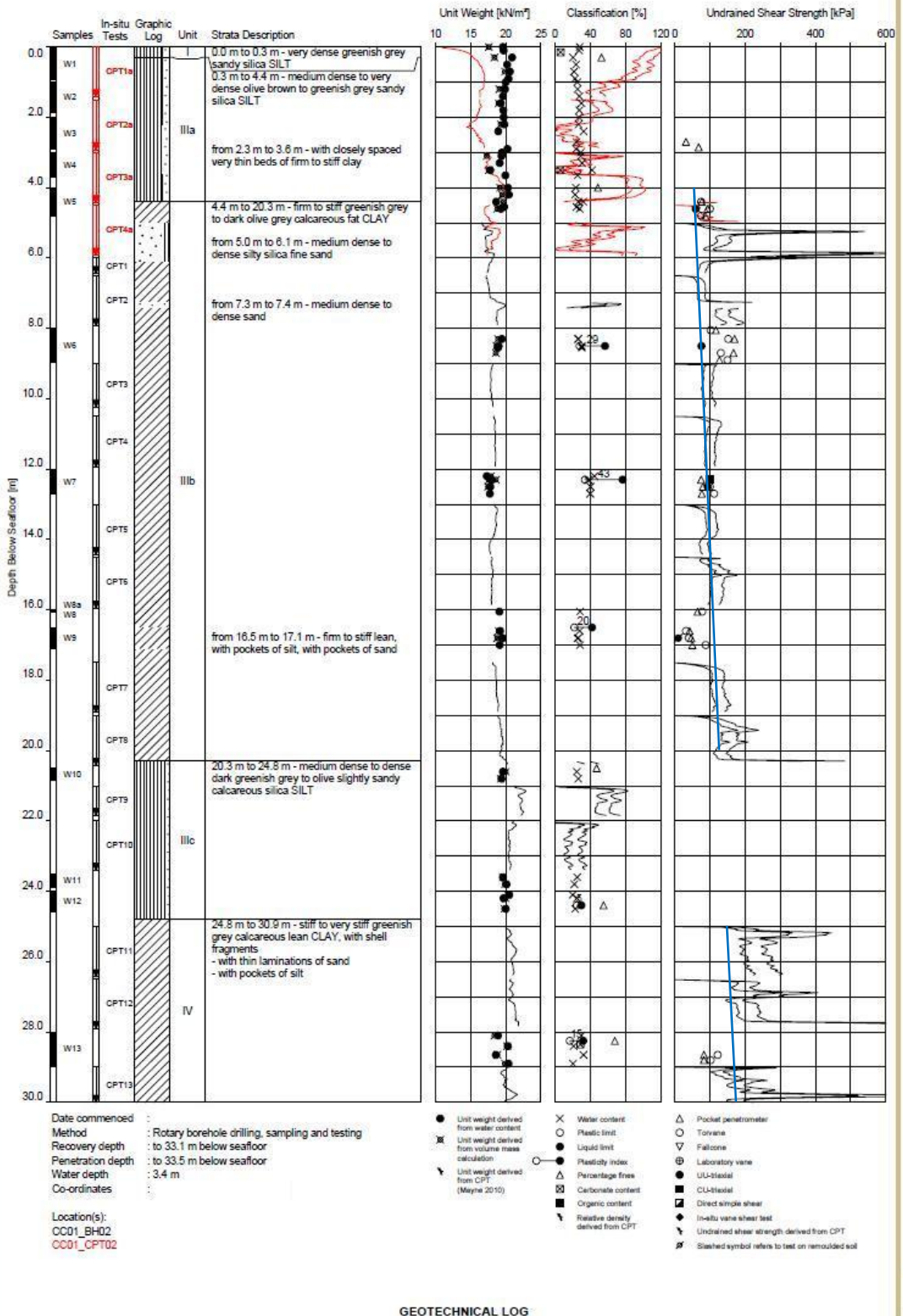
Samples
In-situ Tests
Graphic Log
Unit
Strata Description
Unit Weight [kN/m³]
Classification [%]
Undrained Shear Strength [kPa]
Depth Below Seafloor [m]
0.0 m to 0.3 m - very dense greenish grey sandy silica SILT
0.3 m to 4.4 m - medium dense to very dense olive brown to greenish grey sandy silica SILT
from 2.3 m to 3.6 m - with closely spaced very thin beds of firm to stiff clay
4.4 m to 20.3 m - firm to stiff greenish grey to dark olive grey calcareous fat CLAY
from 5.0 m to 6.1 m - medium dense to dense silty silica fine sand
from 7.3 m to 7.4 m - medium dense to dense sand
from 16.5 m to 17.1 m - firm to stiff lean, with pockets of silt, with pockets of sand
20.3 m to 24.8 m - medium dense to dense dark greenish grey to olive slightly sandy calcareous silica SILT
24.8 m to 30.9 m - stiff to very stiff greenish grey calcareous lean CLAY, with shell fragments
- with thin laminations of sand
- with pockets of silt
Date commenced :
Method : Rotary borehole drilling, sampling and testing
Recovery depth : to 33.1 m below seafloor
Penetration depth : to 33.5 m below seafloor
Water depth : 3.4 m
Co-ordinates :
Location(s):
CC01_BH02
CC01_CPT02
GEOTECHNICAL LOG

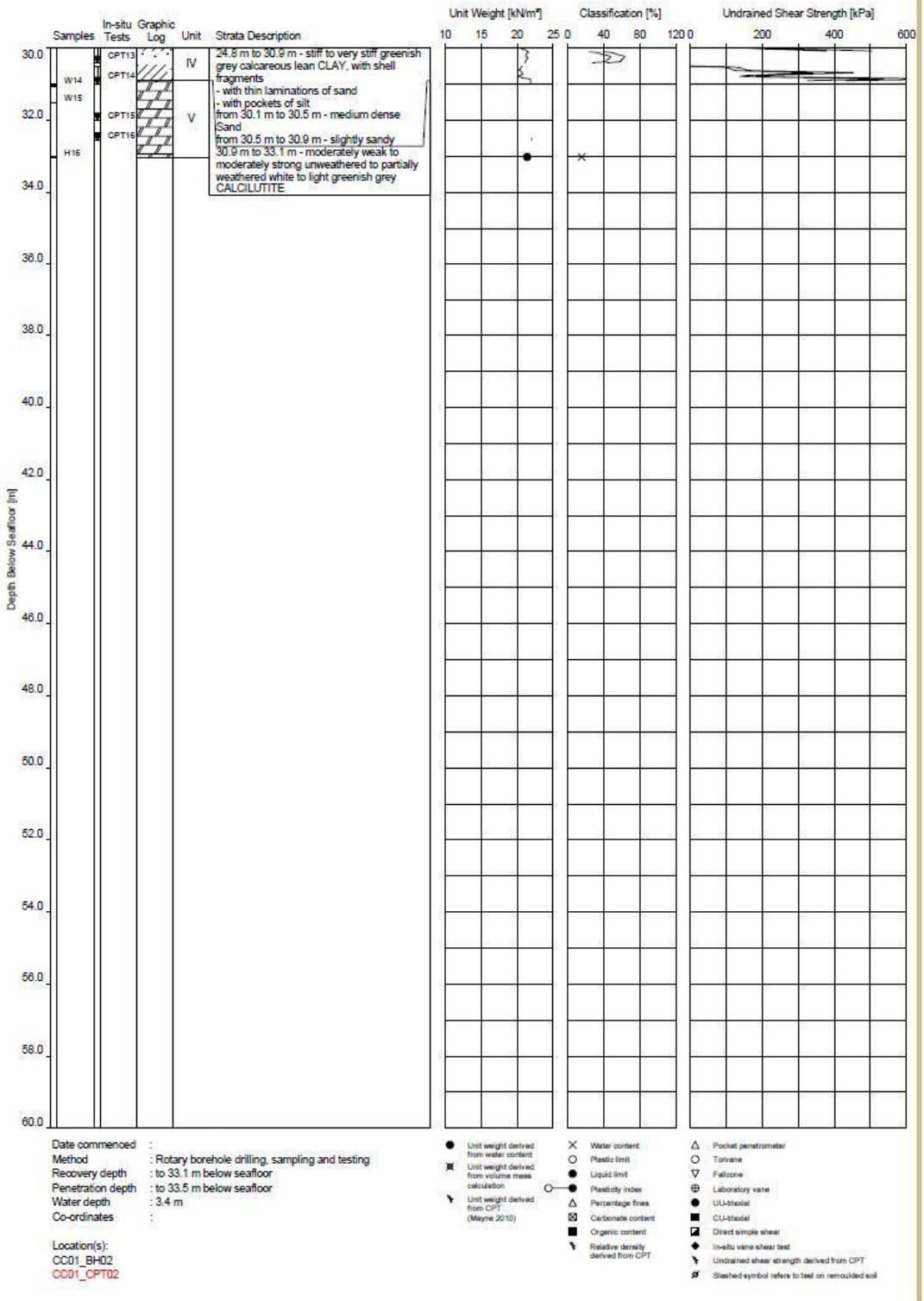

GEOTECHNICAL LOG

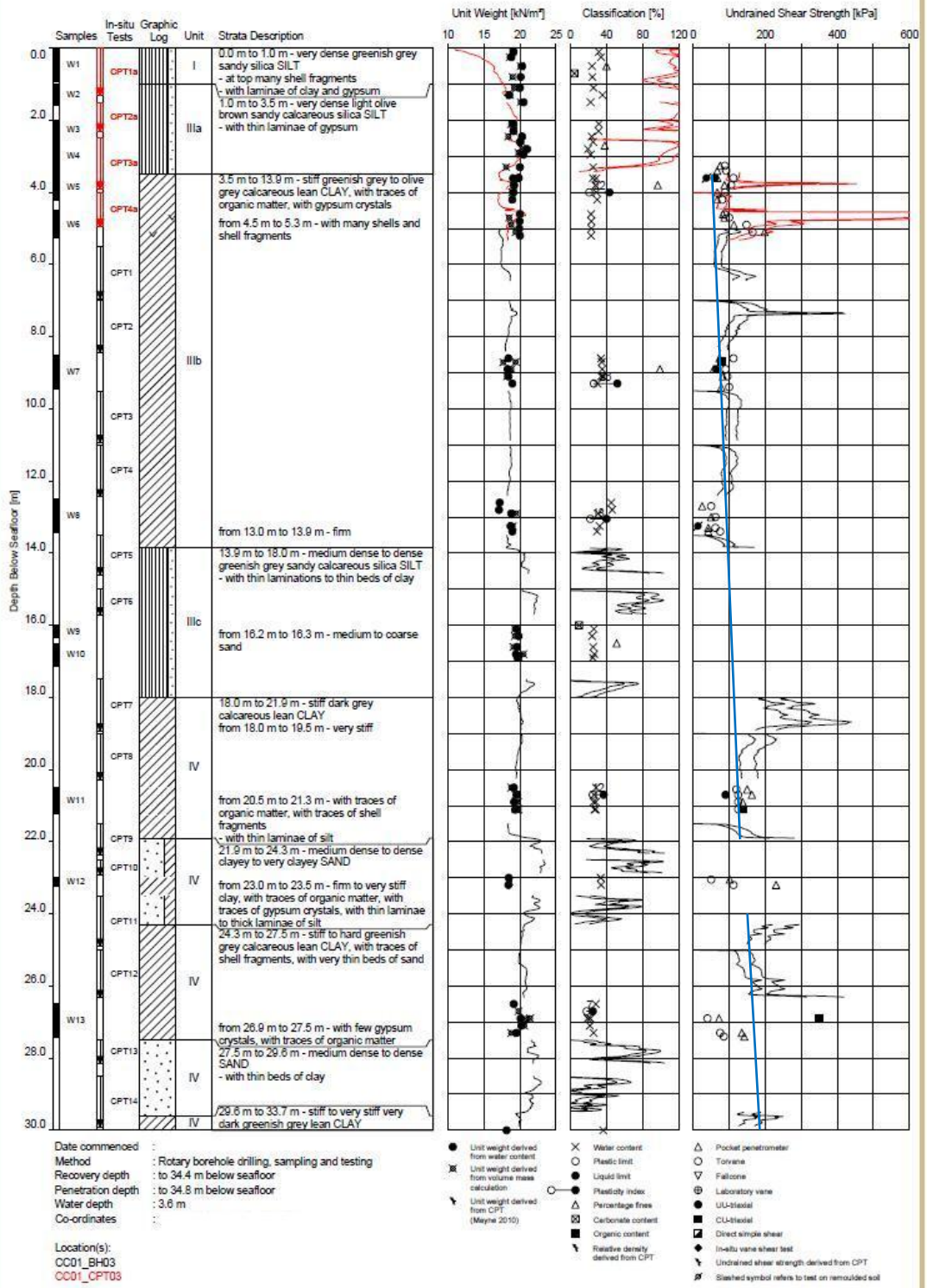

GEOTECHNICAL LOG

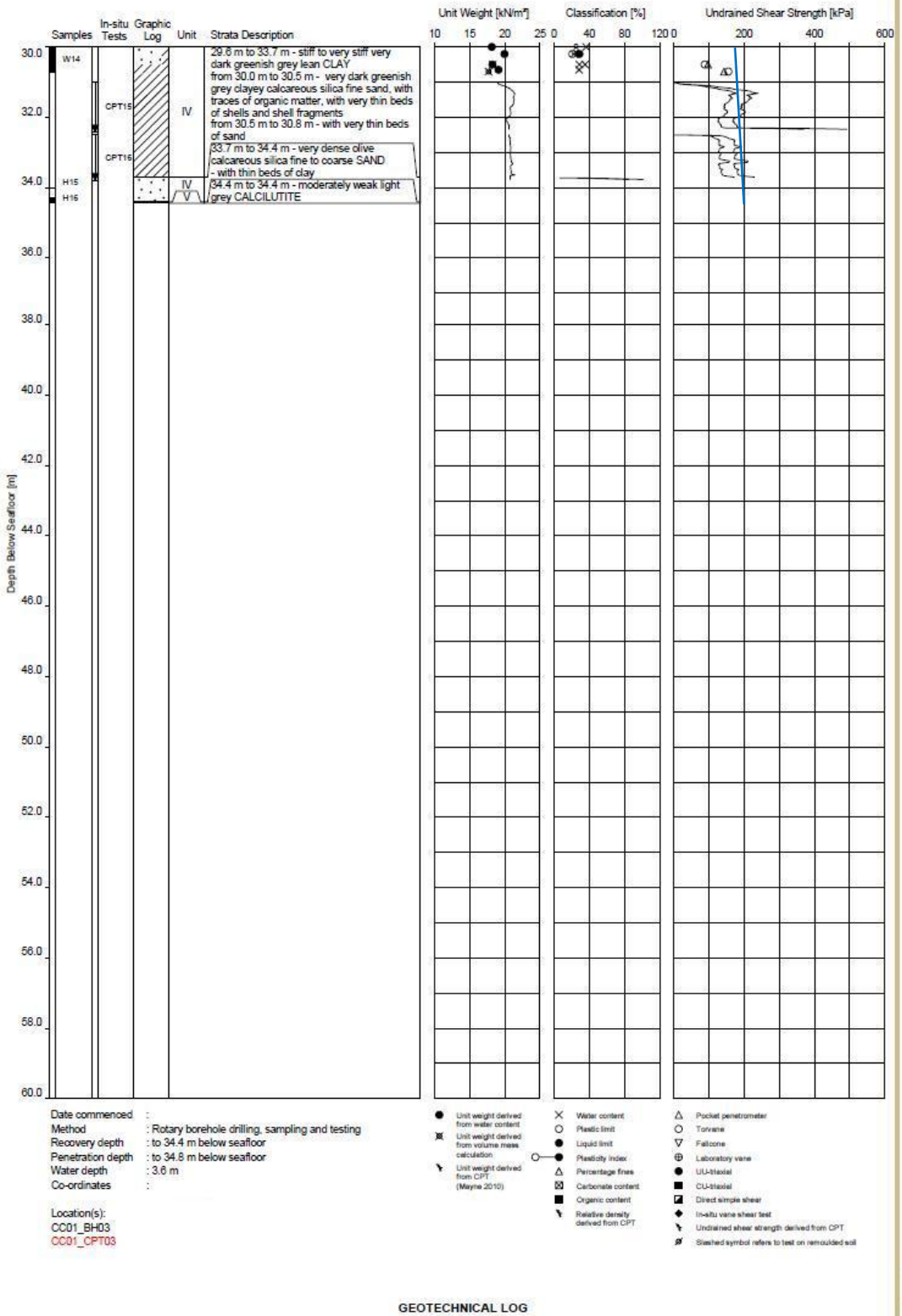

GEOTECHNICAL LOG

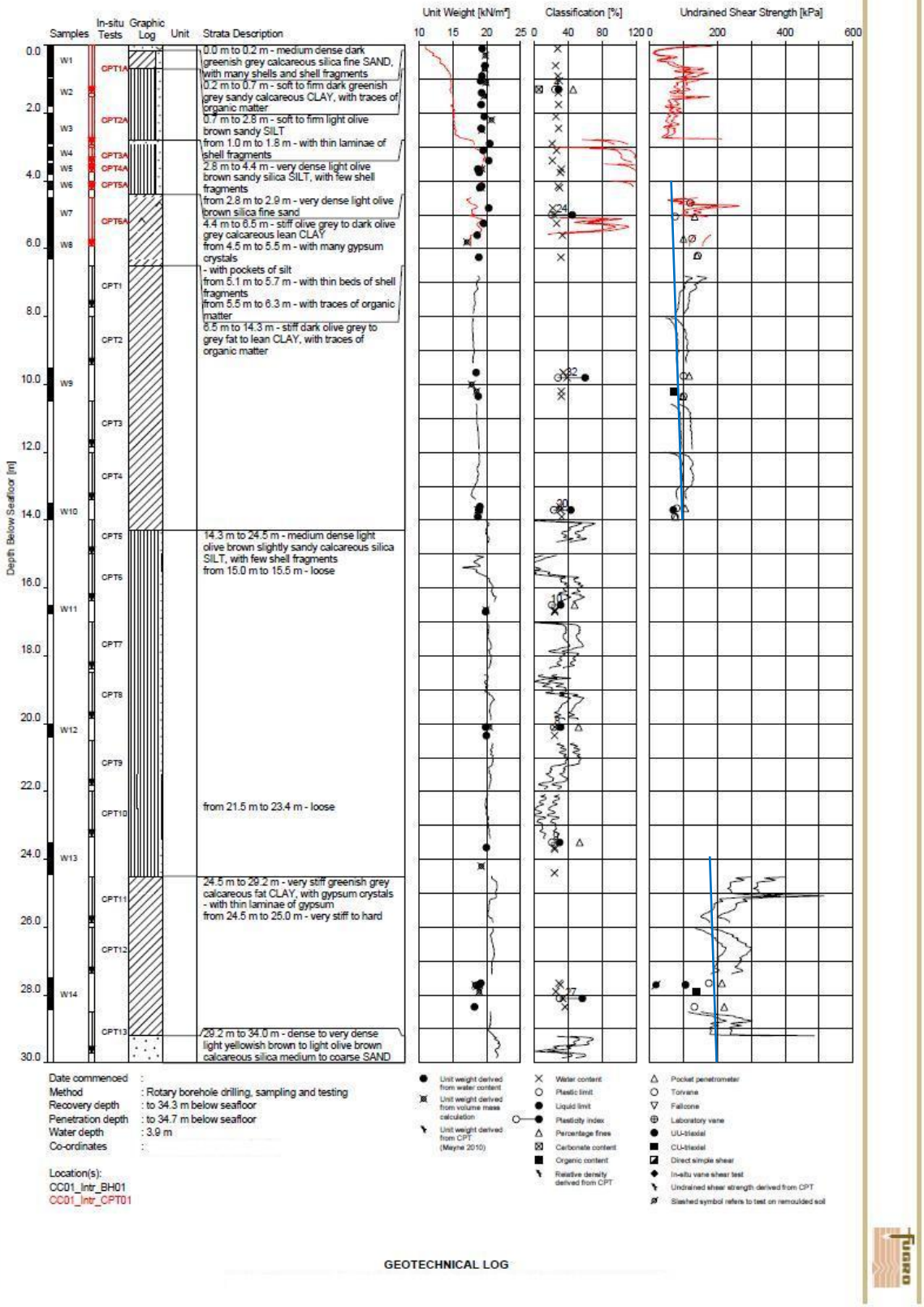

GEOTECHNICAL LOG

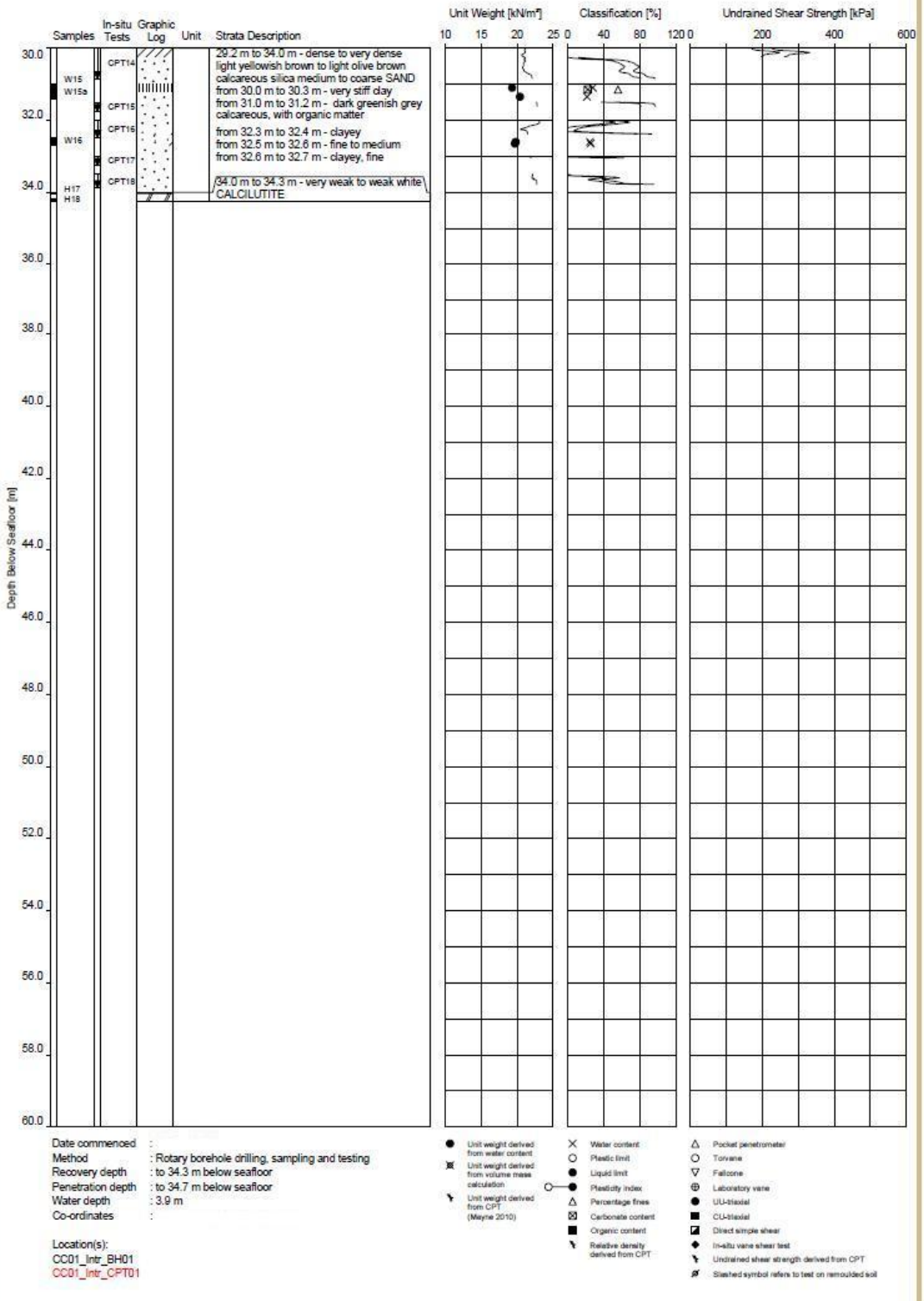

GEOTECHNICAL LOG

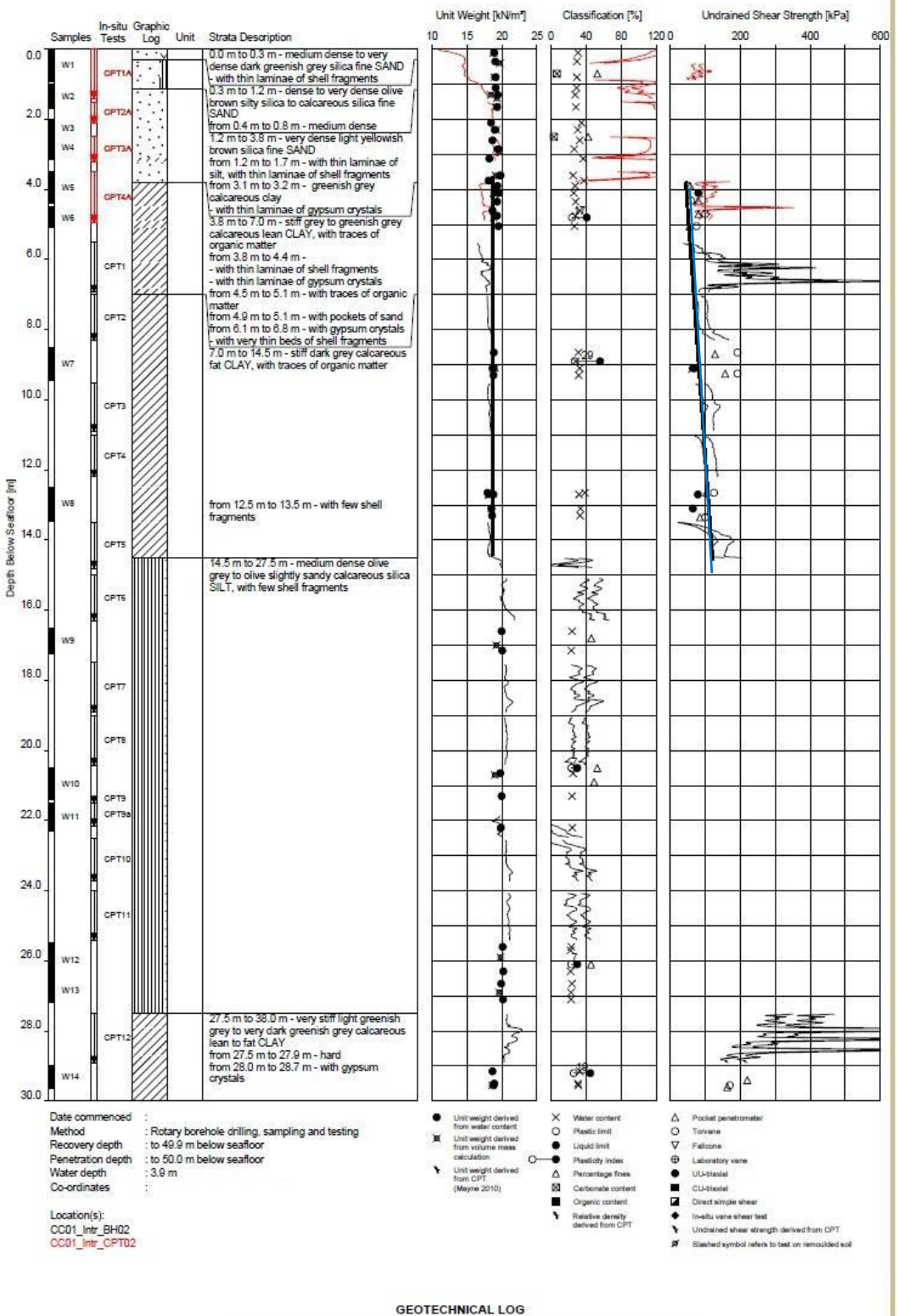
Samples
In-situ Tests
Graphic Log
Unit
Strata Description
Unit Weight [kN/m³]
Classification [%]
Undrained Shear Strength [kPa]
Depth Below Seafloor [m]
0.0 m to 0.3 m - medium dense to very dense dark greenish grey silica fine SAND
- with thin laminae of shell fragments
0.3 m to 1.2 m - dense to very dense olive brown silty silica to calcareous silica fine SAND
from 0.4 m to 0.8 m - medium dense
1.2 m to 3.8 m - very dense light yellowish brown silica fine SAND
from 1.2 m to 1.7 m - with thin laminae of silt, with thin laminae of shell fragments
from 3.1 m to 3.2 m - greenish grey calcareous clay
- with thin laminae of gypsum crystals
3.8 m to 7.0 m - stiff grey to greenish grey calcareous lean CLAY, with traces of organic matter
from 3.8 m to 4.4 m -
- with thin laminae of shell fragments
- with thin laminae of gypsum crystals
from 4.5 m to 5.1 m - with traces of organic matter
from 4.9 m to 5.1 m - with pockets of sand
from 6.1 m to 6.8 m - with gypsum crystals
- with very thin beds of shell fragments
7.0 m to 14.5 m - stiff dark grey calcareous fat CLAY, with traces of organic matter
from 12.5 m to 13.5 m - with few shell fragments
14.5 m to 27.5 m - medium dense olive grey to olive slightly sandy calcareous silica SILT, with few shell fragments
27.5 m to 38.0 m - very stiff light greenish grey to very dark greenish grey calcareous lean to fat CLAY
from 27.5 m to 27.9 m - hard
from 28.0 m to 28.7 m - with gypsum crystals
Date commenced :
Method : Rotary borehole drilling, sampling and testing
Recovery depth : to 49.9 m below seafloor
Penetration depth : to 50.0 m below seafloor
Water depth : 3.9 m
Co-ordinates :
Location(s):
CC01_Intr_BH02
CC01_Intr_CPT02
GEOTECHNICAL LOG

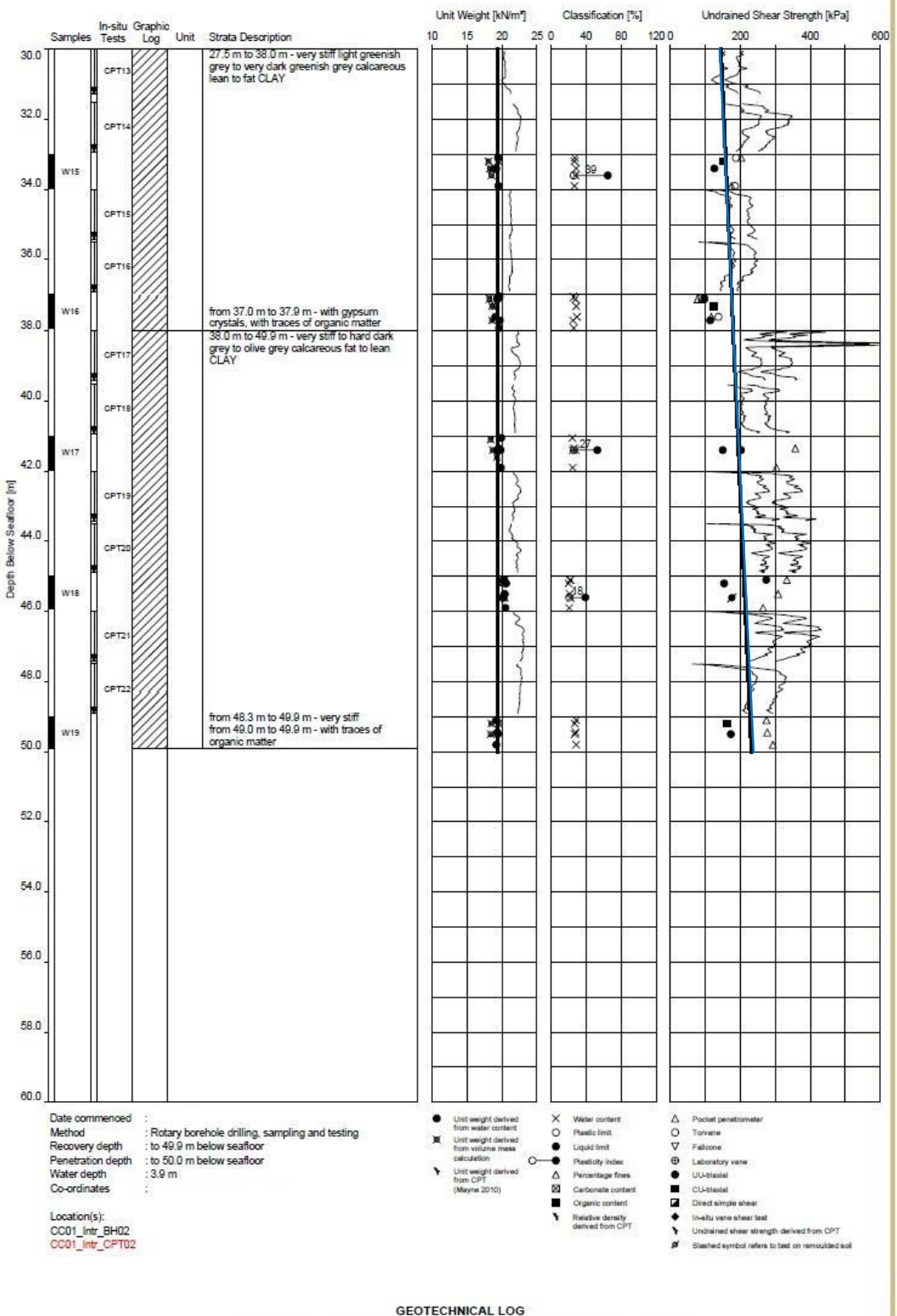
Samples
In-situ Tests
Graphic Log
Unit
Strata Description
Unit Weight [kN/m³]
Classification [%]
Undrained Shear Strength [kPa]
Depth Below Seafloor [m]
27.5 m to 38.0 m - very stiff light greenish grey to very dark greenish grey calcareous lean to fat CLAY
from 37.0 m to 37.9 m - with gypsum crystals, with traces of organic matter
38.0 m to 49.9 m - very stiff to hard dark grey to olive grey calcareous fat to lean CLAY
from 48.3 m to 49.9 m - very stiff
from 49.0 m to 49.9 m - with traces of organic matter
CPT13
CPT14
CPT15
CPT16
CPT17
CPT18
CPT19
CPT20
CPT21
CPT22
W15
W16
W17
W18
W19
Date commenced :
Method : Rotary borehole drilling, sampling and testing
Recovery depth : to 49.9 m below seafloor
Penetration depth : to 50.0 m below seafloor
Water depth : 3.9 m
Co-ordinates :
Location(s):
CC01_Intr_BH02
CC01_Intr_CPT02
GEOTECHNICAL LOG

APPENDIX C

Msettle Input; “Benchmark” Soil Profile

Report for MSettle 8.2

Settlement Calculations
Developed by Deltares

Date of report:	5-9-2012
Time of report:	14:03:00
Date of calculation:	5-9-2012
Time of calculation:	14:02:30
Filename:	C:\..\0. Benchmark Situation\onetimestep_load\Msettle_benchmark

1 Echo of the Input

1.1 Layer Boundaries

Boundary number	Co-ordinates [m]				
2 - X -	0,000	100,000			
2 - Y -	0,000	0,000			
1 - X -	0,000	100,000			
1 - Y -	-10,000	-10,000			
0 - X -	0,000	100,000			
0 - Y -	-15,000	-15,000			

1.2 PL Lines

PL line number	Co-ordinates [m]				
1 - X -	0,000	100,000			
1 - Y -	5,000	5,000			

1.3 General Data

Soil model:	NEN Bjerrum
Consolidation model:	Darcy
Strain model:	Linear
Groundwater level:	Initial determined by PL-line number 1
Unit weight of water:	10,00 [kN/m³]
Stress distribution	
- Soil:	Buisman
- Loads:	None
End of consolidation:	100000,00 [days]
No maintain profile	
Pc (initial):	Variable parallel to the initial effective stress
Pc (per step):	Automatic increased to the final effective stresses
Creep rate reference time:	1,000 [days]
No imaginary surface	
No submerging	
Load column width	
- Non-Uniform Loads :	1,00 [m]
- Trapezoidal Loads :	1,00 [m]

1.4 Soil Profiles

Layer number	Material name	PL-line top	PL-line bottom
2	Stiff Clay	1	1
1	Impermeable Layer	1	1

1.5 Soil Properties

Layer number	Drained	Unit weight	
		Unsaturated [kN/m³]	Saturated [kN/m³]
2	No	18,00	18,00
1	No	20,00	20,00

Layer number	Storage type	Vert. consolid. coefficient Cv [m²/s]	Vertical permeability [m/s]	Permeability strain mod. [m/s]	Initial vertical permeability [m/s]
2	Const. perm.	-	3,000E-09	-	-
1	Const. perm.	-	1,000E-13	-	-

Layer number	POP [kN/m²]	OCR [-]	Equiv. age [days]
2	0,00	-	-
1	400,00	-	-

Layer number	Secondary swelling type	Secondary swelling factor[-]	Unloading stress ratio[-]
2	Full	-	-
1	Full	-	-

Layer number	Reloading/ swelling ratio RR [-]	Compression ratio CR [-]	Reloading/ swelling index Ca [-]	Compression index Cr [-]	Coeff. of sec. compression Cc [-]	Initial void ratio (e0) [-]
2	-	-	0,0000000	0,0800000	0,3000000	1,000000
1	-	-	0,0000000	0,0000001	0,0000001	0,000000

1.6 Non-Uniform Loads

Load number	Time [days]	Unit weight	
		Unsaturated [kN/m³]	Saturated [kN/m³]
1	0	20,00	20,00

Load number	Co-ordinates [m]					
1 - X -	0,00	0,00	100,00	100,00		
1 - Y -	0,00	7,50	7,50	0,00		

1.7 Verticals

Vertical number	X co-ordinates [m]				
1 - 5	0,000	10,000	20,000	30,000	40,000
6 - 10	50,000	60,000	70,000	80,000	90,000
11	100,000				

Calculation of cross section at Z = 0,000 m
Discretisation = 100

End of Report

APPENDIX D

Msettle Input; “Centrifuge” Soil Profile

Report for MSettle 8.2

Settlement Calculations
Developed by Deltares

Date of report:	5-9-2012
Time of report:	14:01:02
Date of calculation:	27-8-2012
Time of calculation:	13:14:55
Filename:	C:\..\2. Centrifuge Soil model\Msettle\1timesteplaod\Centrifuge Sample

1 Echo of the Input

1.1 Layer Boundaries

Boundary number	Co-ordinates [m]				
3 - X -	0,000	100,000			
3 - Y -	0,000	0,000			
2 - X -	0,000	100,000			
2 - Y -	-4,500	-4,500			
1 - X -	0,000	100,000			
1 - Y -	-14,000	-14,000			
0 - X -	0,000	100,000			
0 - Y -	-20,000	-20,000			

1.2 PL Lines

PL line number	Co-ordinates [m]				
1 - X -	0,000	100,000			
1 - Y -	5,000	5,000			

1.3 General Data

Soil model:	NEN Bjerrum
Consolidation model:	Darcy
Strain model:	Linear
Groundwater level:	Initial determined by PL-line number 1
Unit weight of water:	10,00 [kN/m³]
Stress distribution	
- Soil:	Buisman
- Loads:	None
End of consolidation:	50000,00 [days]
No maintain profile	
Pc (initial):	Variable parallel to the initial effective stress
Pc (per step):	Automatic increased to the final effective stresses
Creep rate reference time:	1,000 [days]
No imaginary surface	
No submerging	
Load column width	
- Non-Uniform Loads :	1,00 [m]
- Trapezoidal Loads :	1,00 [m]

1.4 Soil Profiles

Layer number	Material name	PL-line top	PL-line bottom
3	Soft Clay	1	1
2	Stiff Clay	1	1
1	Impermeable	1	1

1.5 Soil Properties

Layer number	Drained	Unit weight	
		Unsaturated [kN/m³]	Saturated [kN/m³]
3	No	18,00	18,00
2	No	18,00	18,00
1	No	18,00	18,00

Layer number	Storage type	Vert. consolid. coefficient Cv [m²/s]	Vertical permeability [m/s]	Permeability strain mod. [m/s]	Initial vertical permeability [m/s]
3	Const. perm.	-	2,000E-09	-	-
2	Const. perm.	-	1,000E-09	-	-
1	Const. perm.	-	1,000E-13	-	-

Layer number	POP [kN/m²]	OCR [-]	Equiv. age [days]
3	0,00	-	-
2	200,00	-	-
1	0,00	-	-

Layer number	Secondary swelling type	Secondary swelling factor[-]	Unloading stress ratio[-]
3	Full	-	-
2	Full	-	-
1	Full	-	-

Layer number	Reloading/ swelling ratio RR [-]	Compression ratio CR [-]	Reloading/ swelling index Ca [-]	Compression index Cr [-]	Coeff. of sec. compression Cc [-]	Initial void ratio (e0) [-]
3	-	-	0,0000000	0,0800000	0,3000000	1,000000
2	-	-	0,0000000	0,0800000	0,3000000	1,000000
1	-	-	0,0000000	0,0000001	0,0000001	0,000000

1.6 Non-Uniform Loads

Load number	Time [days]	Unit weight	
		Unsaturated [kN/m³]	Saturated [kN/m³]
1	0	20,00	20,00

Load number	Co-ordinates [m]					
1 - X -	0,00	0,00	100,00	100,00		
1 - Y -	0,00	7,50	7,50	0,00		

1.7 Verticals

Vertical number	X co-ordinates [m]				
1 - 5	0,000	10,000	20,000	30,000	40,000
6 - 10	50,000	60,000	70,000	80,000	90,000
11	100,000				

Calculation of cross section at Z = 0,000 m
Discretisation = 100

End of Report

APPENDIX E

Plaxis Input

BENCHMARK SOIL PROFILE

		Material Model	Material Type	y unsat	y sat	kx	ky	e init	E ref	lambda*	kappa*	lambda	kappa	E50	Eoed	Eur	power (m)	p ref	c	phi	psi	v ur	K0 nc	M	POP
				[kN/m3]	*[kN/m3]*	*[m/day]*	*[m/day]*	*[-]*	*[kN/m2]*	*[-]*	*[-]*	*[-]*	*[-]*	*[kN/m2]*	*[kN/m2]*	*[kN/m2]*	*[-]*	*[kN/m2]*	*[kN/m2]*	*[deg]*	*[deg]*	*[-]*	*[-]*	*[-]*	*[kN]*
Soft Soil																									
Layer I	Rock Fill	Linear Elastic	Drained	20	20	1	1	0,5	1,00E+10	-	-	-	-	-	-	-	-	-	-	-	-	0,3	-	-	0
Layer II	Clay	Soft Soil	Undrained	18	18	2,592E-04	2,592E-04	1	-	0,065	0,035	-	-	-	-	-	-	-	15	29	0	0,2	0,515	1,363	0
Modified Cam Clay																									
Layer I	Rock Fill	Linear Elastic	Drained	20	20	1	1	0,5	1,00E+10	-	-	-	-	-	-	-	-	-	-	-	-	0,3	-	-	0
Layer II	Clay	Modified Cam Clay	Undrained	18	18	2,592E-04	2,592E-04	1	-	-	-	0,1304	0,0696	-	-	-	-	-	15	29	0	0,2	0,515	1,2	0
Hardening Soil																									
Layer I	Rock Fill	Linear Elastic	Drained	20	20	1	1	0,5	1,00E+10	-	-	-	-	-	-	-	-	-	-	-	-	0,3	-	-	0
Layer II	Clay	Hardening Soil	Undrained	18	18	2,592E-04	2,592E-04	1	-	-	-	-	-	1916	1533	5175	1	100	15	29	0	0,2	0,515	-	0

Dimensoins		Top	Bottom
		[m]	[m]
Layer I	Rock Fill	7,5	0
Layer II	Clay	0	-10
Water level		5	

CENTRIFUGE SOIL PROFILE

		Material Model	Material Type	y unsat	y sat	kx	ky	e init	E ref	lambda*	kappa*	lambda	kappa	E50	Eoed	Eur	power (m)	p ref	c	phi	psi	v ur	K0 nc	M	POP
				[kN/m3]	*[kN/m3]*	*[m/day]*	*[m/day]*	*[-]*	*[kN/m2]*	*[-]*	*[-]*	*[-]*	*[-]*	*[kN/m2]*	*[kN/m2]*	*[kN/m2]*	*[-]*	*[kN/m2]*	*[kN/m2]*	*[deg]*	*[deg]*	*[-]*	*[-]*	*[-]*	*[kN]*
Soft Soil																									
Layer I	Rock Fill	Linear Elastic	Drained	20	20	1	1	0,5	1,00E+10	-	-	-	-	-	-	-	-	-	-	-	-	0,3	-	-	0
Layer II	Soft Clay	Soft Soil	Undrained	18	18	2,592E-04	2,592E-04	1	-	0,065	0,035	-	-	-	-	-	-	-	8	29	0	0,2	0,515	1,363	0
Layer III	Stiff Clay	Soft Soil	Undrained	18	18	2,592E-04	2,592E-04	1	-	0,065	0,035	-	-	-	-	-	-	-	15	29	0	0,2	0,515	1,363	200
Modified Cam Clay																									
Layer I	Rock Fill	Linear Elastic	Drained	20	20	1	1	0,5	1,00E+10	-	-	-	-	-	-	-	-	-	-	-	-	0,3	-	-	0
Layer II	Soft Clay	Modified Cam Clay	Undrained	18	18	2,592E-04	2,592E-04	1	-	-	-	0,1304	0,0696	-	-	-	-	-	8	29	0	0,2	0,515	1,2	0
Layer III	Stiff Clay	Modified Cam Clay	Undrained	18	18	2,592E-04	2,592E-04	1	-	-	-	0,1304	0,0696	-	-	-	-	-	15	29	0	0,2	0,515	1,2	200
Hardening Soil																									
Layer I	Rock Fill	Linear Elastic	Drained	20	20	1	1	0,5	1,00E+10	-	-	-	-	-	-	-	-	-	-	-	-	0,3	-	-	0
Layer II	Soft Clay	Hardening Soil	Undrained	18	18	2,592E-04	2,592E-04	1	-	-	-	-	-	1916	1533	5175	1	100	8	29	0	0,2	0,515	-	0
Layer III	Stiff Clay	Hardening Soil	Undrained	18	18	2,592E-04	2,592E-04	1	-	-	-	-	-	1916	1533	5175	0,6	100	15	29	0				200

Dimensoins		Top	Bottom
		[m]	[m]
Layer I	Rock Fill	7,5	0
Layer II	Soft Clay	0	-5
Layer III	Stiff Clay	-5	-14
Water level		5	

APPENDIX F

JPIV images

Image Number	Time step
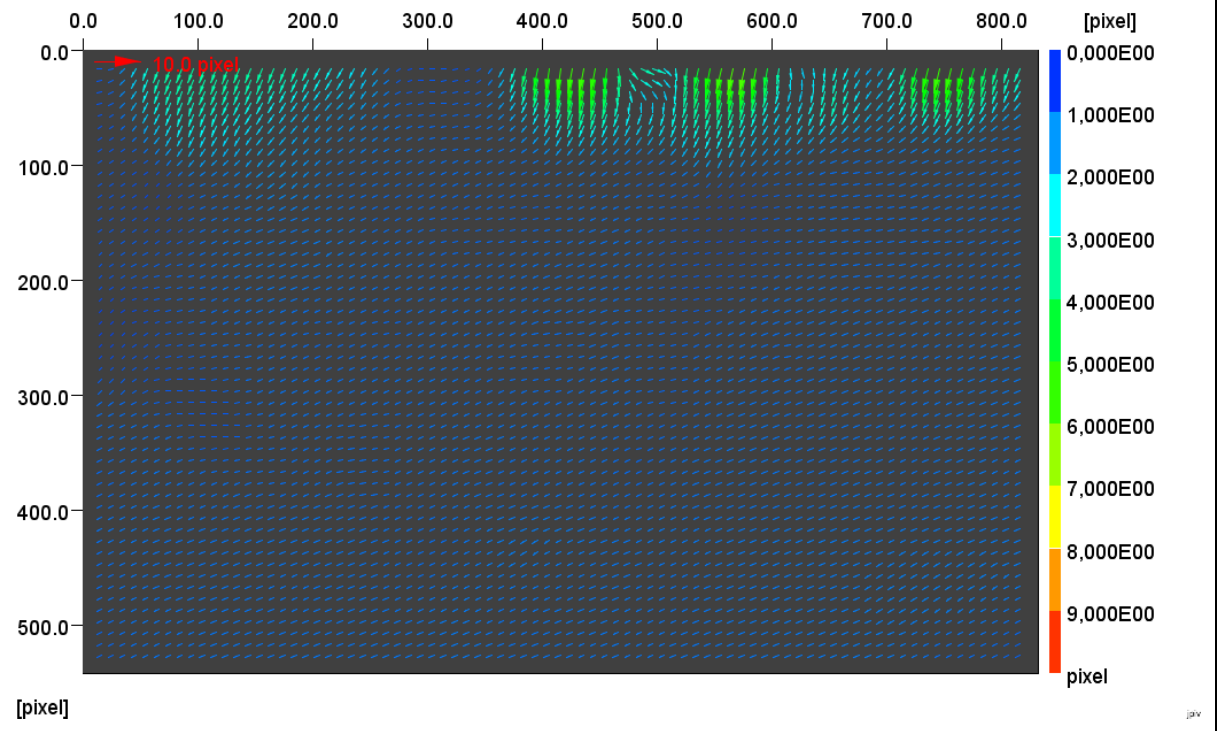	
JPIV image 0	**0:00 – 0:05**
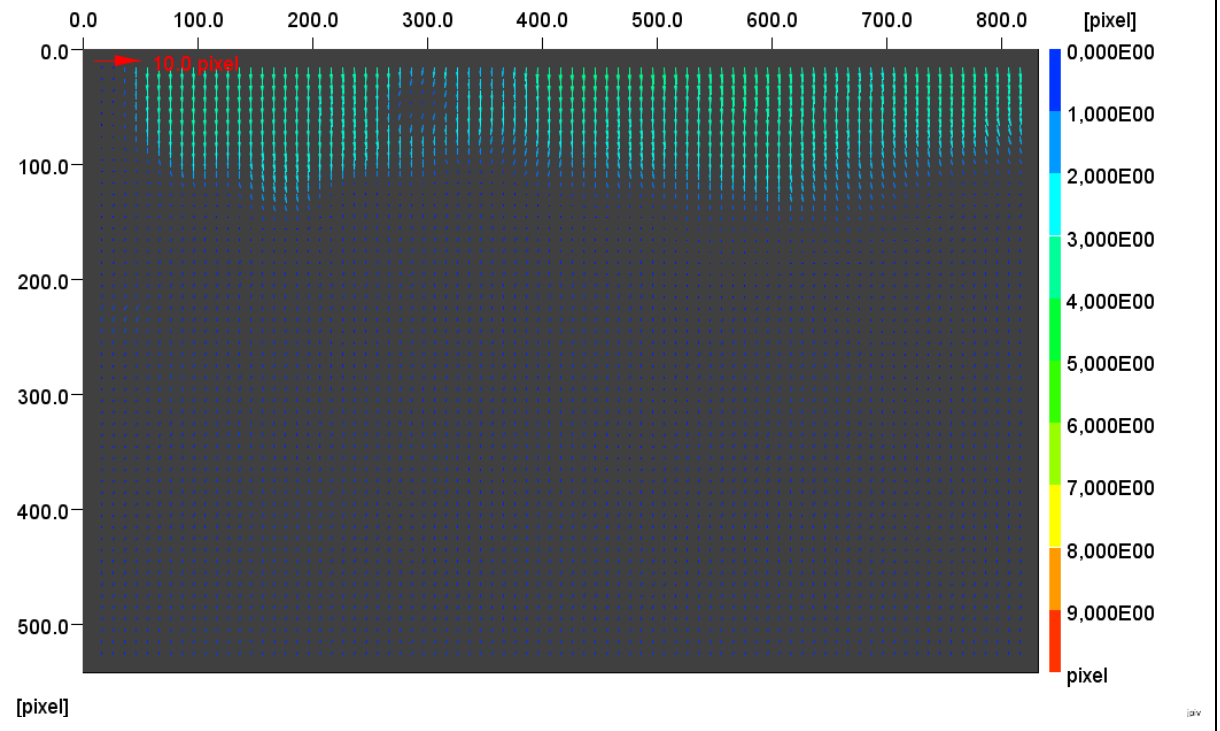	
JPIV image 1	**0:05 – 0:10**

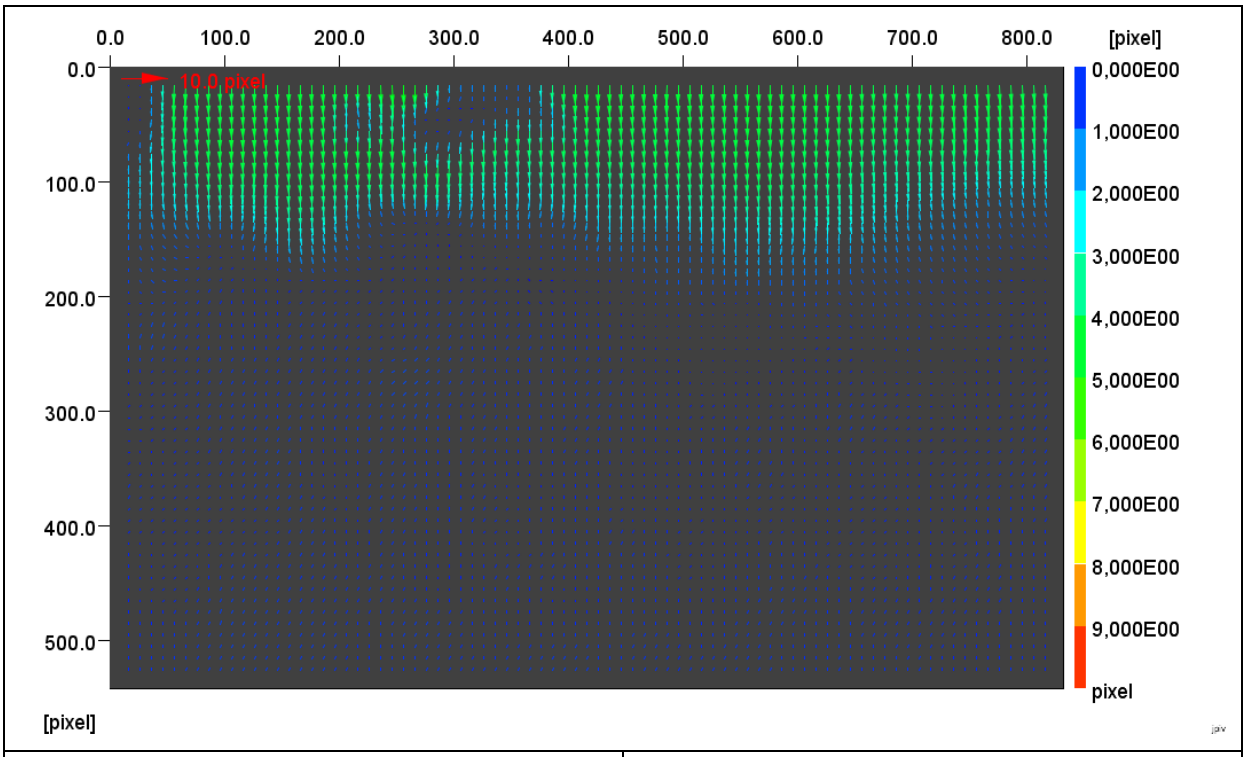

JPIV image 2	0:10 – 0:20

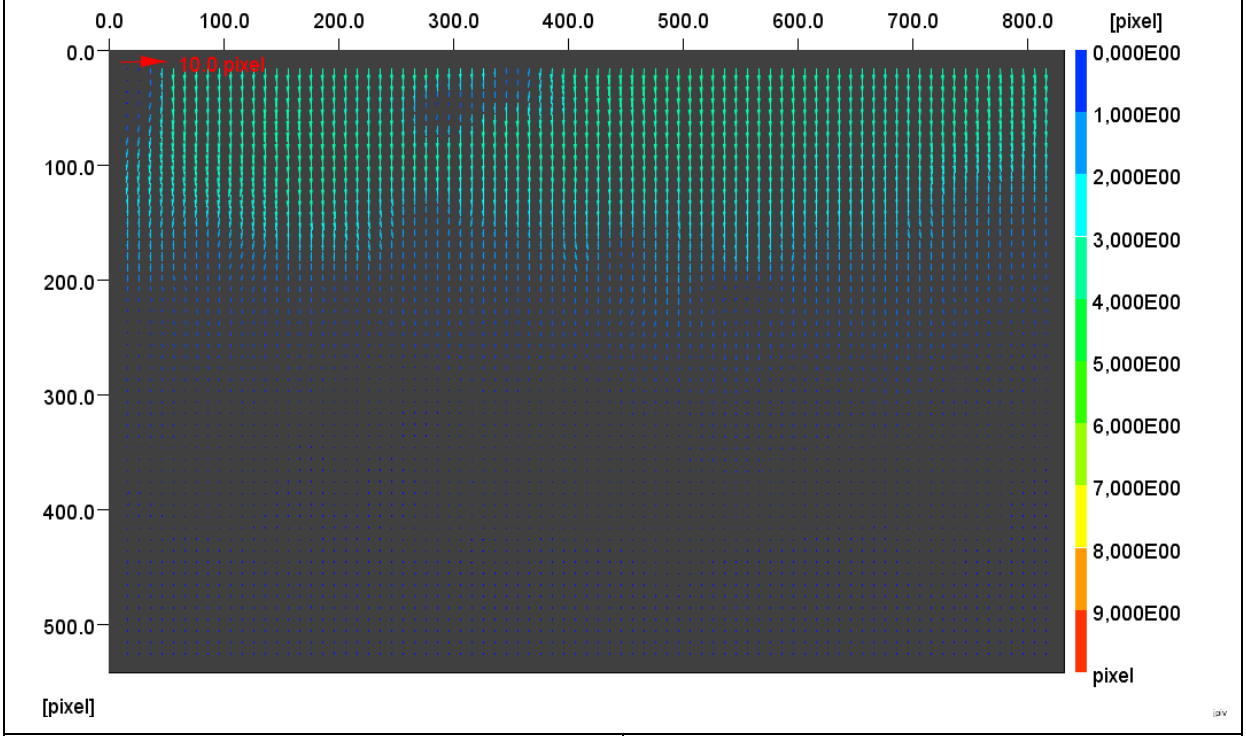

JPIV image 3	0:20 – 0:30

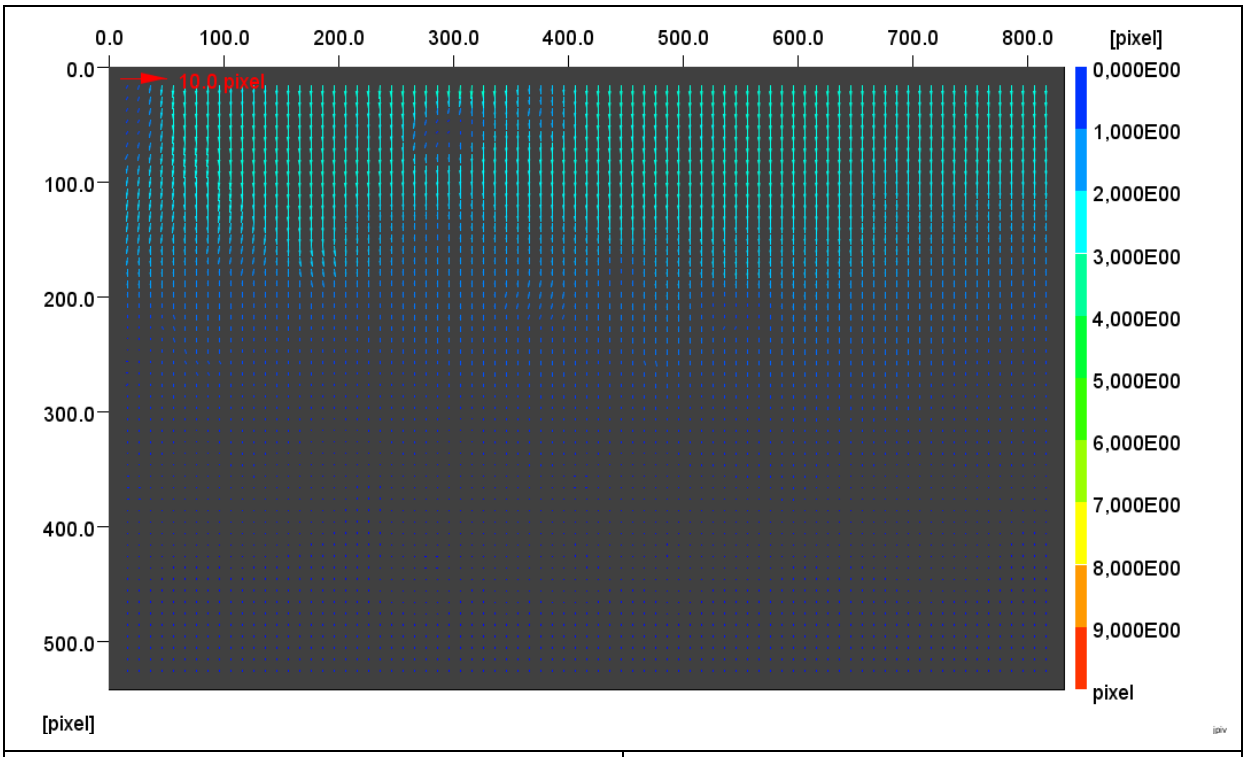

JPIV image 4	0:30 – 0:40

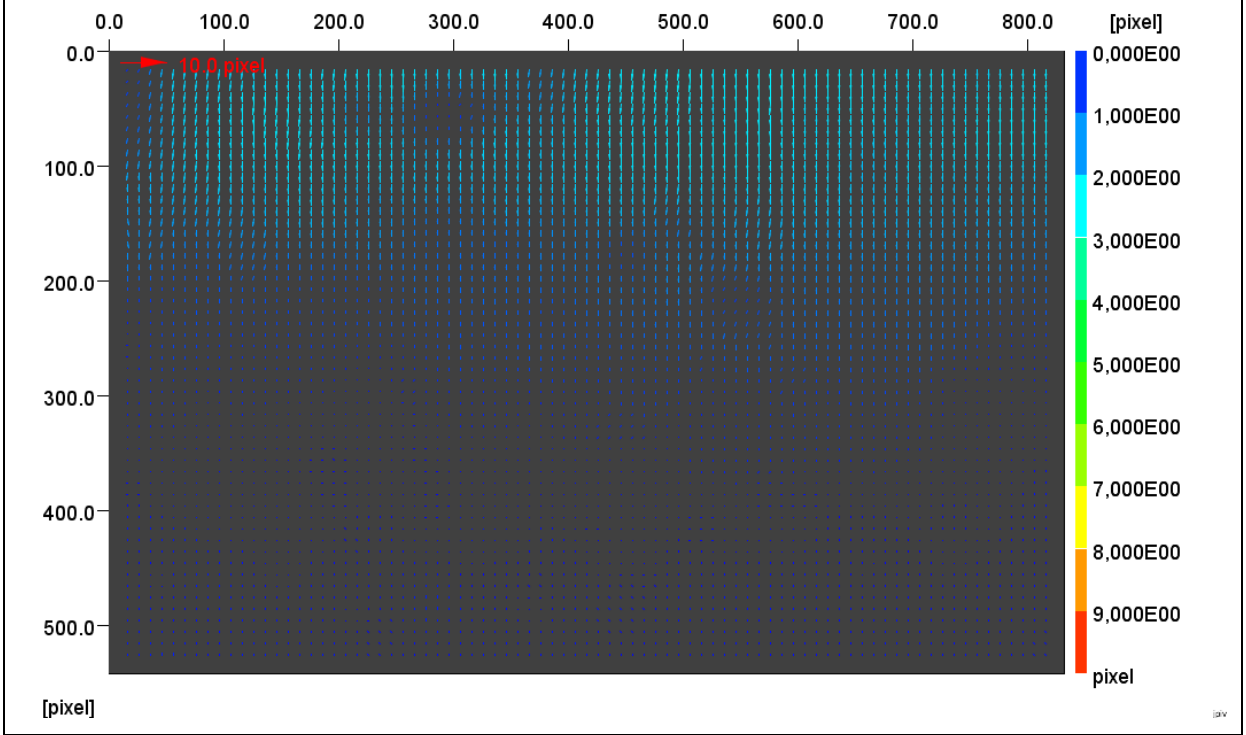

JPIV image 5	0:40 – 0:50

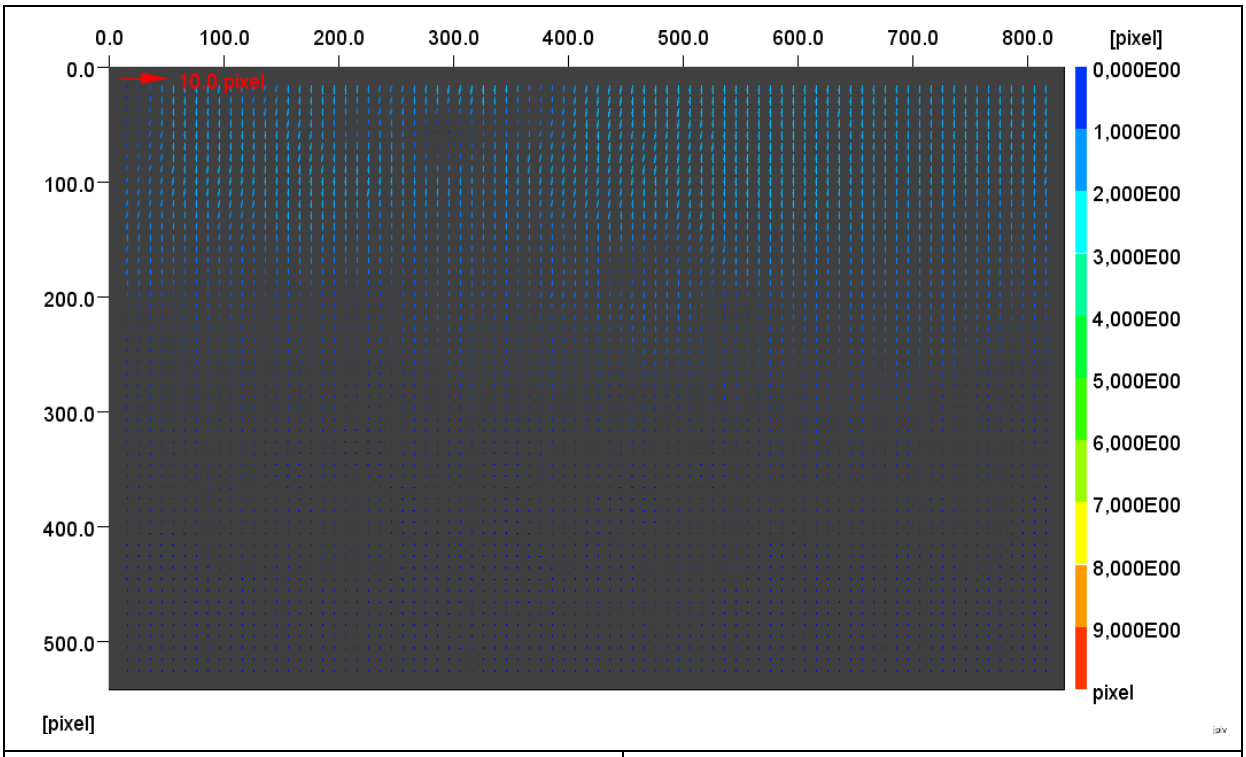

JPIV image 6	0:50 – 1:00

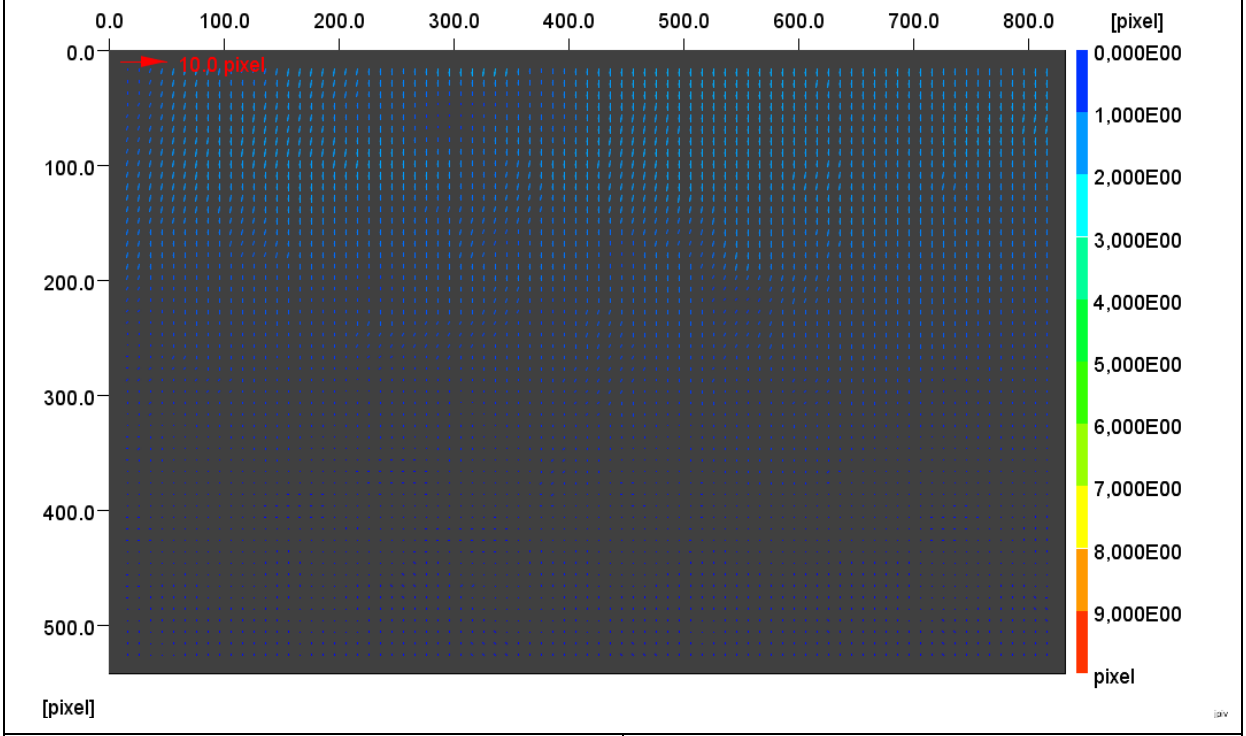

JPIV image 7	1:00 – 1:10

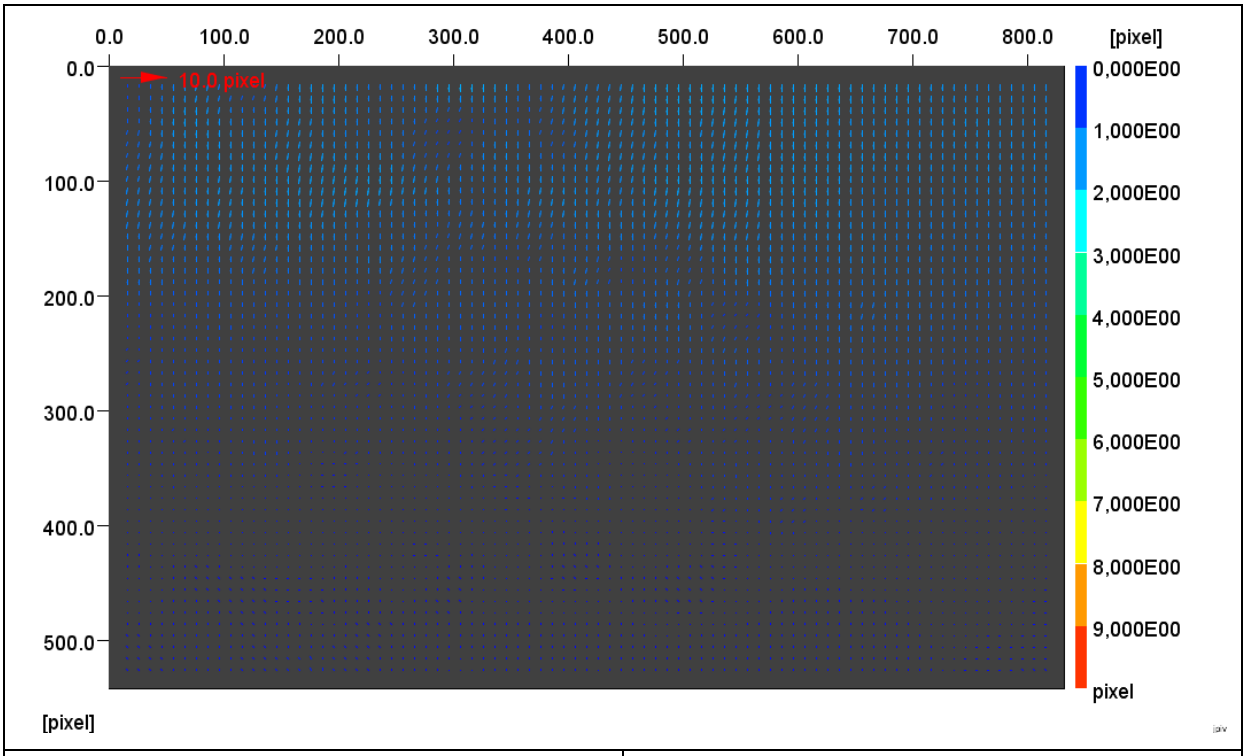

JPIV image 8	1:10 – 1:20

JPIV image 9	1:20 – 1:45

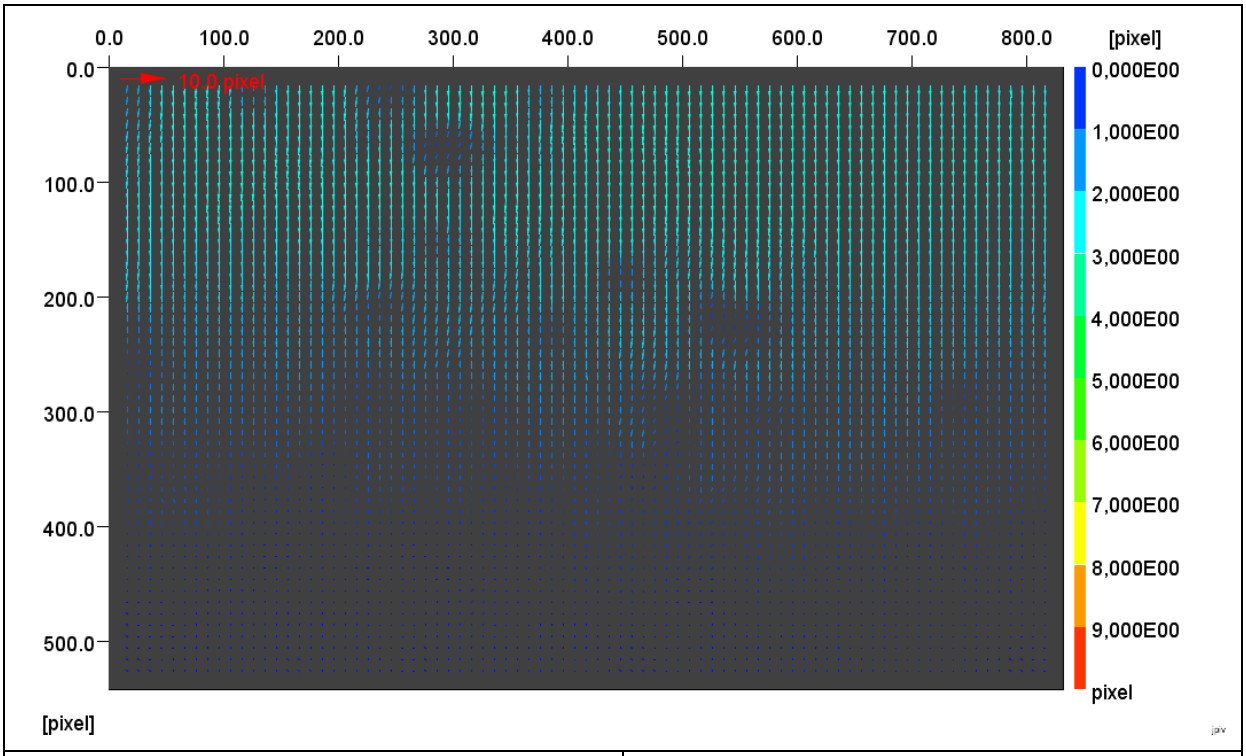

JPIV image 10	1:45 – 2:10

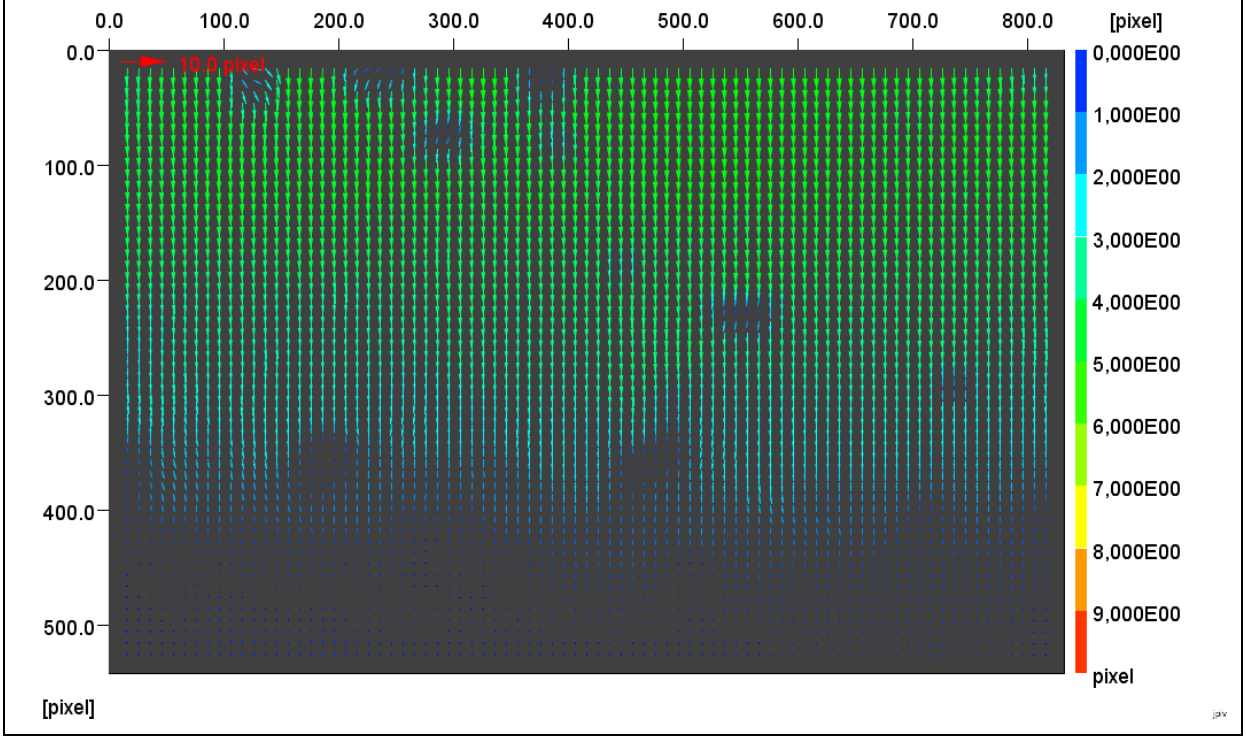

JPIV image 11	2:10 – 3:10

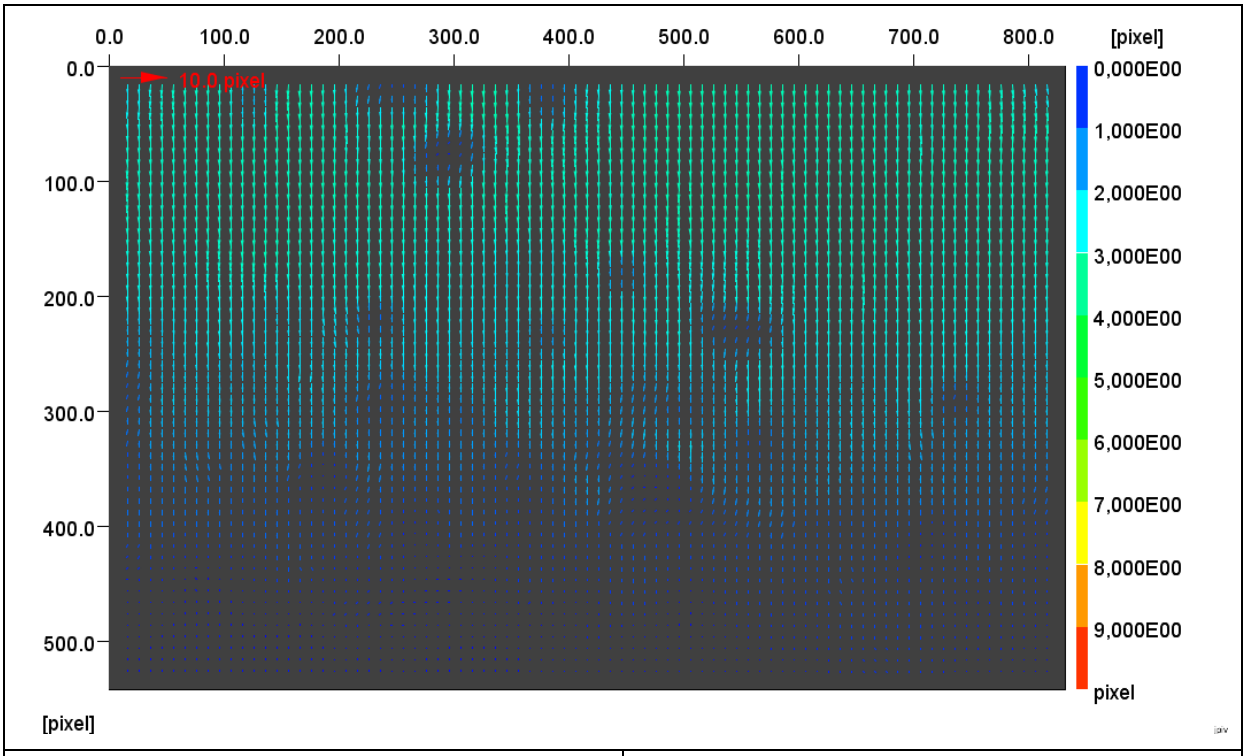

JPIV image 12	3:10 – 4:10

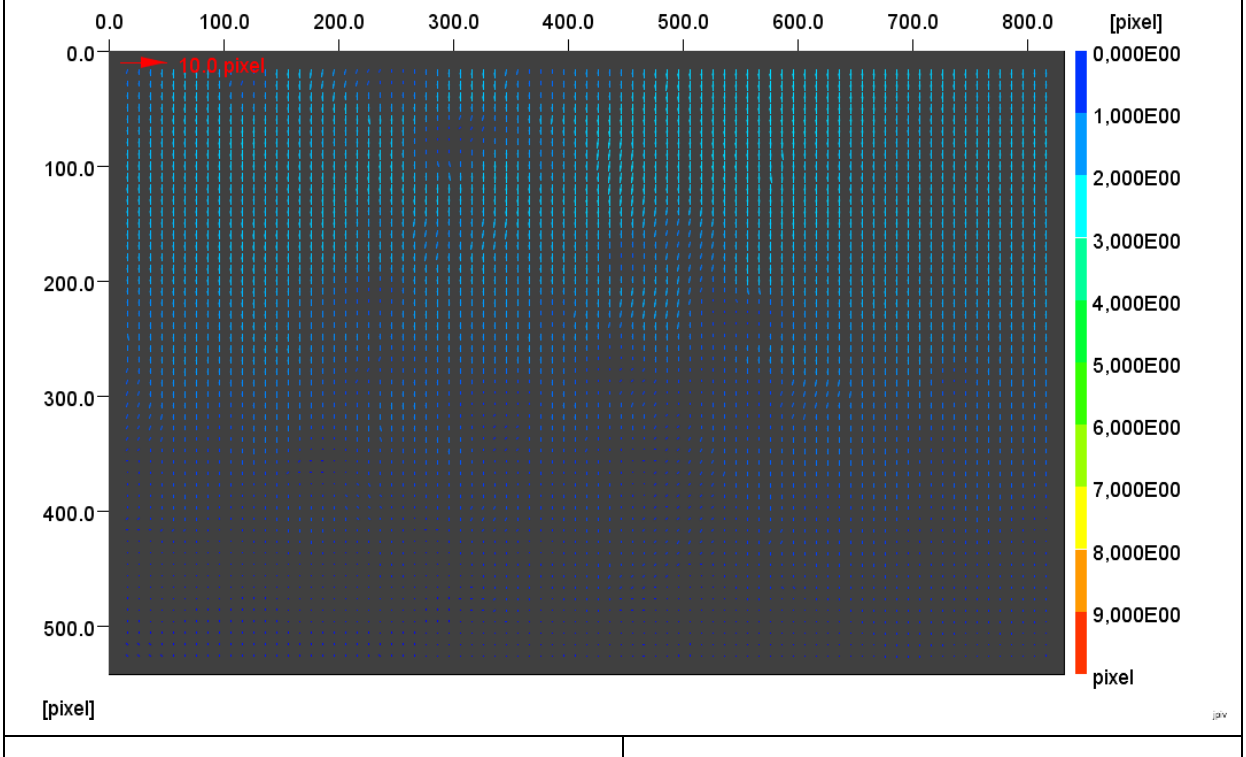

JPIV image 13	4:10 – 5:10

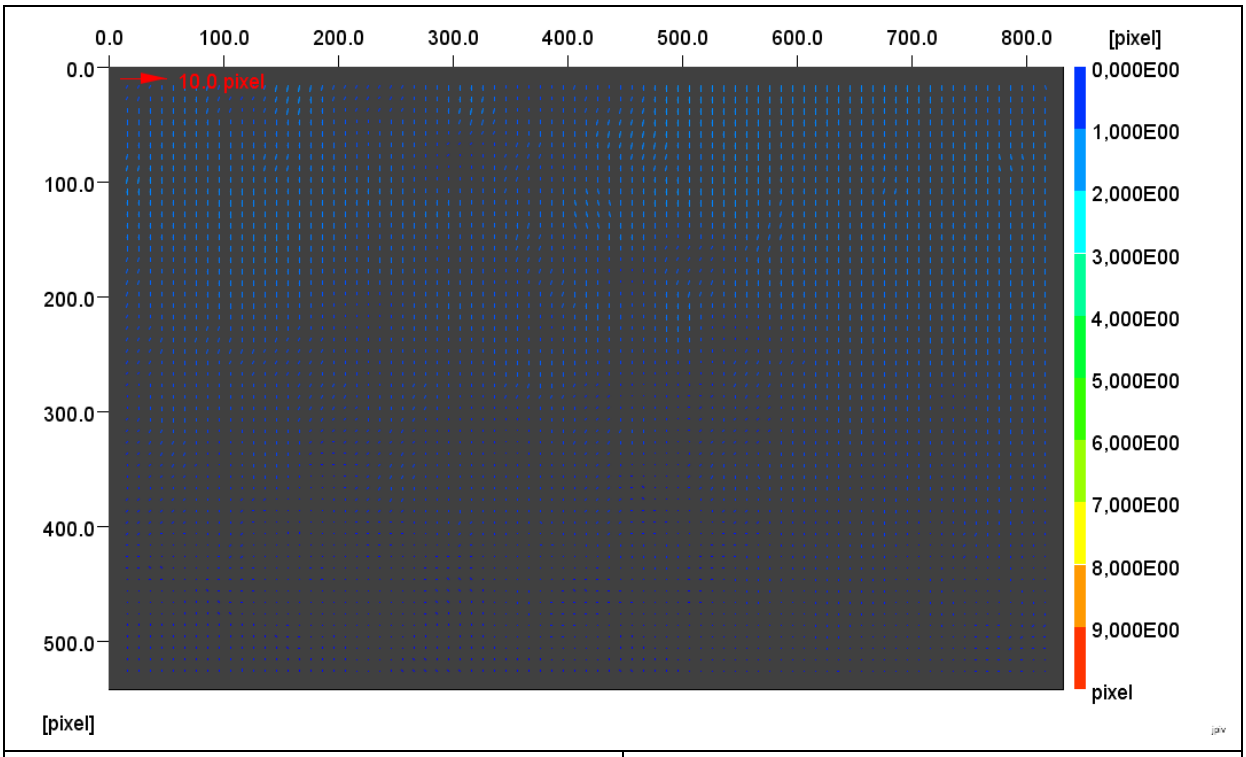

JPIV image 14	5:10 – 6:10

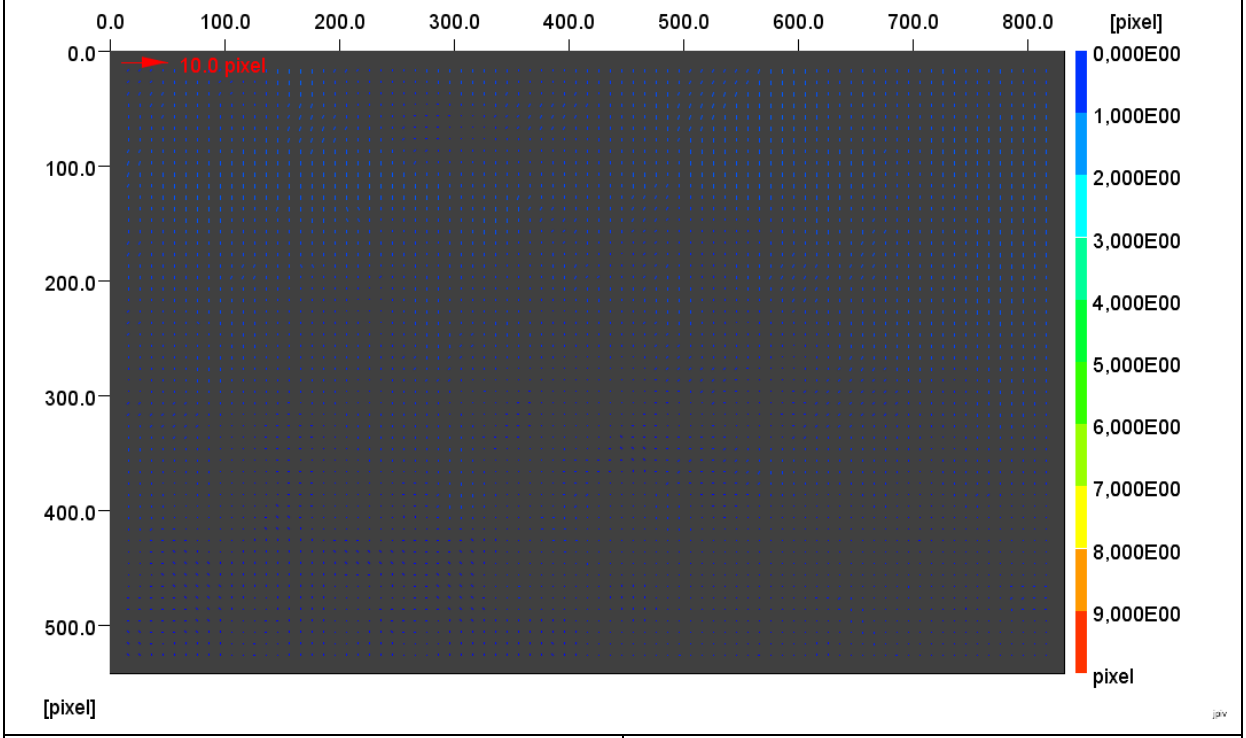

JPIV image 15	6:10 – 7:10

APPENDIX G

Direct Shear Box Tests

To test the reaction on the interface between pile and soil shear tests have been performed. These shear tests are done specifically on the interface between a smooth aluminium plate and kaolin clay. The performed tests will be drained, since the in situ situation also leads to drained loading from consolidation induced displacements.

1.1 Test setup

The shear box apparatus at Delft University of Technology is used to perform the tests. A box containing of an upper and lower half is placed in the apparatus. The lower half of the shear box is fixed in place by bolts. This part will be moved and the reaction forces resulting from this movement at the top half are measured by a load cell. A schematization can be found in Figure 1.

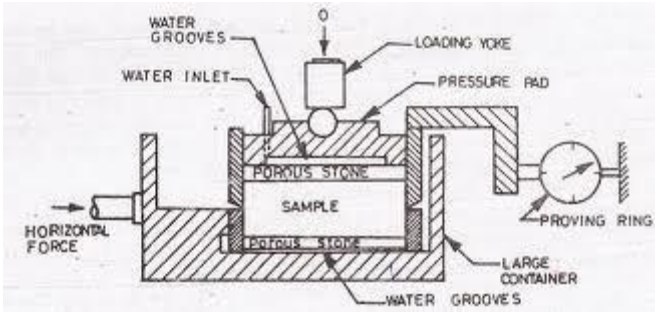

Figure 1: Schematization of direct shear box test

The sample will be loaded vertically by a top plate, resulting in a normal stress to recreate an in situ stress situation. Measurements are done on the settlements of this top plate as well. Just as an oedometer test the sample is unable to deform in horizontal direction. Therefore the deformation in vertical direction can be directly related to volume change.

The overburden is applied through a loading frame which attempts to keep the load centralized on top of the sample. This loading frame has an arm of 1:10, which means that a load placed on the arm will cause a load 10 times as big on the sample.

In general the box is filled with one soil sample. Either a cohesive of non-cohesive soil can be tested in this apparatus. Because for this research the interface is of interest, the shear box will be partly filled with a soil sample. In the bottom half of the box an aluminium plate is placed, with the clay sample in the box on top of this.

Figure 2: Bottom shear box with aluminium plate

Figure 3: Shearbox test assembly

Figure 2 shows the bottom half of the shear box placed in the test apparatus. Both parts of the shear box are projected in Figure 3. Besides that the aluminium plate, the ring including a sample and the top cap can be seen as well. The ring is used to cut the clay sample into the right size to fit it into the shear box.

1.2 Test Procedure

The test is performed on clay samples prepared in the centrifuge. The sample has been consolidated under its own weight and are thus Normally Consolidated. The bottom half of the box is placed in the test apparatus and will be fixed in place, as depicted in Figure 2. The box projected in this picture is later on filled with water to prevent the clay sample from drying out.

The clay sample with ring is placed in the top half of the shear box and placed in the apparatus. The cutting ring is added in the shear box upside down, to prevent the cutting side to be pressed into the aluminium plate.

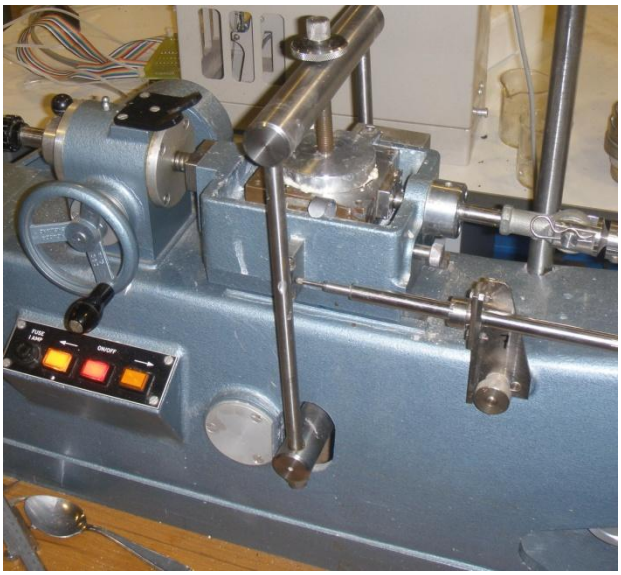

Figure 4: Shear box with test sample installed

The top cap has been designed to fit into the cutting ring. In this way the overburden is transferred to the clay sample without support of the ring on the side. The amount of overburden is presented per sample. Figure 4 shows a test during execution. The overburden is placed on the clay sample through an arm. The sample is left to consolidate, when this consolidation has finished the test can be started.

Measured are the horizontal displacement of the box, the vertical displacement of the top cap and the force on the top half of the shear box.

1.3 Drained Shear Box Tests

These shear tests have been performed drained. That means that shearing is done at such a rate that excess pore pressures get the opportunity to dissipate. Especially in highly impermeable material like clay this leads to very low shearing rates.

The rate of shearing has been determined with the help of [ASTM D3080]. An estimation of the displacement rate is given by the time it takes to reach 50% consolidation. Also the estimated displacement at failure should be implemented. The t50 can be calculated with an estimation of the permeability. Estimated permeability is $1*10^{-9}$ m/s and the estimated displacement at failure is 1 mm. This led to a shearing rate of 0.0024 mm/min.

		Test 1	Test 2
Sample Diameter	*[mm]*	75	75
Sample Height	*[mm]*	25	25
Surcharge	*[kg]*	2	2
	[kN/m2]	45	45
Shearing rate	*[mm/min]*	0.0024	0.0024
Peak shear stress	*[kN/m2]*	20.0	18.8
Peak friction angle	*[deg]*	23.8	22.6
Residual shear stress	*[kN/m2]*	15.0	15.5
Residual friction angle	*[deg]*	18.4	19.0

The graphs of the two different tests are presented in the next paragraph. It can be seen that these samples were contractant because of the increase in settlement (or decrease in void ratio) occurring during shear. The samples have been normally consolidated in the centrifuge and are then loaded up to its described overburden pressure in the shear box.

1.4 Drained Shear Box Tests; Results

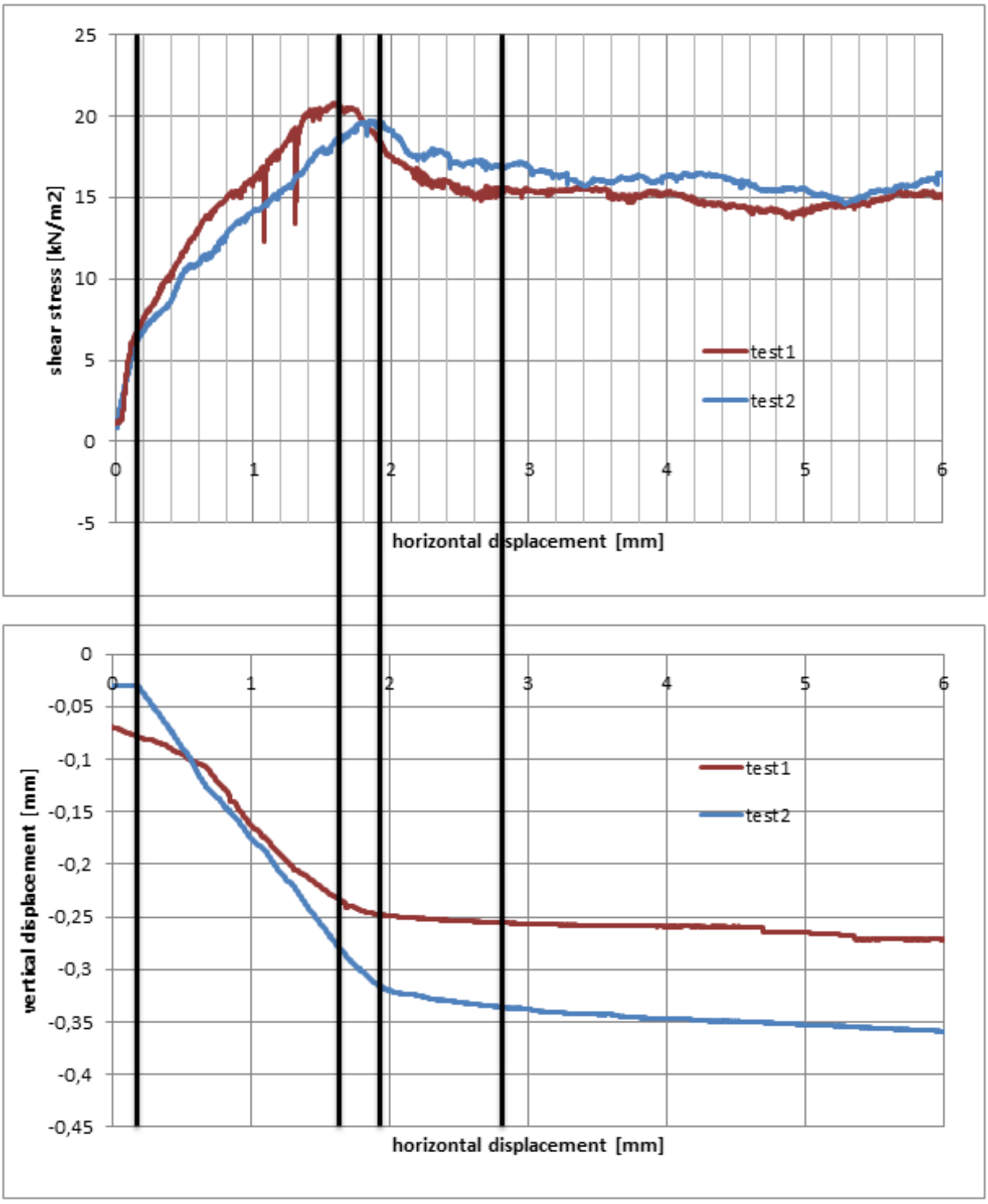

Report for MSettle 8.2

Settlement Calculations
Developed by Deltares

Date of report:	5-9-2012
Time of report:	14:03:00
Date of calculation:	5-9-2012
Time of calculation:	14:02:30
Filename:	C:\..\0. Benchmark Situation\onetimestep_load\Msettle_benchmark

1 Echo of the Input

1.1 Layer Boundaries

Boundary number	Co-ordinates [m]				
2 - X -	0,000	100,000			
2 - Y -	0,000	0,000			
1 - X -	0,000	100,000			
1 - Y -	-10,000	-10,000			
0 - X -	0,000	100,000			
0 - Y -	-15,000	-15,000			

1.2 PL Lines

PL line number	Co-ordinates [m]				
1 - X -	0,000	100,000			
1 - Y -	5,000	5,000			

1.3 General Data

Soil model:	NEN Bjerrum
Consolidation model:	Darcy
Strain model:	Linear
Groundwater level:	Initial determined by PL-line number 1
Unit weight of water:	10,00 [kN/m³]
Stress distribution	
- Soil:	Buisman
- Loads:	None
End of consolidation:	100000,00 [days]
No maintain profile	
Pc (initial):	Variable parallel to the initial effective stress
Pc (per step):	Automatic increased to the final effective stresses
Creep rate reference time:	1,000 [days]
No imaginary surface	
No submerging	
Load column width	
- Non-Uniform Loads :	1,00 [m]
- Trapezoidal Loads :	1,00 [m]

1.4 Soil Profiles

Layer number	Material name	PL-line top	PL-line bottom
2	Stiff Clay	1	1
1	Impermeable Layer	1	1

1.5 Soil Properties

Layer number	Drained	Unit weight	
		Unsaturated [kN/m³]	Saturated [kN/m³]
2	No	18,00	18,00
1	No	20,00	20,00

Layer number	Storage type	Vert. consolid. coefficient Cv [m²/s]	Vertical permeability [m/s]	Permeability strain mod. [m/s]	Initial vertical permeability [m/s]
2	Const. perm.	-	3,000E-09	-	-
1	Const. perm.	-	1,000E-13	-	-

Layer number	POP [kN/m²]	OCR [-]	Equiv. age [days]
2	0,00	-	-
1	400,00	-	-

Layer number	Secondary swelling type	Secondary swelling factor[-]	Unloading stress ratio[-]
2	Full	-	-
1	Full	-	-

Layer number	Reloading/ swelling ratio RR [-]	Compression ratio CR [-]	Reloading/ swelling index Ca [-]	Compression index Cr [-]	Coeff. of sec. compression Cc [-]	Initial void ratio (e0) [-]
2	-	-	0,0000000	0,0800000	0,3000000	1,000000
1	-	-	0,0000000	0,0000001	0,0000001	0,000000

1.6 Non-Uniform Loads

Load number	Time [days]	Unit weight	
		Unsaturated [kN/m³]	Saturated [kN/m³]
1	0	20,00	20,00

Load number	Co-ordinates [m]					
1 - X -	0,00	0,00	100,00	100,00		
1 - Y -	0,00	7,50	7,50	0,00		

1.7 Verticals

Vertical number	X co-ordinates [m]				
1 - 5	0,000	10,000	20,000	30,000	40,000
6 - 10	50,000	60,000	70,000	80,000	90,000
11	100,000				

Calculation of cross section at Z = 0,000 m
Discretisation = 100

End of Report

Report for MSettle 8.2

Settlement Calculations
Developed by Deltares

Date of report:	5-9-2012
Time of report:	14:01:02
Date of calculation:	27-8-2012
Time of calculation:	13:14:55
Filename:	C:\..\2. Centrifuge Soil model\Msettle\1timesteplaod\Centrifuge Sample

1 Echo of the Input

1.1 Layer Boundaries

Boundary number	Co-ordinates [m]				
3 - X -	0,000	100,000			
3 - Y -	0,000	0,000			
2 - X -	0,000	100,000			
2 - Y -	-4,500	-4,500			
1 - X -	0,000	100,000			
1 - Y -	-14,000	-14,000			
0 - X -	0,000	100,000			
0 - Y -	-20,000	-20,000			

1.2 PL Lines

PL line number	Co-ordinates [m]				
1 - X -	0,000	100,000			
1 - Y -	5,000	5,000			

1.3 General Data

Soil model:	NEN Bjerrum
Consolidation model:	Darcy
Strain model:	Linear
Groundwater level:	Initial determined by PL-line number 1
Unit weight of water:	10,00 [kN/m³]
Stress distribution	
- Soil:	Buisman
- Loads:	None
End of consolidation:	50000,00 [days]
No maintain profile	
Pc (initial):	Variable parallel to the initial effective stress
Pc (per step):	Automatic increased to the final effective stresses
Creep rate reference time:	1,000 [days]
No imaginary surface	
No submerging	
Load column width	
- Non-Uniform Loads :	1,00 [m]
- Trapezoidal Loads :	1,00 [m]

1.4 Soil Profiles

Layer number	Material name	PL-line top	PL-line bottom
3	Soft Clay	1	1
2	Stiff Clay	1	1
1	Impermeable	1	1

1.5 Soil Properties

Layer number	Drained	Unit weight	
		Unsaturated [kN/m³]	Saturated [kN/m³]
3	No	18,00	18,00
2	No	18,00	18,00
1	No	18,00	18,00

Layer number	Storage type	Vert. consolid. coefficient Cv [m²/s]	Vertical permeability [m/s]	Permeability strain mod. [m/s]	Initial vertical permeability [m/s]
3	Const. perm.	-	2,000E-09	-	-
2	Const. perm.	-	1,000E-09	-	-
1	Const. perm.	-	1,000E-13	-	-

Layer number	POP [kN/m²]	OCR [-]	Equiv. age [days]
3	0,00	-	-
2	200,00	-	-
1	0,00	-	-

Layer number	Secondary swelling type	Secondary swelling factor[-]	Unloading stress ratio[-]
3	Full	-	-
2	Full	-	-
1	Full	-	-

Layer number	Reloading/ swelling ratio RR [-]	Compression ratio CR [-]	Reloading/ swelling index Ca [-]	Compression index Cr [-]	Coeff. of sec. compression Cc [-]	Initial void ratio (e0) [-]
3	-	-	0,0000000	0,0800000	0,3000000	1,000000
2	-	-	0,0000000	0,0800000	0,3000000	1,000000
1	-	-	0,0000000	0,0000001	0,0000001	0,000000

1.6 Non-Uniform Loads

Load number	Time [days]	Unit weight	
		Unsaturated [kN/m³]	Saturated [kN/m³]
1	0	20,00	20,00

Load number	Co-ordinates [m]					
1 - X -	0,00	0,00	100,00	100,00		
1 - Y -	0,00	7,50	7,50	0,00		

1.7 Verticals

Vertical number	X co-ordinates [m]				
1 - 5	0,000	10,000	20,000	30,000	40,000
6 - 10	50,000	60,000	70,000	80,000	90,000
11	100,000				

Calculation of cross section at Z = 0,000 m
Discretisation = 100

End of Report

BENCHMARK SOIL PROFILE

		Material Model	Material Type	y unsat	y sat	kx	ky	e init	E ref	lambda*	kappa*	lambda	kappa	E50	Eoed	Eur	power (m)	p ref	c	phi	psi	v ur	K0 nc	M	POP
				[kN/m3]	*[kN/m3]*	*[m/day]*	*[m/day]*	*[-]*	*[kN/m2]*	*[-]*	*[-]*	*[-]*	*[-]*	*[kN/m2]*	*[kN/m2]*	*[kN/m2]*	*[-]*	*[kN/m2]*	*[kN/m2]*	*[deg]*	*[deg]*	*[-]*	*[-]*	*[-]*	*[kN]*
Soft Soil																									
Layer I	Rock Fill	Linear Elastic	Drained	20	20	1	1	0,5	1,00E+10	-	-	-	-	-	-	-	-	-	-	-	-	0,3	-	-	0
Layer II	Clay	Soft Soil	Undrained	18	18	2,592E-04	2,592E-04	1	-	0,065	0,035	-	-	-	-	-	-	-	15	29	0	0,2	0,515	1,363	0
Modified Cam Clay																									
Layer I	Rock Fill	Linear Elastic	Drained	20	20	1	1	0,5	1,00E+10	-	-	-	-	-	-	-	-	-	-	-	-	0,3	-	-	0
Layer II	Clay	Modified Cam Clay	Undrained	18	18	2,592E-04	2,592E-04	1	-	-	-	0,1304	0,0696	-	-	-	-	-	15	29	0	0,2	0,515	1,2	0
Hardening Soil																									
Layer I	Rock Fill	Linear Elastic	Drained	20	20	1	1	0,5	1,00E+10	-	-	-	-	-	-	-	-	-	-	-	-	0,3	-	-	0
Layer II	Clay	Hardening Soil	Undrained	18	18	2,592E-04	2,592E-04	1	-	-	-	-	-	1916	1533	5175	1	100	15	29	0	0,2	0,515	-	0

Dimensoins		Top	Bottom
		[m]	[m]
Layer I	Rock Fill	7,5	0
Layer II	Clay	0	-10
Water level		5	

CENTRIFUGE SOIL PROFILE

		Material Model	Material Type	y unsat	y sat	kx	ky	e init	E ref	lambda*	kappa*	lambda	kappa	E50	Eoed	Eur	power (m)	p ref	c	phi	psi	v ur	K0 nc	M	POP
				[kN/m3]	*[kN/m3]*	*[m/day]*	*[m/day]*	*[-]*	*[kN/m2]*	*[-]*	*[-]*	*[-]*	*[-]*	*[kN/m2]*	*[kN/m2]*	*[kN/m2]*	*[-]*	*[kN/m2]*	*[kN/m2]*	*[deg]*	*[deg]*	*[-]*	*[-]*	*[-]*	*[kN]*
Soft Soil																									
Layer I	Rock Fill	Linear Elastic	Drained	20	20	1	1	0,5	1,00E+10	-	-	-	-	-	-	-	-	-	-	-	-	0,3	-	-	0
Layer II	Soft Clay	Soft Soil	Undrained	18	18	2,592E-04	2,592E-04	1	-	0,065	0,035	-	-	-	-	-	-	-	8	29	0	0,2	0,515	1,363	0
Layer III	Stiff Clay	Soft Soil	Undrained	18	18	2,592E-04	2,592E-04	1	-	0,065	0,035	-	-	-	-	-	-	-	15	29	0	0,2	0,515	1,363	200
Modified Cam Clay																									
Layer I	Rock Fill	Linear Elastic	Drained	20	20	1	1	0,5	1,00E+10	-	-	-	-	-	-	-	-	-	-	-	-	0,3	-	-	0
Layer II	Soft Clay	Modified Cam Clay	Undrained	18	18	2,592E-04	2,592E-04	1	-	-	-	0,1304	0,0696	-	-	-	-	-	8	29	0	0,2	0,515	1,2	0
Layer III	Stiff Clay	Modified Cam Clay	Undrained	18	18	2,592E-04	2,592E-04	1	-	-	-	0,1304	0,0696	-	-	-	-	-	15	29	0	0,2	0,515	1,2	200
Hardening Soil																									
Layer I	Rock Fill	Linear Elastic	Drained	20	20	1	1	0,5	1,00E+10	-	-	-	-	-	-	-	-	-	-	-	-	0,3	-	-	0
Layer II	Soft Clay	Hardening Soil	Undrained	18	18	2,592E-04	2,592E-04	1	-	-	-	-	-	1916	1533	5175	1	100	8	29	0	0,2	0,515	-	0
Layer III	Stiff Clay	Hardening Soil	Undrained	18	18	2,592E-04	2,592E-04	1	-	-	-	-	-	1916	1533	5175	0,6	100	15	29	0				200

Dimensoins		Top	Bottom
		[m]	[m]
Layer I	Rock Fill	7,5	0
Layer II	Soft Clay	0	-5
Layer III	Stiff Clay	-5	-14
Water level		5	